

1-2005

Simulating the Oil Spill in the Arabian Gulf Marine Environment: A Risk Assessment in Association with UAE Coastal Desalination Plants

Abubaker Awad El-Hakeem

Follow this and additional works at: https://scholarworks.uaeu.ac.ae/all_theses

Part of the [Environmental Sciences Commons](#)

Recommended Citation

El-Hakeem, Abubaker Awad, "Simulating the Oil Spill in the Arabian Gulf Marine Environment: A Risk Assessment in Association with UAE Coastal Desalination Plants" (2005). *Theses*. 660.
https://scholarworks.uaeu.ac.ae/all_theses/660

This Thesis is brought to you for free and open access by the Electronic Theses and Dissertations at Scholarworks@UAEU. It has been accepted for inclusion in Theses by an authorized administrator of Scholarworks@UAEU. For more information, please contact fadl.musa@uaeu.ac.ae.



United Arab Emirates University
Deanship of Graduate Studies
Master Degree Program in Environmental Sciences

**SIMULATING THE OIL SPILL IN THE ARABIAN GULF MARINE
ENVIRONMENT:
A RISK ASSESSMENT IN ASSOCIATION WITH UAE COASTAL
DESALINATION PLANTS**

By

Abubaker Awad El-Hakeem

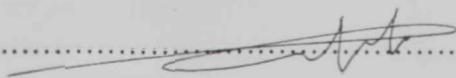
A Thesis

Submitted to

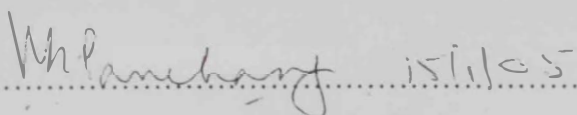
United Arab Emirates University
in partial fulfillment of the requirements
For the Degree of M.Sc. in Environmental Sciences

January 2005

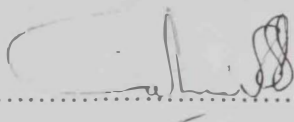
The Thesis of Abubakier Awad El-Hakeem for the Degree of Master of Science in Environmental is approved.



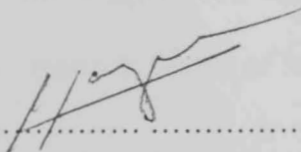
Examining Committee Member, Dr. Walid Elshorbagy



Examining Committee Member, Prof. Vijay G Panchang



Examining Committee Member, Dr. Saif M. Al Ghais



Director of the Program, Dr. Hazem A. H. Kataya



Dean of the Graduate Studies, Professor James E. Fletcher

United Arab Emirates University
2004/2005

ACKNOWLEDGMENT

I would like to express my deep appreciation and thanks to the UAE University and in particular the Graduate Studies Deanship under the leadership of his Excellency, Professor James Fletcher for providing all needed resources and support to accomplish this thesis. Acknowledgment is also due to the research affairs under the leadership of her Excellency, Dr Maitha AlShamsi, in addition to TAKREER and JCCP (Japanese Cooperation Center, Petroleum) Companies for providing access to research papers produced by the JCCP-B Externally Funded Research Project.

I hereby also wish to express my sincere appreciation and thanks to Dr. Walid Elshorbagy and Prof. Rashid Chebbi for their guidance and patients without which this work could have never been materialized. I should also raise my gratitude to Dr. Mir Hammadul Azam, former Research Assistant in the UAE University, for his distinguishable support with regard to the use of the modeling software MIKE3.

I would thank my dear wife for her patients and strong support during all stages of my study.

I finally wish to express my deep appreciation to the Civil and Environmental Engineering Dept. family for continues support and encouragement.

I present this work to the sole of my father, Professor. Awad Salim El-Hakeem the founder Dean of the College of Engineering– UAE University (1982-1992) and to my dear mother for her continuous prayers.

ABSTRACT

The current study is directed towards the development of oil spill hazard contour maps for the prediction of oil spill travel times and critical wind directions in association with major strategic desalination plants in United Arab Emirates. Five desalination plants in are selected along the UAE coastline to be the potential destination points of oil spill hazards. These plants are Al-Shuwayhat, Al-Mirfa, Umm AlNar & Taweelah, Jebel Ali and Al-Layah.

In order to reach the set target, a coastal hydraulics simulation model is employed to adopt the real sea-state dynamic conditions. The hydrodynamic simulated results are tuned and tested against actual documented measurements of tides and currents. The simulated flow pattern of the surface currents produced by the model is also compared with common cited patterns.

Oil spill simulation is then conducted employing the resolved flow field and other hydrodynamic results. The oil spill model parameters are tested to verify their sensitivity for final model setup. A validation of the model performance is also carried out utilizing well documented actual observations of oil spill incidents in the Arabian Gulf. At that stage, the coupled hydrodynamic and oil spill model are set to perform a series of simulations on hypothetical oil spills based on extreme case conditions. The study area is divided into zones covering the oil export loading terminals and the oil tanker routs. The shortest traveling times of the oil spill from various zones to each desalination plant are identified in association with the critical wind directing the oil slick to that plant. At last, the simulated travel maps for shortest arrival desalination plants.

Key words: Arabian Gulf, numerical modeling, hydrodynamic modeling, oil spill modeling, spill hazard maps.

LIST OF CONTENTS

<u>Chapter</u>	<u>Page</u>
Chapter 1 Introduction.....	1-1
1.1 Introduction.....	1-1
1.2 Problem Significance.....	1-4
1.3 Objectives.....	1-7
1.4 Methodology.....	1-7
Chapter 2 Literature Review.....	2-1
2.1 Arabian Gulf Hydrodynamic Characteristics and Modeling.....	2-1
2.2 Bathymetry.....	2-2
2.3 Fresh Water Exchange and Evaporation.....	2-3
2.4 Wind.....	2-4
2.5 Currents.....	2-5
2.6 Residual Circulation.....	2-6
2.7 Hydrodynamic and Oil Spill Modeling.....	2-8
2.7.1 Hydrodynamic Modeling Studies.....	2-8
2.7.2 Oil Spill Processes and Modeling.....	2-10
2.8 Types of Oil.....	2-16
2.9 Oil Spills in UAE.....	2-18
Chapter 3 Mike3 Hydrodynamic Flow Model.....	3-1
3.1 General Description of Modules.....	3-1
3.1.1 Conservation Equations of Mass And Momentum.....	3-2
3.1.2 Advection-Dispersion Schemes.....	3-2
3.1.3 Turbulence Closure Module.....	3-3
3.1.4 Heat Flux Module.....	3-5
3.2 HD Module Data and Setup.....	3-11

3.2.1 Bathymetry.....	3-11
3.2.2 Grid Generation for Hydrodynamics.....	3-11
3.2.3 Initial Salt and Temperature Fields.....	3-12
3.2.4 Initial Boundary Salt and Temperature Time Series.....	3-13
3.2.5 Tidal Boundary.....	3-13
3.2.6 Wind Field.....	3-14
3.2.7 River Inflow.....	3-15
3.2.8 Heat Exchange Parameters.....	3-16
3.2.9 Turbulence.....	3-17
3.3 Hydrodynamic Simulation Results and Tuning.....	3-17
3.3.1 Computed and Measured Tides.....	3-17
3.3.2 Computed and Measured Residual Currents.....	3-18
3.3.3 Arabian Gulf Residual Flow Pattern.....	3-19
Chapter 4 Oil Spill Model.....	4-1
4.1 MIKE3 SA Numerical Models.....	4-1
4.1.1 Basic Equations.....	4-2
4.1.2 Advection/Diffusion.....	4-2
4.1.3 Evaporation.....	4-3
4.1.4 Natural Dispersion.....	4-4
4.1.5 Mechanical Spreading.....	4-5
4.1.6 Dissolution.....	4-5
4.1.7 Emulsification.....	4-6
4.2 Oil Spill Sensitivity Analysis.....	4-6
4.2.1 Source and Source Flux.....	4-7
4.2.2 Dispersion Criteria: no wind conditions.....	4-7
4.2.3 Wind Field.....	4-10

4.2.4 Other Selected Parameters	4-12
4.2.5 Sensitivity to Crude Oil Types.....	4-16
4.2.6 Sensitivity Analysis Conclusion.....	4-20
4.3 Spill Analysis Model Validation.....	4-21
4.3.1 Al-Ahmadi Oil Spill	4-22
4.3.2 Al Ahmadi Oil Spill Simulation Using MIKE3 S A	4-25
4.3.3 Results of Al Ahmadi Oil Spill Simulation Using MIKE3 SA	4-28
4.3.4 Discussion and Conclusion	4-29
 Chapter 5 Desalination Plants and Source Zoning	5-1
5.1 Desalination Plants Selection	5-1
5.2 Zoning	5-3
 Chapter 6 Oil Spill Model.....	6-1
6.1 Results of Sample Oil Spill Event.....	6-1
6.2 Oil Spill Impact Assessment On Desalination Plants.....	6-5
6.2.1 Release Conditions.....	6-5
6.2.2 Approaches of Identifying Critical Trajectories.....	6-7
6.2.3 Shuwayhat Desalination Plant.....	6-10
6.2.4 Mirfa Desalination Plant.....	6-12
6.2.5 Abu Dhabi Desalination Plants.....	6-14
6.2.6 Jebel-Ali Desalination Plant.....	6-16
6.2.7 Layah Desalination Plant.....	6-18
 Chapter 7 Summary and Recommendations.....	7-1

LIST OF TABLES

<u>Table</u>	<u>Page</u>
Table 1.1 Major tanker spills of over 5,000 tones in the Gulf Region since 1974.....	1-3
Table 2.1 Different types of oil and their estimated impact.....	2-17
Table 2.2 Oil spills in the UAE	2-19
Table 3.1 The harmonic tidal constituents.....	3-13
Table 3.2 Arabian Gulf average effective monthly wind velocities.....	3-14
Table 3.3 Major rivers into the northern Gulf.....	3-15
Table 3.4 Heat flux module parameters.....	3-16
Table 3.5 Empirical constants in the k- ϵ Turbulence Model.....	3-17
Table 4.1 Results of total oil dispersion: all dimensions are in grid number.....	4-8
Table 4.2 Results of total oil spreading due to wind change: all dimensions are in cell.....	4-10
Table 4.3 Sensitivity analysis parameters	4-13
Table 4.4 Selected crude oil samples and their characteristics.....	4-16
Table 4.5 Hydrocarbon cuts data for selected crudes.....	4-17
Table 4.6 Characteristics of medium and light crudes used in oil spill simulation ...	4-17
Table 4.7 Summary results at 14 day, oil slick trajectory and weathering.....	4-18
Table 4.8 Average effective monthly wind velocities.....	4-22
Table 4.9 Al Ahmadi spill Simulation wind data.....	4-25
Table 4.10 SA Parameters for validation simulation.....	4-27
Table 4.11 Al-Ahmadi oil spill, Actual and predicted trajectory comparison.....	4-27
Table 4.12 Speculated February wind data.....	4-31

Table 5.1 selected desalination plants along the UAE coast.....	5-1
Table 5.2 zone significance and relative oil spill source	5-5
Table 6.1 Total oil thickness and weathering estimates in	6-2
Table 6.2 Reported oil spill events, approximate location and volume spilled.....	6-5
Table 6.3 Shore arrival time using different release modes.....	6-6
Table 6.4 Critical arrival times and corresponding wind direction for Shuwayhat desalination plant.....	6-10
Table 6.5 critical arrival times and corresponding wind direction for Mirfa desalination plant.....	6-12
Table 6.6 critical arrival times and corresponding wind direction for Abu Dhabi desalination plant.....	6-14
Table 6.7 Critical arrival times and corresponding wind direction for Jebel-Ali desalination plant.....	6-16
Table 6.8 critical arrival times and corresponding wind direction for Layah desalination plant.....	6-18

LIST OF FIGURES

<u>Figure</u>	<u>Page</u>
Figure 1.1 Arabian Gulf region.....	1-1
Figure 1.2 Oil and gas fields in the Arabian Gulf	1-4
Figure 2.1 Arabian Gulf Bathymetry.....	2-2
Figure 2.2 Rivers of the northern Gulf (Reynolds, 1993).....	2-3
Figure 2.3 Classification of tides in the Arabian Gulf	2-6
Figure 2.4 Rough locations of oil incidents in the Gulf region adjacent to the UAE Coast.	2-18
Figure 3.1 Arabian Gulf Bathymetry- model setup	3-11
Figure 3.2 Computational Grid.....	3-12
Figure 3.3 Winter, Temperature & Salinity fields.....	3-13
Figure 3.4 Definition of wind direction	3-15
Figure 3.5 comparison of model and measured water level for Abu Dhabi & Dubai.	3-18
Figure 3.6 Comparison of measured and model current components U and V.....	3-19
Figure 3.7 a Wind and Density driven one month residual surface flow for (Winter).....	3-20
Figure 3.7 b Wind and Density driven one month residual surface flow for (Summer).....	3-20
Figure 4.1 Oil Dispersion criteria, 14 Day age	
Case I : Dispersion proportional to current.....	4-9
Case II : Dispersion independent of current	4-9

Figure 4.2 a Wind conditions effect 5m/s constant wind field, Day14 Oil slick....	4-11
Figure 4.2 b No wind conditions, Day14 Oil slick.....	4-11
Figure. 4.3 Location of Mina Al-Ahmadi.....	4-21
Figure 4.4 Al-Ahmadi actual trajectory of leading edge from the beginning of release.....	4-23
Figure 4.5 Predicted oil trajectory KFUPM model.....	4-25
Figure 4.6a Al Ahmadi oil spill trajectory at January 25, 1991- monthly average wind.....	4-29
Figure 4.6b Al Ahmadi oil spill trajectory at January 31, 1991- monthly average Wind.....	4-29
Figure 4.6c Al Ahmadi oil spill trajectory at February 7, 1991- monthly average Wind.....	4-30
Figure 4.6d Al Ahmadi oil spill trajectory at March 17, 1991- monthly average Wind.....	4-30
Figure 4.7a Al Ahmadi oil spill trajectory at February 12, 1991-specified wind field.....	4-33
Figure 4.7b Al Ahmadi oil spill trajectory at February 18, 1991-specified wind field.....	4-33
Figure 4.7c Al Ahmadi oil spill trajectory at February 24, 1991-specified wind field.....	4-34
Figure 4.7d Al Ahmadi oil spill trajectory at March 17, 1991-specified wind field.....	4-34
Figure 4.8 Al Ahmadi oil spill trajectory with speculated wind field.....	4-35

Figure 5.1 The locations of the selected desalination plants.....	5-2
Figure 5.2 Oil spill source zones.....	5-3
Figure 5.3 zoning based on oil terminals locations and navigation lines.....	5-4
Figure 6.1a Trajectory and total thickness of spill- 1week age.....	6-3
Figure 6.1b Trajectory and total thickness of spill - 2week age.....	6-4
Figure 6.1c Trajectory and total thickness of spill - 3week age.....	6-4
Figure 6.2 Locations of oil spills sources and destinations.....	6-8
Figure 6.3 Supplementary enhancement zones.....	6-9
Figure 6.4a Shortest arrival times to Shuwayhat desalination plant.....	6-11
Figure 6.4b Critical wind direction in association with shortest arrival times to Shuwayhat plant.	6-11
Figure 6.5a Shortest arrival time to Mirfa desalination plant.....	6-13
Figure 6.5b Critical wind direction in association with shortest arrival times to Mirfa Plant.....	6-13
Figure 6.6 Approximate location of Mina Zayed, Taweelah and Umm AlNar desalination plants in Abu Dhabi.....	6-14
Figure 6.7a Shortest arrival time to Abu Dhabi desalination plants.....	6-15
Figure 6.7b Critical wind direction in association with shortest arrival times to Abu Dhabi desalination Plants.....	6-15
Figure 6.8a Shortest arrival time to Jebel-Ali desalination plant.....	6-17
Figure 6.8b Critical wind direction in association with shortest arrival times to Jebel-Ali desalination plant.....	6-17
Figure 6.9a Shortest arrival time to Layah desalination plant.....	6-19

Figure 6.9b Critical wind direction in association with shortest arrival times to Layah des.

Plant.....6-19

CHAPTER 1

INTRODUCTION

1.1 Background

The Arabian Gulf is a semi-enclosed, tropical, marginal sea located at the southeastern end of the Arabian Peninsula with an average length of 1000 km and a width that varies between 55 and 340 km, having an area of 240 000 km². The Gulf water borders the United Arab Emirates, Qatar, Bahrain, Saudi Arabia, Kuwait, Iraq, Iran, and Oman (figure 1).



Figure 1.1 Arabian Gulf region

The Gulf, which affords one of the busiest and most important shipping lanes in the world, is a shallow embayment with a mean depth of 35 m and is connected through the Straits of Hormuz with the Gulf of Oman. The bathymetry is markedly asymmetrical, with deeper water along the Iranian coast and shallow water on the Arabian side (Chu et al.

1988). The Gulf lies entirely north of the Tropic of Cancer, so it is strictly sub-tropical, though its location within the large, arid, East Asian land mass means that the climate is more fiercely tropical in summer and more temperate in winter than most seas of equivalent latitude. In the summer, it experiences very high temperatures, while in the winter, water and air temperatures fall to well below values associated with tropical marine ecosystems (Sheppard, 1993).

From a historic point of view, people have been attracted to the shores of the Arabian Gulf for millennia. An early maritime civilization, Dilmun, prospered some 4000-5000 years ago, encompassing what is known as Bahrain now and the eastern coast of Saudi Arabia. Before the tenth century AD, the Arabs had established a trade network extending from the gulf as far eastward as China. Using stitched, lateen rigged craft, cargoes of textile and spices were accompanied by the exchange of new ideas, science, and religion. Such voyages were made possible through the Arab's sophisticated knowledge of astronomy and navigation (Tibbetts, 1971; Price et al. 1982; Severin, 1982). Nowadays, there is still some trade using the traditional craft, that is now equipped with diesel motors, between the Gulf, Pakistan and East Africa (Price, 1993).

The discovery of oil in the 1930s and 1940s was principally responsible for the immense economic wealth and geopolitical importance of the region today. Oil currently supplies about 40% of the world energy, and recent estimates suggest that the Middle East has over 65% of the world petroleum reserves. The countries bordering the Arabian Gulf produce almost 6 billion barrels (798 million metric tones) of oil a year, about 27% of the world's production in 1993 (World Resources Institute, 1996).

The same waterway serves its old role in linking the Gulf States to the outer world by being the major route of transporting the produced oil to the world market. Historically, about half of the oil transported through the global marine environment has come through the Arabian Gulf countries from 1993 to 1980 with an annual average of 59% (Gupta et al. 1993). Linden et al. 1990, reported that the Gulf is among the busiest tanker navigation routs. For instance, there are 20 000-35 000 individual tanker passages annually at the Straits of Hormuz.

Due to this heavy traffic, transported oil constitutes the most significant source of oil pollution in the Gulf. The annual oil input is 4 000 MT from tanker accidents. About 14

tanker accidents of various kinds occur annually in the Arabian Gulf and at least 13% of these release oil (Linden et al.1990). Thirty-nine confirmed incidents of oil pollution, out of a total 422 reported incidents, were recorded from May 1981 to June 1987 in the Gulf where the incidents varied from sighting of oil sheens to oil well blow-out. The volume varied from a trickle to 500 000 barrels (68 000 tones) reported from the Nowruz oil well blow-out due to military action (Linden et al. 1990).Beside the dramatic and well-publicized catastrophic oil spills, a substantial amount of oil enters the marine and coastal waters of the Arabian Gulf from a variety of sources: ballast water discharges, fueling spills, platform blow-outs, pipeline leaks, and natural seeps (Pearson, Al-Ghais et al.1994).

A study conducted by the world information system in 1981 on oil pollution of the Arabian Gulf estimated that more than 1.5 million tones of oil would pollute the Gulf waters between 1981 and 1989. In fact, this estimate was surpassed in 1985 itself. The hazards of oil pollution in the Arabian Gulf have increased significantly over the past few decades owing to increased urbanization, industrialization, oil production and transportation and political tension.

The negative impact of oil spills in the Arabian Gulf is pronounced because of expected adverse impacts on desalination plants on the coast. Continuous need for desalinated water supplies dictates the prevention of pollution of source waters.

A summary of accidental tanker spills in the Region since 1974 is given in the Table (1.1) below.

Table 1.1 Major tanker spills of over 5,000 tones in the Region since 1974.
(source: www.itopf.com)

Quantity spilled	Vessel Name		Country	Year	Cause
	(tones)	(Type)			
NOVA	70,000	CRUDE	IRAN	1985	COLLISION
ASSIMI	52,500	CRUDE	OMAN	1983	FIRE/EXPLOSION
PERICLES GC	46,000	CRUDE	QATAR	1983	FIRE/EXPLOSION
SEKI	16,000	CRUDE	UAE	1994	COLLISION
PONTOON300	5,500	FUEL (CARGO)	UAE	1998	SINKING

In addition, it is estimated that 840,000 tones of oil entered the marine environment during the Gulf War in 1991(source: www.itopf.com). More recently there have been concerns about the number of illegal discharges from the large volume of shipping within the region and the frequency of oil spills resulting from sub-standard vessels which were illegally transporting oil from Iraq. Unofficial records show that nearly 26,000 tones of oil entered the marine environment from these illegal operations (source: www.itopf.com)

1.2 Problem Significance

In recent years, there has been a growing concern over the increasing contamination of water bodies and adjacent shoreline areas caused by oil spills. This concern is magnified in the Arabian Gulf where the surrounding countries produce and export more than 6 billion bbl of crude oil per annum to the world market via the Arabian Gulf waterway, the major transport route for the super tankers. Another incentive is the lack of fresh water resources in this dynamically developing region which has dictated the employment of desalination technology with mega plants along the Arabian Gulf shoreline. The Arabian Gulf coastal and marine environment is becoming increasingly important in fulfilling social and economic development and strategic objectives of its member states. Coastal uses and other human activities have strongly burdened the Gulf environment, with the extent and scale varying geographically. The Arabian Gulf is a naturally stressed environment. and at the same time has been subjected to unprecedented development pressures over the past two to three decades (Price & Shepperd, 1991); see figure 1.2.



Figure 1.2 Oil and gas fields in the Arabian Gulf

Being a coastal community, the related renewable and non-renewable resources remain the cornerstones for life and development in the Gulf States since they contribute to food, transport, industrial, recreational and other needs of local people.

The Gulf waters play a particularly vital role in providing most of the population with fresh water from desalination plants. The region's oil and gas are of course the major non-living resources, but increasingly important is clean sea water for desalination. During the Gulf war, substantial effort was directed at preventing oil from reaching the intakes of desalination plants. In July, 1997, diesel fuel spilled from a grounded barge in Sharjah, UAE entered the intake of a desalination plant, and contaminated the water supply of an estimated half million people.

In recent years there has been a growing concern over the increasing contamination of water bodies and adjacent shoreline areas by oil spills in general and in the Arabian Gulf in particular. Activities related to the oil industry, mainly oil exploration and transport in the region have increased the risk of oil spill accidents. Oil spillage into the marine environment represents a very complex situation to deal with as it is highly dependant on the sea state, and the type and the scale of spilled oil. From an environmental and health point of view, an oil spill accident is very harmful to the marine and the health of mankind. Despite the long-term damage to aquatic environment, a major oil spill will immediately cause contamination of the shoreline which causes malfunctioning of desalination plants, and foul harbor facilities and vessels.

To combat such accidents, many government agencies have prepared oil spill contingency plans. An important component of these plans is the use of mathematical models to predict the oil slick motion and distribution of oil particle concentration. Such models act as real time prediction tools during an oil spill incident when quick response is needed. The realization of the adverse effects of spilled oil in the water bodies has focused attention on the behavior of oil spills. Over the past few years, considerable research has been directed towards the development of such mathematical models to describe the behavior and fate of pollutants such as oil and oil products. This research has been motivated primarily by the practical consideration that the successful model would be of great value in ringing the warning bell for harbors, and power and desalination plants that may be affected. An efficient model would also help in selecting locations for the

deployment of the oil spill containment, collection and combat systems such as booming, dispersing and burning in order to mitigate the effects of the pollutant on the environment.

United Arab Emirates

Power and water are the most important sectors in the UAE after oil and gas. An increase of 7,000 MW in the power generation will be required over the next 10 years for the whole of the UAE. The investment on these sectors is estimated to be around \$30 billion over the next 5-10 years. There is currently a rapid rate of growth in the demand for water for Abu Dhabi and its surrounding regions. This increase is being driven by population growth, increasing consumption per capita and increasing requirement for water in irrigation. (source: www.trade.uktradeinvest.gov.uk/water/abu_dhabi/).

The total gross water produced from all desalination plants in the UAE, excluding the remote areas in 2001 was approximately 86,000 Million Imperial Gallons (MIG) of desalinated water. More recent figures of the desalination capacity are still higher and future scheduled expansions will follow. The Umm Al Nar desalination plant will increase its fresh water production capacity from 70 million gallons to 100 million gallons after its latest expansion, scheduled on the 1st of June 2005. The Al-Taweelah desalination plant produces 95 million gallons of fresh water per day, Al Marfa plant produces 38.7 million gallons per day, while Bainounah plant produces 15 million gallons per day (source: www.water-technology.net/projects/umm/). Also along the coast while facing northeast, the Jebel Ali Power and Desalination Station, serving Dubai State, has a total desalination capacity of 188 million gallons per day (source: www.dewa.gov.ae). All these huge plants are located along the coast, and are extending their intake terminals to pump-in saline water from the Gulf waters to the desalination plants.

The strategic dependence on desalination plants in the United Arab Emirates to secure fresh water is not a choice. Hence, strict measures to secure continuous supply of clean water to this industry is a very serious commitment that should be continuously fulfilled by protecting the intakes of the desalination plants from pollutants, namely the oil spill risk.

1.3 Objectives

The objectives of the research thesis are as follows:

- Setting up and calibrating the hydrodynamic numerical model for the Arabian Gulf region with special reference to the UAE coastal region using MIKE3 software.
- Setting-up and validating the oil spill model for the Arabian Gulf region based on the flow field produced from the hydrodynamic simulation.
- Evaluating the developed crises scenarios using the oil spill model, identifying critical scenarios, and evaluating the risk associated with oil spills on the intake points of selected desalination plants based on trajectory and arrival time.
- Developing risk alarm maps of arrival time based on the modeling results of spills initiated at locations (zones) adjacent to the UAE coast.

1.4 Methodology

- Literature review to survey the international and regional efforts made in hydrodynamics and oil spill modeling and types of models.
- Collect physical data; bathymetry, tide, wind, current, initial temperature and salinity fields.
- Set up of the numerical hydrodynamic model for the Arabian Gulf region.
- Tune the hydrodynamic model to simulate tidal fluctuation that resembles what is seen in Abu-Dhabi and Dubai harbors.
- Tune the current flow pattern to the general directions recovered from published available observations.
- Conduct sensitivity analysis on the oil spill model to identify critical parameters and their effect on model performance and conduct validation study for the spill analysis model based on published observations
- Set-up the numerical spill analysis model for the Arabian Gulf region and determine the spill analysis simulation inputs (e.g. amount released, mode of release, duration, wind condition, etc.)
- Divide the Arabian Gulf area adjacent to the UAE coast into several zones and apply oil spillage.

- Identify major desalination plants along the UAE coast as destination points of the impact assessment process.
- Evaluate simulation results and determine the arrival time of various scenarios.

CHAPTER 2

LITERATURE REVIEW

2.1 Arabian Gulf Hydrodynamic Characteristics and Modeling

The oceanic region comprised of the Gulf, Straits of Hormuz, and the Gulf of Oman is one of the most important waterways in the world. In peak periods, one ship passes the Strait of Hormuz every 6 min (Al-Hajri, 1990), and approximately 60 % of the world's marine transport of oil occurs at this region. Surprisingly, the number of direct oceanographic observations from this region is small. Investigations have been undertaken by individual countries in their coastal waters, but only two basin-wide studies are widely cited. Emery (1956) reported on a 1948 summer cruise by the German ship Meteor, and Brewer & Dyrssen (1985) reported on the 1976 wintertime expedition of the Atlantis from Woods Hole Oceanographic Institution. The primary reason for the unavailability of basin-wide data is the political unrest between the countries bordering the Gulf that prevents scientific access.

Among other studies, the Mt Mitchell expedition, launched on February 1992 preceding the second Gulf war, was named after the research vessel Mt Mitchell provided by the National Oceanic and Atmospheric Administration (NOAA) in an international program to study the effects of the oil spill that resulted from the hostility acts in the region. The cruise lasted from 26 February to 12 June 1992. Reynolds (1993) described the physical oceanography related findings of the Mt Michel expedition in the Gulf. The Mt Mitchell study was broad in scope and provided valuable information on areas of interest and gave a holistic description of the hydrodynamics of the Gulf.

In what follows, a description of the physical characteristics of the Arabian Gulf and its physical oceanography and meteorology are presented. The review has been collected from Grasshoff (1956), Hughes and Hunter (1979), Hunter (1982 a,b), Emery (1956), Evans-Roberts (1981), IMCOS (1981), Persian Gulf Pilot (1967), Sugden (1963), Lehr (1984), Reynolds (1993), Privett (1959), Elshorbagy et al. (2004a), Lardner et al. (1993), Sheppard (1993) and Spaulding et al. (1993).

2.2 Bathymetry

The Arabian Gulf is located between 24° and 30° latitude. The bathymetry of the Gulf as seen in figure 2.1 is shallow in the North-West and the Western coast which includes the Arabian States. Inter-tidal areas are extensive with very gradual slopes from the supra-littoral to several km offshore. In several areas, uplifted rocky areas (commonly reef) frequently add relief to a generally very level terrain (Sheppard, 1993). The broad region of shallow water off the coast of the United Arab Emirates features many small islands and lagoons. This area is a region of intense evaporation, and a significant contribution to the deep circulation of the Gulf is made there.

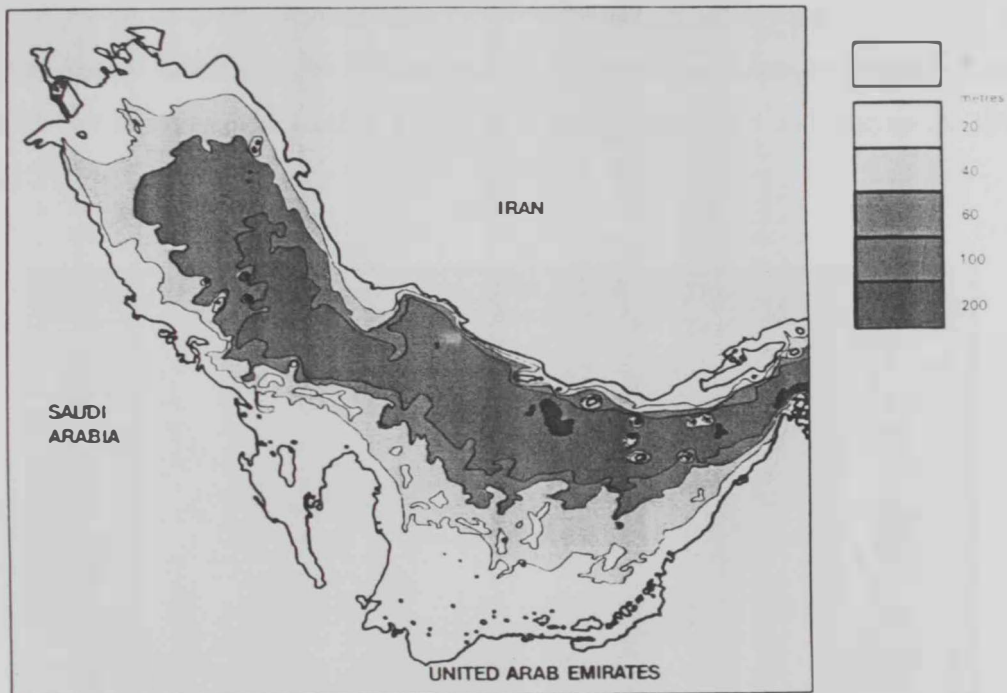


Figure 2.1 Arabian Gulf Bathymetry

An isolated trough extends Northward from the Strait of Hormuz along the Iranian coast approximately 100 km. The trough collects denser bottom water and interferes with existing bottom flow slowing it down. The slope of the Gulf floor is gentle leading to the deepest trough which is >100 m depth.

2.3 Fresh water exchange and evaporation

Most of the river inflow into the Arabian Gulf occurs at the north end of the Gulf primarily on the Iranian side

The Shatt Al-Arab is the collecting point for three major rivers: the Tigris and Euphrates rivers together provide an annual average of $708 \text{ m}^3 \text{ s}^{-1}$ and the Karun adds $748 \text{ m}^3 \text{ s}^{-1}$. Thus the total average outflow of Shatt Al Arab is $1456 \text{ m}^3 \text{ s}^{-1}$. Other major rivers are the Handijan with $203 \text{ m}^3 \text{ s}^{-1}$, the Hilleh $444 \text{ m}^3 \text{ s}^{-1}$, and the Mand $1387 \text{ m}^3 \text{ s}^{-1}$ (Reynolds, 1993). The total river runoff is $1.1 \times 10^{12} \text{ km}^3 \text{ yr}^{-1}$, equivalent to 46 cm yr^{-1} of depth. These values need to be verified due to the fact that the annual runoff from Shatt Al Arab has decreased substantially over the past 20 years after the construction of some huge dams along most of the rivers. Annual rainfall in the arid climate of the Gulf region has an insignificant role in the fresh water budget of the Gulf as it falls in the order of 7 cm yr^{-1} (Reynolds, 1993) see figure (2.2).

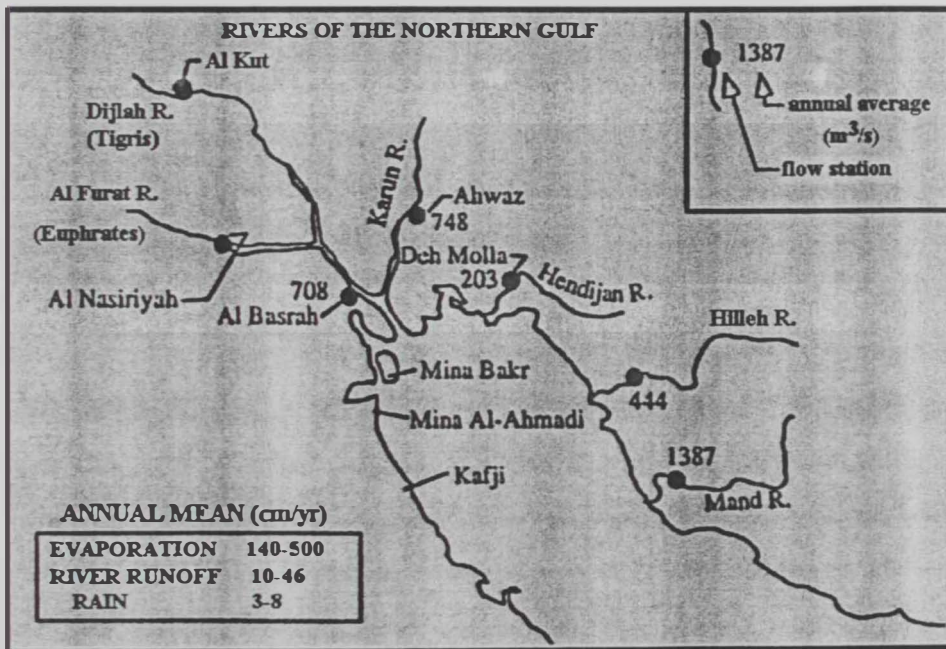


Figure 2.2 Rivers of the northern Gulf (Reynolds, 1993)

Evaporation in the Gulf is much higher than both rivers' inflow and precipitation. Estimates of evaporation vary from 500 to 144 cm yr^{-1} . The lower figure from Privett (1959) is in agreement with Meshal & Hassan (1986) who estimated 200 cm yr^{-1} . Measurements

indicate that even though the water temperature is considerably higher in summer, most evaporation occurs in wintertime. This is mainly referred to the higher wind speeds in the winter season. Evaporation of fresh water enhances mixing by increasing the salinity and density of the surface water thus reducing the surface stability

The Gulf has mild winters and very hot summers with temperatures ranging from 0 °C in winter to 45-50 °C in summer. Water temperatures increase from 18 °C in February to 30-33 °C in August. The shallow waters of the gulf are well mixed, while the deeper waters can have vertical temperature difference of 4 °C (Spaulding, 1993).

2.4 Wind

Being the most evident feature of the weather system, the winds in the Gulf are well recognized as the principal driving force of oil on the sea surface. The Gulf is located in the arid region between latitudes 24°-30°, in which the earth's deserts are mostly located. This region marks the boundary between tropical circulation and the relating weather systems of mid-latitudes. Descending dry air in these latitudes produces clear skies and arid conditions. In the north, the local climate is influenced by the mountainous nature of the surrounding topography. The Taurus and Pontic mountains of Turkey, the Caucasus Mountains in Iran, and Al-Higaz Mountains of the Arabian Peninsula together with the Tigris-Euphrates Valley, form a northwest-southeast axis that strongly tracks extra-tropical storms to a southeast direction.

The climate in the Gulf of Oman is markedly different from the climate in the Arabian Gulf. While the Gulf is affected mainly by the extra-tropical weather systems from the northwest, the Gulf of Oman is at the northern edge of the tropical weather system in the Arabian Sea and the Indian ocean. This monsoon circulation produces southerly winds in the summer and strong northerlies in the winter (Reynolds, 1993). The Straits of Hormuz approximates the boundary between the two systems.

The most well known and famous, weather phenomenon in the Gulf is the *Shamal* (meaning north in Arabic), which is a northwesterly wind which occurs year round during winter and summer. The winter Shamal is a wind that sets with great abruptness and force, and is related to relating weather system in the North West. It seldom exceeds 10 m s^{-1} but lasts several days. The summer Shamal is practically continuous from early June through

July and is associated with the relative strengths of the Indian and Arabian thermal lows. The winter Shamal brings some of the strongest winds and highest seas of the season. During the great Shamal, which occur during June and July, wind speeds can reach 15 m s^{-1} .

Generally, the Shamal winds come predominantly from the northwest throughout the year and display no seasonal reversal. At the lower end of the Gulf, the predominant winds come from the southwest during May through September and are called Suhaili. Sea breeze occurs within 30 km from the coast but generally have wind speeds of 5 m s^{-1} or less (Spaulding, 1993). Wind driven flows can be strong in the shallow waters of the western side of the Gulf including the UAE coastline. These flows are directed to the southeast, parallel to the coast in response to the northwesterly winds.

2.5 Currents

The water motion can be related to three driving forces: tidal forces, wind forces, and density differences. The kinetic energy of the water velocity can be partitioned among the three terms approximately as 100,10,1 respectively. Each type of currents has a different scaling time: tidal currents vary over few hours at diurnal or semi-diurnal periods; wind-driven currents develop a subsidence over a few days; and density driven currents take weeks to change in response to seasonal forcing (Reynolds, 1993).

The currents due to tidal motion in the Gulf are dominated by M_2 , S_2 , K_1 and O_1 constituents (Hydrographer of Navy, 1976). The resonance amplification of tidal current patterns are complex having an amphidromic point near either end for the semi-diurnal tide and one in the center for the diurnal tide. The tides rotate anti-clockwise around these points for all constituents. They vary from semi-diurnal to diurnal, and back to semi-diurnal as one moves from the lower to the upper Gulf (Figure 2.2) (Spaulding, 1993). Lehr, (1984), states that "The tidal range is large, with values larger than 1m everywhere". Tides are important in stirring and mixing waters vertically and on horizontal scale of 10 km, but they do not make an important contribution to the residual circulation of the Gulf. Tidal currents averaged over a day or more has negligible residual energy, and as a result, basin-scale advection from tides is not considered by oil trajectory models or general circulation models. Tides are important in smaller scales of horizontal length less than 10 km and time less than 24 hrs. The strong tidal currents also create a bottom turbulent friction layer.

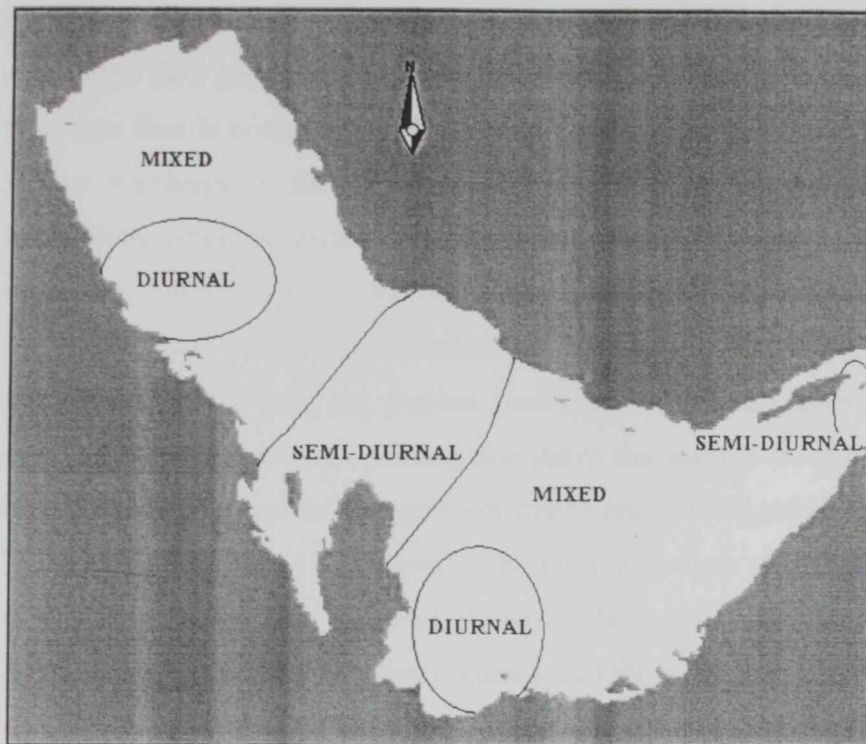


Figure 2.3 Classification of tides in the Arabian Gulf (adapted: Delft Hydraulics Lab. Report)

2.6 Residual Circulation

Residual currents are mainly responsible for the net transport of pollutants. The residual currents in the Gulf have been attributed to two principal factors: wind forcing which when coupled with Coriolis force, generates a net anti-clockwise circulation, and the effects of density gradients sustained by evaporation and radiative heat transfer and to a lesser extent by fresh water inflow at the north end of the Gulf. The relative importance of these two mechanisms has been the subject of a disagreement in the literature. Hughes & Hunter (1980) argued that the wind-driven currents made the major contribution, but Hunter subsequently concluded that the circulation was probably dominated by density-driven flow, geostrophically balanced across the Gulf and frictionally balanced in the direction of the flow. Galt et al. (1983) using depth average model agreed with this assessment in the southern half of the Gulf, but concluded that wind-driven circulation plus the effects of fresh-water inflow dominates the northern half.

Lardner et al.(1988a, b) and more recently Al-Rabeh et al. (1990) computed the vertical structure of the flow generated by the monthly averaged winds in the region. It was found that the surface flow is considerably stronger and more uniform in direction than the depth average flow. Furthermore, the magnitude of this surface current is consistent over most of the Gulf with the empirical values found by Hunter (1982) from analysis of ship-drift data. A subsequent simulation of surface and bottom currents at the Safaniya sea region (Al-Rabeh and Gunay, 1991), and drift of experimental buoy, (Henaidi, 1984). using actual wind measurements, (Cekirge et al. 1989), has yielded good agreement with observations. Thus there is a general agreement that wind forcing dominates the surface flow in the region adjacent to the Saudi coastline. The density-gradient effects are more significant at the lower half of the Gulf and near the Strait of Hormuz. The net fresh water to the atmosphere is replaced by a surface inflow in the Strait of Hormuz. Throughout the year and against prevailing Shamal winds, relatively low-salinity water enters through the Strait of Hormuz to freshen the hyper-saline water. High evaporation increases the density of the surface water so that it sinks to exit as a high-salinity under current. It was stated by Reynolds, 1993 that high evaporation in the broad coastal areas on the coast of the Emirates provides much of the saline bottom water that feeds the bottom outflow through the deeper portion of the Strait of Hormuz (Reynolds, 1993). Lardner and Das (1991) argued later that wind-driven currents dominate the whole Gulf except at the Strait of Hormuz and the vicinity of Shatt Al-Arab.

In a more recent study Elshorbagy et al.(2004b) stated that the effect of wind forcing is not observed very close to the Straits of Hormuz and that almost the entire northern and central portions of the Gulf shows southward current generated by the wind forcing with almost no visual effect from the density driving force. An important, secondary current in the Gulf is a coastal, reverse circulation along the Iranian coast which is mainly driven by the density differences that result from river runoff (Reynolds, 1993). In a simulation conducted by Lardner et al (1993), the circulation in the northern portion of the Gulf was described to comprise coastal jets directed towards the southeast on both the Saudi and the Iranian coasts, while in the central region the surface speeds are much smaller. This is consistent with the observed behavior of the drifter buoys released during the Mt Mitchell cruise which took place between February and June 1992 and reported to hardly move at all over the 3 month

period. Lardner et al, 1993 also reported in their simulation that the surface jet current along the Saudi coast continues around Qatar peninsula and joins the flow along the Emirates coast. It appears from this picture that the surface flow is generally dominated by wind forcing except at Shatt Al-Arab due to density changes from the river inflow and at the Straits of Hormuz which includes strong tidal currents and active density gradients mainly fed by the Emirates coast contribution of heavy saline water and along the Iranian coast as far as the Qatar peninsula.

It is concluded from the above review that, in a general view, the wind driven currents were found to be much dominant and larger than the combined effect of density and thermally driven currents (Al-Rabeh et al., 1992). It is also concluded that wind data is the principal parameter necessary for accurate spill forecasting.

The residence time for the Arabian Gulf basin has been studied by number of scientists (Hughes & Hunter, (1979); Hunter, (1983), Elshorbagy et. al., (2004). An estimate of 2-5 years was suggested by those studies. However, other field measurements by John and Olson, (1998) revealed that the mean outflow ranged between 350-500 days. The rate of exchange and the circulation in the Strait of Hormuz plays a key role in understanding the basin-wide behavior of the gulf.

2.7 Hydrodynamic and Oil Spill Modeling

2.7.1 Hydrodynamic Modeling Studies

Modeling efforts can be divided between tidal models and estuarine circulation models. Most of the early studies conducted on the physical processes of the Arabian Gulf (Al-Rabeh et al. 1990. Lardner & Das, 1991) focused on the mean flow characterization under extreme seasonal conditions. Such studies provide valuable information in the context of long-term understanding and implementation of environmental management issues. However in the cases of sudden environmental disasters like accidental oil spillage, tidal flow dynamics are crucially important. Real-time models are needed to forecast and report the pollutant movement in order to direct the mitigation efforts. Reynolds (1993) listed three comprehensive mathematical models that were available during the Mt Mitchell expedition and used for estuarine circulation modeling. The first was developed by the US Naval oceanographic Office (Horton et al., 1992) which they described as a three dimensional,

primitive-equation circulation model with complete thermodynamics and imbedded turbulent-closure sub-models. Next is the Catholic University of America model (Chao et al. 1992) that uses 20 km grid size and 11 levels in a diagnostic formulation. Lastly, King Fahad University of Petroleum and Minerals (KFUPM) in Al-Dahran, Saudi Arabia (Lardner et al. 1987; Lardner et al. 1988a, b; Lardner et al. 1991; Lardner et al. 1993), that covers the Gulf with a rectangular grid of 10 km size. It is three dimensional but has the option to be run in two-dimensional vertically integrated mode. The algorithm uses a mode-splitting method by which the depth-averaged equations are first solved for the barotropic mode, and then the momentum equations are stepped forward to compute the velocity profiles. The bottom friction and advective terms are computed for use in the average-depth equations on the next step.

In a more recent publication (Al-Rabeh et al. 2000), the team working in the KFUPM has launched a new software package for modeling the hydrodynamics for the Arabian Gulf and in arbitrary small sub-regions in the Gulf. GULFHYDRO Version 2.0 is a modification of the later software described by Reynolds, 1993 and has been released as a single package comprising of two models called HYDRO1 and HYDRO2. The main difference between the two models is the grid size, while HYDRO1 has a 10 km grid, while HYDRO2 has 5 km grid. HYDRO2 is designed to provide more detailed computation of flow in a selected sub-region of the Gulf using a fine grid size specified by the user. This property improvement in HYDRO2 gives the flexibility to the user to focus on the required study area, which was not available in other previous models. It is well understood that the higher resolution always comes on the expense of the CPU computational time and the storage requirements.

Other commercial packages are available for use, (MIKE3, DELFT3D). Such softwares are programmed to be user friendly with Windows interface and with exceptional statistical and graphical capabilities. However, more efforts, training in addition to more data are needed to allow using them professionally. For example, not as in the Arabian Gulf KFUPM models, the user of such commercial softwares needs to specify bathymetry and shoreline, physical characteristics, initial conditions, boundary conditions, environmental conditions, and tidal specifications for the simulation. Also, the need to tune the parameters and calibrate the model in a real condition status requires much understanding of the physical

meanings of the parameters and much effort to work with them. Also the need for the capability of judgment and optimization plays a key role.

2.7.2 Oil Spill Processes and Modeling

There is a vital need to understand and verify the oil spill performance in the marine environment of the Gulf in order to enable scientists and environmental response agencies to act efficiently in oil spill occasions.

The numerical modeling of oil spill weathering processes and trajectory is a very important component in this effort. It is receiving continuous development by scientists based on advances in understanding the nature and close interdependence among the weathering processes.

Spill models are divided into three major components: input, trajectory and fate algorithms, and output. The input modules are normally subdivided into two components: oil data and environmental data. The oil information defines the spill scenario to include oil type and physical-chemical properties, release schedule, location and start/end times. Definition of the wind, current, and temperature fields in space and time constitute the typical environmental typical parameters. This data can be derived from other models or field observations and in either case, accurate spill predictions require high quality environmental data that is carefully integrated into the spill model. The output module is normally a presentation of the spatial extent of the oil spill (eg. surface/subsurface oil) and the oil mass balance by the environmental compartments (eg. surface, atmosphere, subsurface. etc.) and components as a function of time.

The heart of oil spill models is a series of algorithms that represent the processes describing the transport and fate of oil released into the environment. The fate is most commonly described by the following processes: advection, spreading, evaporation, dispersion, dissolution, emulsification, photo-oxidation, biodegradation, sinking/sedimentation. Each of these algorithms is typically formulated on an individual basis with linkages made to relate processes and environmental parameters as necessary (Spaulding, 1988). However, since there is a significant lack of data for reliable analytical formulation to be established for many of the weathering processes, it is impractical to include all of them in an oil spill simulation model. It would be more useful to include the most significant

processes, i.e., those accounting for the bulk of the oil, while omitting others so that uncertainty in the outcome can be reduced (Shen et al., 1987).

In the following part a presentation of the development of each algorithm is provided.

Advection

Oil moves horizontally in the marine environment under forcing from wind, waves, and currents. Being itself a fluid with a density only slightly less than that of water, oil is also transported vertically in the water column in the form of droplets of various sizes. Both vertical and horizontal current shears are therefore important factors in the net motion of oil at sea. Current fields are generally considered to be the vectoral sum of wind, tidal, density, and pressure gradient induced currents. Of these various components, the wind-induced drift is often the most important factor determining surface oil slick trajectories over time scale greater than one day. The extremely simple empirical approach, which assumes that the surface drift current is approximately 3-4% of the wind velocity at 10m height above the water surface, has been used by most existing models and continues to be the most widely accepted methodology. A deflection angle of 20 degrees was suggested in the northern hemisphere (Stolzenbach et al., 1977). A deflection angle of 3 degrees and drift factor of 0.03 was used in the ASA model (Spaulding et al., 1992) which is based on experimentation in the Norwegian Sea (Reed et al., 1991). The drift deflection angle is due to the coriolis forcing and is directed to the right of the wind direction in the northern hemisphere and to the left in the southern hemisphere. Audunson et al., (1980) assumed a wind drift factor of 0.027 and a deflection angle of 12 degrees for the north sea. Samuels et al. (1982) suggest a variable deflection angle being a function of wind speed between 0 and 20 degrees.

Al-Rabeh et al. (1993) stated that "In modeling oil spill transport in the Gulf, oil spill models employing the wind-drift factor approach used values for the wind drift factor and deflection angle that were originally found suitable for other water bodies. This has resulted in poor prediction. Given the empirical nature of the approach it is necessary that suitable values for these critical parameters be derived for the Gulf". On the basis of least square method analysis of the motion of the MEPA buoys (Henaidi, 1984), it was found that the optimal values for the Arabian Gulf for these two parameters are: a drift factor of 0.031 and a deflection drift angle of 26.03 degrees (Al-Rabeh, 1994).

Spreading

Spreading determines the areal extent of spilled oil and effects the various weathering processes influenced by the surface area, including evaporation, dissolution, dispersion, and photo-oxidation. Spreading is normally considered to be controlled by the driving forces of gravity and surface tension and the retarding forces of inertia and viscosity. Various researchers have investigated this process and several methods are available for use in its modeling. Fay's (1969, 1971) three-regime spreading theory is the most widely used (Huang, 1983). Other methods include variations of Fay's spreading theory. In Mackay's algorithm, two expressions are used for the spreading of the thick slick and the total area of the thick and thin slicks (Mackay and Leinonen, 1977; Mackay et al., 1980a, b). For the thick slick, spreading consists of two parts, one a loss of area due to oil flowing from the thick to the thin slicks and the second corresponds to Fay's gravity-viscous phase of spreading (Fay, 1969, 1971).

Based on extensive research on spreading scenarios the following directions were made by Reed et al. (1999). For instantaneous spills, Fay-type spreading models may provide adequate predictions of the film thickness in the thick part of the slick, where the major fraction of the oil volume is found. Such models are appropriate at least during the early stages of release. For continuous spills in open sea conditions, where lateral spreading are dominant some distance down-stream from the source, one dimensional Fay spreading models seem to be more relevant than the radial spreading models used for instantaneous spills.

It was also stated that, theoretical and experimental studies of oil spreading from sub-sea blowouts were initiated in the early 80's (Fannelop and Sjoen, 1980; Milgram, 1983; Milgram and Burgess, 1984), and refinements of these models have continued up to the present (Swan and Moros, 1993; Rey and Brandvik, 1997; Zheng and Yapa, 1997). This recent work implies that predictions of the surface spreading may be made with acceptable accuracy for sub-sea blowouts from moderate water depths. However, for releases from greater depths more than 500 m, modifications based on buoyant plume theory should be considered. More recently, Chebbi, (2001) conducted analysis on the viscous-gravity stage of spreading using the integral boundary-layer method and found agreement of results with the

numerical solution for the unidirectional spread. His study extended in an attempt to develop a sound theoretical treatment for the axisymmetric spread geometry.

Evaporation

Estimates of evaporation losses are required in order to assess the lifetime of the spill. Evaporation typically accounts for 20-40% of spilled oil mass balance (Gundlach & Boehm, 1981) and is strongly influenced by spill area, slick thickness, oil vapor pressure, and mass transfer coefficient. Spill area is determined by spreading. While both vapor pressure and mass transfer coefficient depend on wind speed (Spaulding, 1988), Fingas (1997, 1999) argues that wind speed is not a relevant parameter. Vapor pressure changes as hydrocarbon fractions are lost into the atmosphere. The two methods currently in use to characterize evaporation rate are the pseudo-component approach and an analytical approach. In the pseudo-component approach, oil is characterized by a set of hydrocarbon components grouped by molecular weight (Spaulding et al. 1982a) or by boiling point fraction (Payne et al. 1984b). This allows different fractions of the oil to evaporate at different rates and the density of the slick to change as a function of time.

The analytic approach describes vapor pressure as a function of temperature and amount evaporated (Mackay et al. 1980a). Both approaches use a similar mass transfer concept, expressing the mass transfer coefficient as a function of wind speed, vapor pressure, spill size and temperature. Payne et al. (1984a) described oil composition in terms of both specific components and pseudo-components. This approach permits calculation of both the remaining oil mass and its chemical composition and physical properties.

Jones (1997) has modified this method by introducing an empirical relation between molar volumes and boiling point, based on data for n-alkanes. In this way the pseudo-component model maybe used in spite of the common lack of the data on specific gravity of the boiling point cuts. More recently, Fingas (1997, 1999) has proposed a simple empirical method derived from small-scale pan evaporation experiments.

The pseudo-component method proposed by Spaulding et al. (1982a) and the later by Payne et al. (1984b) seems to be the most reliable and flexible of the discussed methods. However the computational intensity and the high data requirements of the method may still justify a search for simpler methods.

Dissolution

Dissolution is most active shortly after a spill and affects some of the same hydrocarbon fractions as evaporation. However dissolution accounts for much less oil loss than evaporation and is generally two or more orders of magnitude smaller (Harrison et al. 1975) although exact measurements are difficult to obtain, even in the laboratory. Other modeling approaches depend on combining the dissolution to other processes such as evaporation (Williams et al. 1975). Also combining dissolution to dispersion (Spaulding et al. 1982a) approach is taken because of the difficulty to distinguish between dissolution and dispersion in the field while together are expected to account for about 1 to 10% of the mass of an oil spill (Mackay et al. 1980b). Payne et al. (1984b) model dissolution is in much the same way as evaporation with a components approach.

Dispersion

Natural dispersion computation is required for the assessment of the life time of an oil spill. The rate of natural dispersion of oil droplets in the water column depends on the sea state, but is also influenced by the oil related parameters, such as oil film thickness and oil properties (density, surface tension and viscosity). Emulsification will contribute significantly to the persistence of oil spills, mainly due to sharp increase in viscosity and the increase in slick thickness with water content which leads to retarding the spreading, increase in volume and hence reduce the natural vertical dispersion of oil droplets in the water column.

The simplest and most primitive approach applied in estimating the dispersion uses tabulations of dispersion as a function of the sea state (temperature, wind, waves, etc...) and time after the spill. Otherwise, loss of oil from the surface slick due to natural dispersion can be computed by equations originally proposed by Mackay et al. (1980a,b). This approach formulates a two stage dispersion process. The equations describing this process treat dispersion from thin and thick slick separately, agree qualitatively with observed behavior.

In some models (Payne et al. 1987; Reed et al. 1989c), only the thick portion of the slick is considered. By neglecting transfer of oil from the thick to the thin portion of the slick, these models may underestimate the overall dispersion rate (Reed et al. 1999).

Delvigne and Sweeney (1988) conducted investigations of natural dispersion of surface oil due to breaking waves in a small laboratory flume and in a larger test basin. On

this basis, an empirical relation was derived for the entrainment rate (dispersed mass per unit area) as a function of oil type and breaking energy. This method is the most common in use today (Reed et al., 1999).

Emulsification

Water droplets are dispersed into the oil, forming what is called 'chocolate mousse', a blend of oil and sea water brown to orange in color of increased viscosity and volume. The process of its formation is termed emulsification (Spaulding, 1988). Emulsification is computed with an implicit algorithm originally proposed by Mackay et al. (1980a, b). Prediction of emulsification and the associated viscosity changes relies on these empirical observations (Reed et al. 1999).

The algorithm contains two parameters, defining the water uptake and the maximum water content. Both parameters may be derived from laboratory experiments, but the parameter for the water uptake rate must in some way be scaled to field conditions and different sea states (Reed et al. 1999). Experimental studies of emulsification for different crude oils have revealed that both the water uptake and maximum water content vary significantly from one crude to another, and these parameters are also influenced by the state of weathering of the oils (Daling and Brandvik, 1988). The mechanism by which this process occurs is not well understood although it has been determined that turbulence, oil composition and temperature are important.

In general, the maximum water content tends to decrease with the viscosity of the parent oil. The differences in the water uptake rate might be related to chemical make-up of the oil (i.e. the content of resins, waxes and asphaltenes). Emulsion stability is a measure of the decrease in the water content of an emulsion when kept in stagnant conditions. Meso-stable emulsions will lose some water when kept at rest for 24 hrs., while unstable emulsions will lose practically all the water when kept at rest for the same period. Another important observation is that while the apparent viscosity of stable emulsion may be two to three order of magnitudes larger than the viscosity of the parent oil, the apparent viscosities of unstable emulsions are typically no more than one order of magnitude greater than that of the parent oil (Reed et al. 1999).

Biodegradation

A long term process that continues for years after the spill occurs, and is affected by a variety of organisms. No mathematical models have been developed to describe the crude oil biodegradation in the marine environment, although a group of studies have been undertaken on the characteristics of petroleum degrading micro-organisms (ZoBell, 1973; Horowitz and Atlas, 1977, Atlas, 1981). The results of the controlled lab experiments are not always applicable to the real marine conditions due to the complexity of the process.

Photo-oxidation:

It is the process by which oil, with energy from sunlight, undergoes oxidation, and polar, water soluble, oxygenated products are generated (Payne and Philips, 1985a, b). This process is unimportant in the first few days of the spill but may be noticeable after a week or more (Spaulding, 1988). A conceptual expression for its rate have been used by Kolpak et al. (1977) based on extrapolation of laboratory results to open ocean slicks but the approach remains unverified.

2.8 Types of oil:

Various types of oil act differently when spilled in the open sea. Due to different physical properties (e.g. viscosity, volatility, toxicity) and the ambient surrounding conditions (e.g. wind, temperature, sea state) the extent of oil movement and degree of weathering differs and hence the expected harm to the environment and cleanup expense differ. Table 2.1 shows the types of oil along with their impact and how each type can affect the shoreline in oil spill incidents, remedies and cleanup are also mentioned.

Table 2.1 Different types of oil and their estimated impact

(source: www.response.restoration.noaa.gov)

Type	Impact
Type1: Very Light Oils (Jet Fuels, Gasoline)	<ul style="list-style-type: none"> - Highly volatile (should evaporate within 1-2 days) - High concentration of toxic (soluble compounds) - Localized, severe impacts to water column and inter-tidal resources. - No cleanup possible
Type2: Light Oils (Diesel, No.2 Fuel Oil, Light Crudes)	<ul style="list-style-type: none"> - Moderately volatile; will leave residue (up to one third of the spill amount) after a few days - Will oil inter-tidal resources with long-term contamination potential. - Cleanup can be very effective
Type3: Medium Oils (Most Crude Oils)	<ul style="list-style-type: none"> - About one third will evaporate within 24 hours - Oil contamination of inter-tidal areas can be severe and long-term - Oil impacts to waterfowl and fur-bearing mammals can be severe - Cleanup most effective if conducted quickly
Type 4: Heavy Oils (Heavy Crude Oils)	<ul style="list-style-type: none"> - Heavy oils with little or no evaporation or dissolution - Heavy contamination of inter-tidal areas likely - Severe impacts to waterfowl and fur-bearing mammals - Long-term contamination of sediments possible - Weathers very slowly - Shoreline cleanup very difficult

2.9 Oil Spills in the UAE

The documented history presented in the “ROPME Oil Spill Incidents report, 1965-2002” counts over 140 cases of oil spilling in the ROPME sea area. The UAE waters received 15 incidents. The main reason is being the substandard ships, vessels, and tankers carrying crude and refined oil products loaded in the UAE or just passing in their way out of the Gulf. It is clearly understood that oil spill incidents are an across-border phenomenon that could take place in one location while its negative impacts would travel to reach far locations in other countries. Figure (3.4) represents rough locations of oil incidents in the region adjacent to the UAE coast. Table (2.2) states the incidents of oil spills in the UAE.

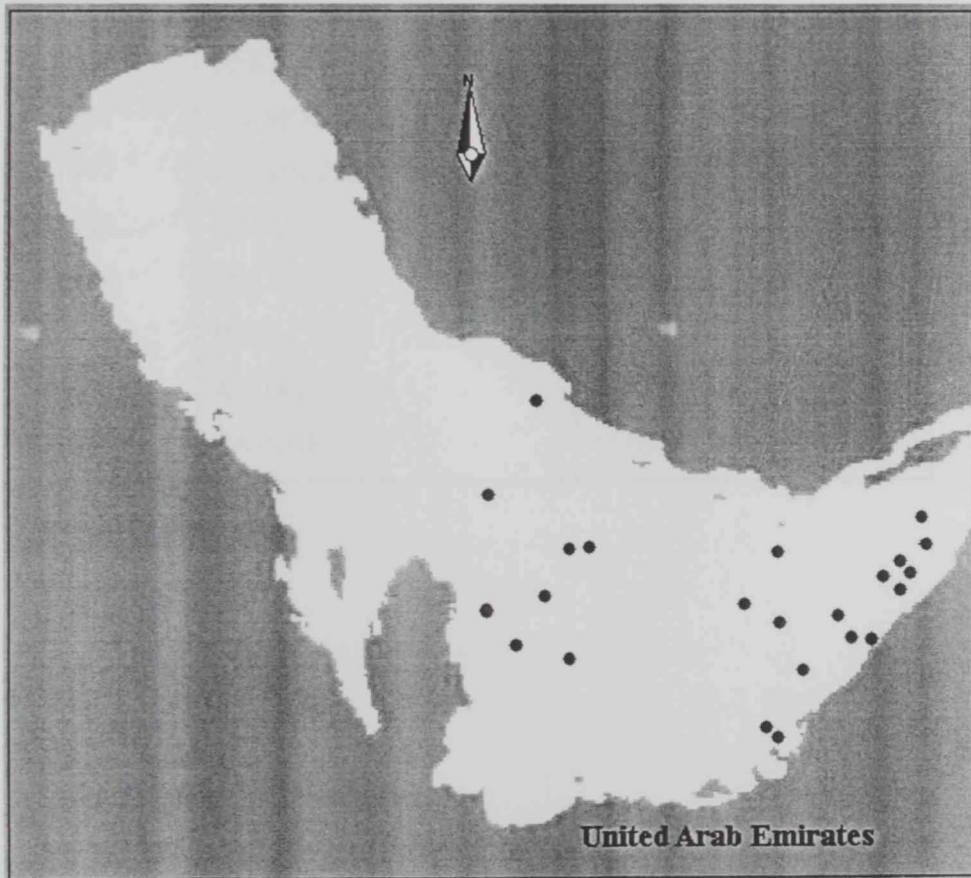


Figure 2.4 Rough locations of oil incidents in the Gulf region adjacent to the UAE Coast.
(Adopted from the MEMAC-ROPME report-2003)

Table 2.2 Oil spills in the UAE (adopted from the MEMAC-ROPME report-2003)

YEAR	NAME	AMOUNT SPILLED (US GALLONS)
1984	QARNINA	7353
1986	AKARITA	0
1987	TEXACO CARIBBEAN	2283470
1987	AKARI	UNKNOWN
1988	HAPPY KARI	UNKNOWN
1988	KARAME MAERSK	1180000
1989	TROPICAL LION	420168
1994	SEKI	4705882
1997	GMMOS-II	617647
1997	ZAPPA 225	1470000
1998	LB 300	1764706
1998	MILAD-I	MINOR
1999	INES	10200
2000	AL JAZIYAH	88235
2000	ZAINAB	411600

CHAPTER 3

MIKE3 HYDRODYNAMIC FLOW MODEL

MIKE3, a 3D modeling software package (educational version) produced by the DHI WATER & ENVIRONMENT -Denmark- was selected for the present study. It is a user-friendly, fully dynamic, 3D modeling system that uses Cartesian (rectilinear) grids. The following section describes the technical information of the hydrodynamic module MIKE3 HD of the software. Major parts of this description are adopted from the software manual (MIKE3 User guide Documentation)

3.1 General Description of Modules

MIKE3 simulates unsteady flow with sigma layer system taking into account density variations, bathymetry and external forcing such as meteorology, tidal elevations, currents and other hydrographic conditions. The hydrodynamic model is dynamically coupled with the temperature and salinity modules, which are resolved by advection-dispersion processes.

The hydrodynamic module (HD) is the core of the MIKE 3 modeling system. It provides the hydrodynamic basis for computations performed in other modules, namely the spill analysis module. The spill analysis module (SA) will be discussed in much detail in the next chapter.

MIKE 3/HD solves the time-dependent classical conservation equations of mass and momentum in three dimensions, the so-called Reynolds-averaged Navier-Stokes equations, where the flow is decomposed into mean quantities and turbulent fluctuations.

The flow field and pressure variation are computed in response to a variety of forcing functions, when provided with the bathymetry, bed resistance, wind field, hydrographic boundary conditions.

The closure problem is solved in the turbulence module through the Boussinesq eddy viscosity concept relating the Reynold stresses to the mean velocity field. To handle density variations, the equations for conservation of salinity and temperature are included and solved in the transport equation module. An equation of state constitutes the relation

between the density and the variations in salinity and temperature. Thus, the turbulence module and the transport equation module are integrated components of the hydrodynamic module, and the suite of those three constitutes the HD module.

3.1.1 Conservation Equations of Mass and Momentum

The governing continuity and momentum equations are as follows (Chao et al.,2000).

Continuity equation:

$$\frac{\partial U}{\partial x} + \frac{\partial V}{\partial y} + \frac{\partial W}{\partial z} = 0 \quad (3.1)$$

Momentum equation in x-direction:

$$\frac{\partial U}{\partial t} + U \frac{\partial U}{\partial x} + V \frac{\partial U}{\partial y} + W \frac{\partial U}{\partial z} = -\frac{1}{\rho} \frac{\partial P}{\partial x} + \frac{\partial}{\partial x} (v_h \frac{\partial U}{\partial x}) + \frac{\partial}{\partial y} (v_h \frac{\partial U}{\partial y}) + \frac{1}{\rho} \frac{\partial (\tau_x)}{\partial z} + \Omega V \quad (3.2)$$

Momentum equation in y-direction:

$$\frac{\partial V}{\partial t} + U \frac{\partial V}{\partial x} + V \frac{\partial V}{\partial y} + W \frac{\partial V}{\partial z} = -\frac{1}{\rho} \frac{\partial P}{\partial x} + \frac{\partial}{\partial x} (v_h \frac{\partial V}{\partial x}) + \frac{\partial}{\partial y} (v_h \frac{\partial V}{\partial y}) + \frac{1}{\rho} \frac{\partial (\tau_x)}{\partial z} + \Omega V \quad (3.3)$$

Hydrostatic pressure equation:

$$\frac{\partial P}{\partial z} + \rho g = 0 \quad (3.4)$$

where U , V and W are time-averaged velocity components in the longitudinal (x), Lateral (y), and vertical (z) directions, respectively; t is the time; ρ is the density of water; P is the time averaged pressure; g is the gravitational acceleration; v_h is the coefficient of horizontal eddy viscosity; τ_x and τ_y are the horizontal shear stresses resulting from vertical turbulent momentum transport; Ω is the coriolis parameter, $\Omega = 2\omega \sin \phi$, where ω is the angular speed of the Earth's rotation and ϕ is the geographical latitude.

The vertical axis is represented by σ -layers that divide the water column in parallel layers. The momentum balance in the vertical direction is introduced into the model by equating the pressure gradient with hydrostatic pressure.

Often estuarine and coastal hydraulics and oceanography imply variations in the density due to varying salinities and temperatures. As even small differences in density may have a decisive influence on the flow properties this is an important part of MIKE 3.

3.1.2 Advection-Dispersion Schemes:

MIKE 3 includes four advection-dispersion schemes:

- QUICKEST/SHARP, is especially suitable for simulations with steep density gradients. It is a fully three-dimensional scheme
- QUICKEST/ULTIMATE scheme with directional splitting.
- SIMPLE UPWIND scheme using directional splitting
- 3D UPWIND scheme.

The schemes applying directional splitting, i.e. QUICKEST/ULTIMATE and simple UPWIND, have a build-in internal loop over components which increase the computational speed when both salinity and temperature variations have been selected. For the fully 3D schemes, i.e. QUICKEST/SHARP and 3D UPWIND, the internal loop over components may optionally be selected to increase computational speed at the expense of requiring more memory.

In this study the SIMPLE UPWIND scheme is selected based upon the fact of regular density gradients in the Arabian Gulf and optimal computational speed and memory requirement.

The description of initial and open boundary conditions as well as proper choices of dispersion factors are very important tasks during the model calibration process.

The transport equation for salt is formulated as:

$$\frac{1}{\rho} \frac{D(\rho S)}{D_t} = \frac{\partial}{\partial x_j} \left(\frac{v_T}{\sigma_T} \frac{\partial S}{\partial x_j} \right) \quad (3.5)$$

and similarly, the transport equation for temperature is

$$\frac{1}{\rho} \frac{D(\rho T)}{D_t} = \frac{\partial}{\partial x_j} \left(\frac{v_T}{\sigma_T} \frac{\partial T}{\partial x_j} \right) + \frac{1}{\rho} Q_H \quad (3.6)$$

Where S is the salinity and T is the temperature, and Q_H is the Heat Exchange (for simplicity SS , the source/sink term for the respective equation, is not displayed in the above equations). The dispersion of salinity and temperature is assumed to be proportional to the effective Eddy Viscosity with the factor of proportionality being $1/\sigma_T$, the dispersion factor. σ_T is the Prandtl/Schmidt number. Values of σ_T greater than one imply that diffusive transport is weaker for salt/temperature than for momentum.

3.1.3 Turbulence Closure Module

The turbulence is modeled in terms of an Eddy Viscosity and a bed shear stress. The turbulent fluctuations (Reynolds stresses) are modeled employing the Boussinesq eddy viscosity concept. In MIKE 3 the eddy viscosity (turbulent closures) can be specified as one of five different models, These are:

- constant eddy viscosity
- Smagorinsky sub-grid scale model
- k -model
- k - ϵ model
- mixed Smagorinsky/ k - ϵ model

The following is the k - ϵ turbulence model description used in the study:

To eliminate the shortcomings of the k -model, the length scale specification inherent in this model can be replaced by a transport equation for a turbulent quantity. The most extensively used quantity is the isotropic energy dissipation rate, ϵ

$$\epsilon = c_D \frac{k^{3/2}}{l} \quad (3.7)$$

which combined with the Kolmogorov-Prandtl expression leads to

$$v_T = c_\mu \frac{k^2}{\epsilon} \quad (3.8)$$

c_μ is an empirical constant to be determined from experiments. The k - ϵ turbulence closure, which has been implemented in MIKE 3, is the one suggested by Rodi (1980),

$$\frac{\partial k}{\partial t} + u_i \frac{\partial k}{\partial x_i} = \frac{\partial}{\partial x_i} \left(\frac{v_T}{\sigma_k} \frac{\partial k}{\partial x_i} \right) + v_T \left(\frac{\partial u_i}{\partial x_j} \frac{\partial u_j}{\partial x_i} \right) \frac{\partial u_i}{\partial x_j} + \beta g_i \frac{v_T}{\sigma_T} \frac{\partial \phi}{\partial x_i} - \epsilon \quad (3.9)$$

$$\frac{\partial \epsilon}{\partial t} + u_i \frac{\partial \epsilon}{\partial x_i} = \frac{\partial}{\partial x_i} \left(\frac{v_T}{\sigma_\epsilon} \frac{\partial \epsilon}{\partial x_i} \right) + c_{1\epsilon} \frac{\epsilon}{k} \left(v_T \left(\frac{\partial u_i}{\partial x_j} \frac{\partial u_j}{\partial x_i} \right) \frac{\partial u_i}{\partial x_j} + c_{3\epsilon} \beta g_i \frac{v_T}{\sigma_T} \frac{\partial \phi}{\partial x_i} \right) - c_{2\epsilon} \frac{\epsilon^2}{k}$$

where $C_{1\epsilon}$, $C_{2\epsilon}$, $C_{3\epsilon}$, σ_k , σ_ϵ and σ_T are empirical constants. β is the volumetric expansion coefficient and f is the buoyancy scalar quantity.

3.1.4 Heat Flux Module

The heat exchange module is used for simulation of heat transfer between the water body and the atmosphere.

The heat exchange is calculated on basis of the four physical processes:

- sensible heat flux (or the heat flux due to Convection)
- latent heat flux (or the heat loss due to Vaporization)
- net Short Wave Radiation
- net Long Wave Radiation

Each process is further described here

Convection

The sensible heat flux, q_c (or the heat flux due to convection) depends on the type of boundary layer between the sea surface and the atmosphere. Generally this boundary layer is turbulent implying the following relationship

$$q_c = \begin{cases} \rho_{air} C_{air} C_c W_{10m} (T_{water} - T_{air}) & \text{for } T_{air} > T_{water} \\ \rho_{air} C_{air} C_c W_{10m} (T_{water} - T_{air}) & \text{for } T_{air} \leq T_{water} \end{cases} \quad (3.10)$$

where

ρ_{air} is the air density (kg/m^3)

C_{air} is the specific heat of air, $1007 \text{ J (kg} \cdot \text{°K)}$

C_w is the specific heat of water, $4186 \text{ J (kg} \cdot \text{°K)}$

W_{10m} is the wind speed 10 m above the sea surface

T_w is the absolute temperature of the sea

T_{air} is the absolute temperature of the air

C_c is the sensible transfer coefficient, given as $1.41 \cdot 10^{-3}$

The convective heat flux typically varies between $0 - 100 \text{ W/m}^2$.

Vaporization

Dalton's law yields the following relationship for the vaporization heat loss (or latent flux):

$$q_v = LC_e (a_1 + b_1 W_{2m}) (Q_{water} - Q_{air}) \quad (3.11)$$

where

L is the latent heat of vaporisation, $2.5 \cdot 10^6 \text{ J/kg}$

C_e is the moisture coefficient, $1.32 \cdot 10^{-3}$

W_{2m} is the wind speed 2 m above the sea surface

Q_{water} is the water vapour density close to the surface

Q_{air} is the water vapor density in the atmosphere constant in Dalton's law. (a_1), and the wind coefficient in Dalton's law (b_1) are user specified coefficients, a_1 is dimensionless and b_1 is in s/m

Sensitivity analysis of a_1 , and b_1 has yielded the following values to give the best agreement with Al-Rabeh et al., 1993 average flow pattern using average June wind.

$$a_1 = 0.5$$

$$b_1 = 0.9 \text{ s m}$$

Short Wave Radiation

Radiation from the sun consists of electromagnetic waves with wave lengths varying from 1,000 to 30,000 Å. Most of this is absorbed in the ozone layer, leaving only a fraction of the energy to reach the surface of the Earth. Furthermore the spectrum changes when sunrays pass through the atmosphere. Most of the infrared and ultraviolet compound is absorbed such that the solar radiation on the Earth mainly consists of light with wave lengths between 4,000 and 9,000 Å. This radiation is normally termed short wave radiation. The intensity depends on the distance to the sun, declination angle and latitude, extraterrestrial radiation and the cloudiness and amount of water vapor in the atmosphere.

Distance between the Earth and the Sun

The ratio between the mean distance, r_0 to the Sun and the actual distance, r is given by

$$E_o = \left(\frac{r_o}{r} \right)^2 = 1.000110 + 0.034221 \cos(\Gamma) + 0.001280 \sin(\Gamma) + 0.000719 \cos(2\Gamma) + 0.000077 \sin(2\Gamma) \quad (3.12)$$

in which Γ is defined by

$$\Gamma = \frac{2\pi(d_n - 1)}{365} \quad (3.13)$$

and d_n is the Julian day of the year.

Solar Declination and Day Length

The daily rotation of the Earth around the polar axes contributes to changes in the solar radiation. The seasonal radiation is governed by the declination angle, which can be expressed by

$$\begin{aligned} \delta = & 0.006918 - 0.399912 \cos(\Gamma) + 0.07257 \sin(\Gamma) \\ & - 0.006758 \cos(2\Gamma) + 0.000907 \sin(2\Gamma) \\ & - 0.002697 \cos(3\Gamma) + 0.00148 \sin(3\Gamma) \end{aligned} \quad (3.14)$$

The day length, N_d varies with d . For a given latitude (positive on the northern hemisphere) the day length is given by

$$N_d = \frac{24}{\pi} \arccos\{-\tan(\phi)\tan(\delta)\} \quad (3.15)$$

and the sunrise angle, ω_{sr} is

$$\omega_{sr} = \arccos\{-\tan(\phi)\tan(\delta)\} \quad (3.16)$$

Extraterrestrial Radiation

The intensity of short wave radiation on the surface parallel to the surface of the Earth changes with the angle of incident. The highest intensity is in zenith and the lowest during sunrise and sunset. Integrated over one day the extraterrestrial intensity in short wave radiation on the surface can be derived as

$$H_o = \frac{24}{\pi} q_{sc} E_o \cos(\phi) \cos(\delta) (\sin(\omega_{sr}) - \omega_{sr} \cos(\omega_{sr})) \quad (3.17)$$

where q_{sc} is a solar constant.

Radiation under cloudy skies

For determination of daily radiation under cloudy skies, H , the following relation is used

$$\begin{aligned}\frac{H}{H_0} &= a_2 + b_2 \frac{n}{N_d} \\ a_2 &= 0.1 + 0.24 \frac{\bar{n}}{\bar{N}_d} \\ b_2 &= 0.38 + 0.08 \frac{\bar{N}_d}{\bar{n}}\end{aligned}\tag{3.18}$$

in which n is the number of bright sunshine hours, N_d the length of the day. The over-bars refer to the mean annual values.

The constants a_2 , b_2 known as sun constants in Angstrom's law are required as inputs in the heat flux module to count for the cloudiness effect on short wave radiation.

Based on the local Arabian Gulf day conditions, an average number of bright sunshine hours (n) = 12 hours, and an average length of the day (N_d) = 14 hours. The following values were obtained from the above formulation for a_2 , b_2 are used with the heat flux module. $a_2 = 0.305$, $b_2 = 0.473$

Beer's Law

The attenuation of the light intensity is described through the modified Beer's law as:

$$I(d) = (1 - \beta) I_0 e^{-kd}\tag{3.19}$$

where

$I(d)$ is the intensity at depth d below the surface

I_0 is the intensity just below the water surface

β is a quantity that takes into account that a fraction of the light energy (the infrared) is absorbed near the surface

λ is the light extinction coefficient

Typical values for β and λ are 0.2-0.6 and 0.5-1.4 m^{-1} , respectively. Typical default values for $\beta = 0.3$, and $\lambda = 1$ were used respectively.

For the short wave and long wave calculations the relative humidity and cloudiness are to be specified in the heat flux module. Elshorbagy et al., (2004) used values for the relative humidity to be 53% in summer and 60% in winter, and clearness coefficient of 65% for the Arabian Gulf.

Long Wave Radiation

A body or a surface emits electromagnetic energy at all wavelengths of the spectrum. The long wave radiation consists of waves with wavelengths between 9,000 and 25,000 Å. The radiation in this interval is termed infrared radiation and is emitted from the atmosphere and the sea surface. The long wave remittance from the surface to the atmosphere minus the long wave radiation from the atmosphere to the sea surface is called the net long wave radiation and is dependent on the cloudiness, air temperature, vapor pressure in the air and relative humidity. In MIKE 3 the net outgoing long wave radiation is given by

$$q_{lr,net} = \sigma_{sb} T_{air}^4 (a - b\sqrt{e_d}) \left(c + d \frac{n}{n_d} \right) \quad (3.20)$$

where a, b, c and d are coefficients given as:

$$a = 0.56; b = 0.77 \text{ mb}^{-1/2}; c = 0.10; d = .90$$

e_d is the vapor pressure at dew point temperature measured in mb

n is the number of sunshine hours

N_d is the number of possible sunshine hours

σ_{sb} is Stefan Boltzman's given as $5.6697 \cdot 10^{-8} \text{ W}/(\text{m}^2 \cdot \text{K}^4)$

T_{air} is the air temperature

3.2 HD Module Data and Setup

3.2.1 Bathymetry

Using the bathymetry editor of MIKE 3, the bathymetry of the study area was constructed to the MIKE 3 format by using digital format data published in the NOAA final report of the Mt-Mitchell cruise in the Arabian Gulf which took place during February-May 1992. Figure (3.1) shows the water depths of the Arabian Gulf.

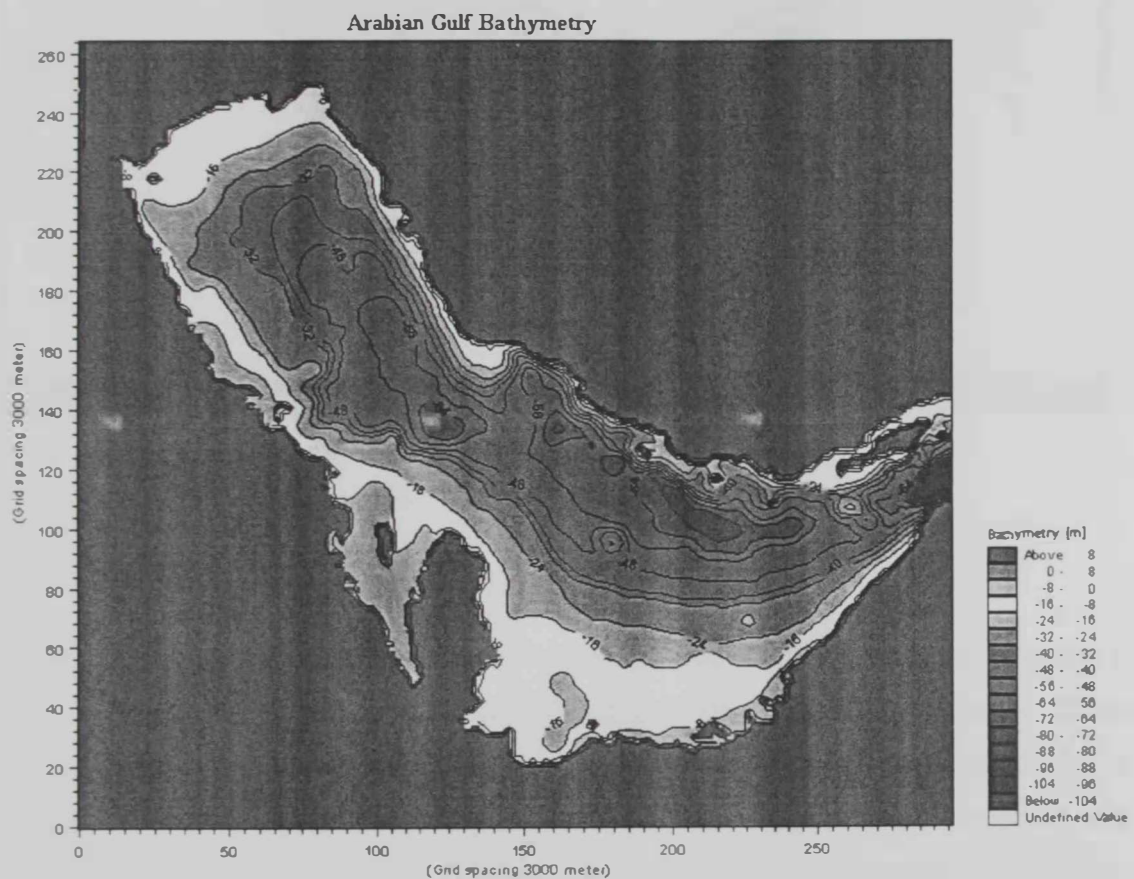


Figure 3.1 Arabian Gulf Bathymetry

3.2.2 Grid Generation for Hydrodynamics

Using the Bathymetry Editor of the MIKE3 software, a Cartesian (rectilinear) grid of 3 km spacing was adopted over the entire region of study (Fig. 3.2). This relatively high modeling resolution enables the possibility of investigating details of coastline flow.

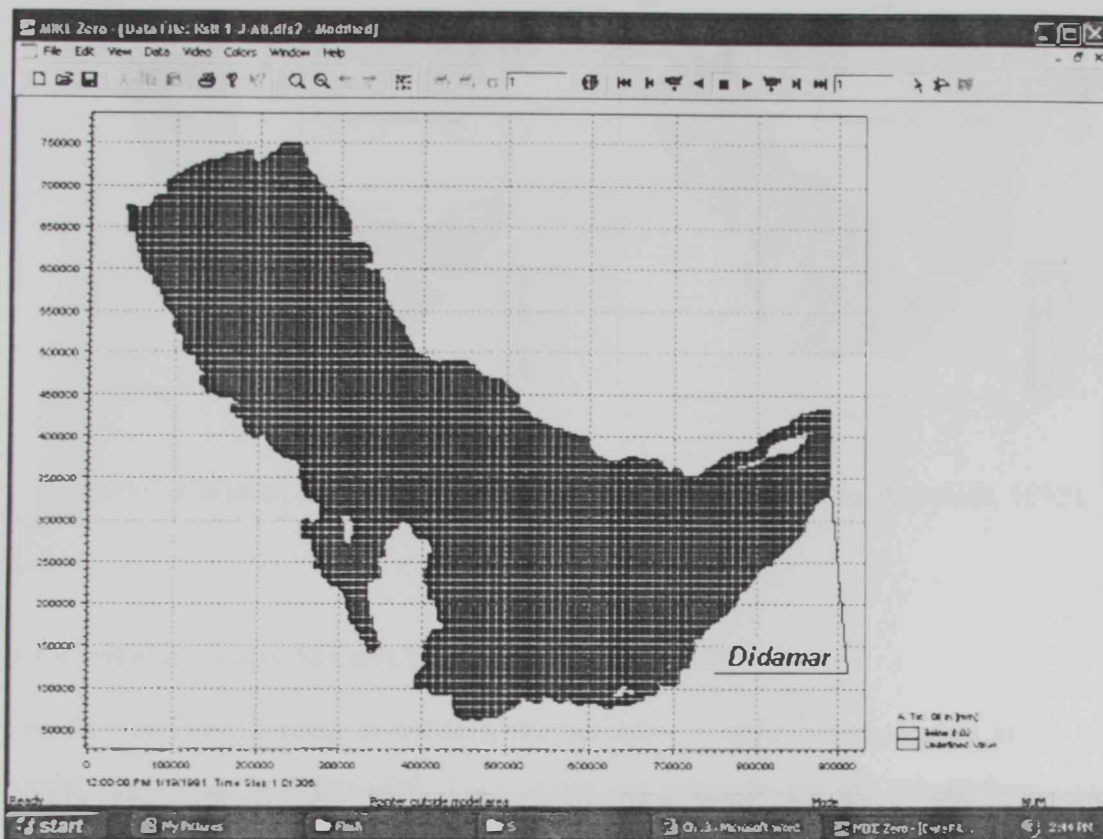


Figure 3.2 Computational Grid

3.2.3 Initial Salt and Temperature Fields

Prior to starting of the simulation, MIKE 3 requires knowledge of the initial salinity/temperature distribution. MIKE3 Type3 (3D) data files are prepared for initial salinity and temperature using the digitizing tool in MIKE3 to couple the Gulf bathymetry with the data. The end product is a 3D file describing the properties in a vertical system of 5 layers of 20 m depth each. Salinity and temperature fields were produced for both winter and summer according to the available data. The data used for salinity and temperature are published in the final NOAA report on the Mt-Mitchell cruise in the Gulf during the February-May 1992. Furthermore, the dispersion was considered to be proportional to the velocity, and dispersion factors were taken equal to $0.01\text{m}^2/\text{s}$ in the horizontal and vertical directions, and were found to satisfy the computational stability requirements set forth in the software manual.

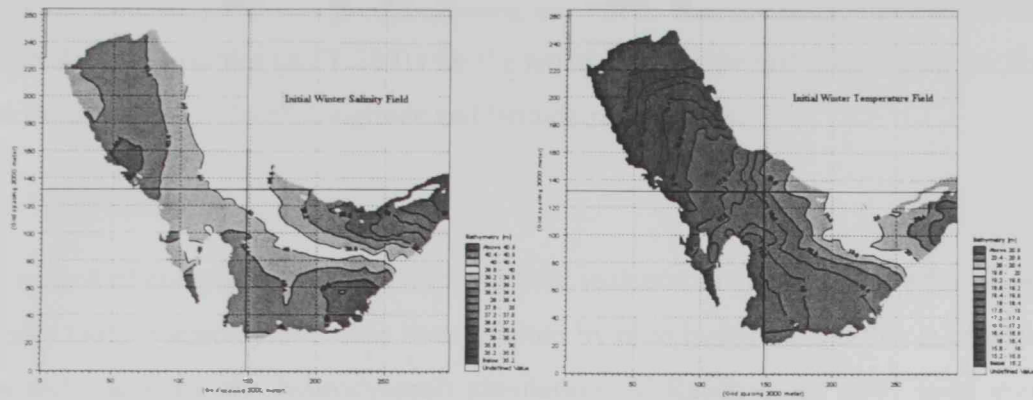


Figure 3.3 Winter, Temperature & Salinity fields (Adopted from Reynolds, 1993).

3.2.4 Initial Boundary Salt and Temperature Time Series

For the baroclinic forcing of MIKE3, the variation of salinity/temperature at the open model boundaries was provided. Time series are prepared for the salinity/temperature boundary data based on a five (5) layer-system, each of 20 meter depth. The Data is adopted from the Mt-Mitchell cruise oceanographic contour results (Reynolds, 1993) at Strait of Hormuz vicinity and is interpolated to cover the total depth (+104m) at the location.

3.2.5 Tidal Boundary

The tidal induced flow into the model area was forced with the principal semi-diurnal, M2 and S2, and diurnal K1 and O1, constituents (see Table 3.1). These components were selected as they were found dominating the tidal motions in the Gulf (Hydrographer of Navy, 1976).

Table 3.1 The harmonic tidal constituents

Tidal Constituent	M2	S2	K1	O1
Phase (H.m)	0.76	0.29	0.29	0.29
Amplitude (g°)	299	335	57	55

The Tidal boundary file was produced using the MIKE tidal prediction tool based on the British Admiralty tables (ATT 2001) for the location of “Didamar” (fig. 3.2) at the Straits of Hormuz at 56.35°,26.5°, longitude and latitude respectively.

3.2.6 Wind Field

Due to lack of comprehensive data on wind field variation in time and space for the entire Arabian Gulf, a simplification has been adopted by introducing a wind that is constant in time and space for the hydrodynamic simulation. Al-Rabeh et al. 1991 used average effective monthly wind velocities values and directions in the Gulf based on the assumption that for any given wind direction and for any month the wind speed is exponentially distributed. The same values were used for summer and winter simulations with the North-Westerly wind dominating the entire region. The data used are represented in Table 3.2 which is adopted from the previous source. A constant wind drag coefficient value of 0.0026 was used.

Table 3.2 Arabian Gulf average effective monthly wind velocities

Season	Speed (ms^{-1})	Direction ($^{\circ}$)
January	5.324	141.7
February	5.487	131.7
March	5.006	132.5
April	4.483	128.5
May	4.724	118.5
June	4.892	127.7
July	3.892	122.8
August	3.000	126.3
September	3.465	132.8
October	3.296	143.4
November	4.689	147.8
December	4.784	135.9
Annual	4.471	132.7

Notice that the direction of the wind in MIKE3 is given in degrees blowing **from** (relative to true north (see Figure 3.4). Hence the above value of wind direction was added to 180 degrees to make up for this change in wind direction definition.

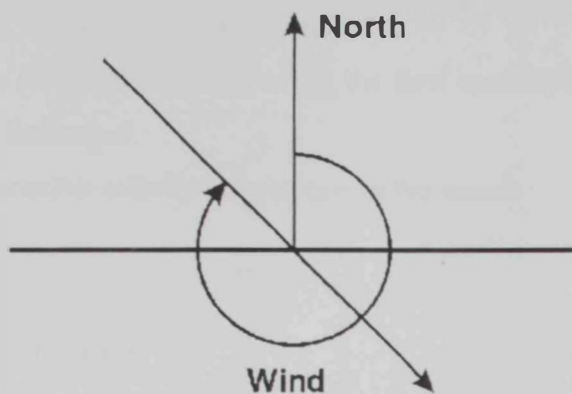


Figure 3.4 Definition of wind direction.

3.2.7 River Inflow

It has been stated in the introduction chapter that most of the river inflow into the Gulf occurs at the northern end. Table 3.3 summarizes the river inflows used in the model. The discharge data and location is adopted from Reynolds, 1993 (see figure 2.2).

Table 3.3 Major rivers into the northern Gulf

River	Discharge (m ³ /s)	Speed (m/s)	Hor. Dir. (degree)	Ver. Dir. (degree)	Salinity (PSU)	Temp. (°C)
Shatt-Al Arab	1456	0.5	90	90	0	20
Hendijan	203	0.5	180	90	0	20
Hilleh	444	0.5	270	90	0	20
Mand	1387	0.5	180	90	0	20

The effects of rivers can be included in the simulation. **MIKE3** enables the user to identify up to a total of 300 sources. For each source the information specified is

- The location (in grid coordinates). It must be placed at a computational point (a wet grid point, not on land or below seabed).
- The discharge (or magnitude) (in m^3/s), the flow speed (in m/s) and the direction at which it is discharged.
- The value of possible salinity/temperature at the source

3.2.8 Heat Exchange Parameters

The heat flux module is a very important tool in seas such as the Arabian Gulf where evaporation plays an important role in the water movement especially in the shallow areas such as the UAE coast. Based on the theoretical background review in the first section of this chapter, the values used in the heat flux module are listed in table 3.4.

Table 3.4 heat flux module parameters

Parameter	Value
Constant a_1 in Dalton's law	0.5
Wind coefficient b_1 in Dalton's law	0.9
Sun constant in a_2 Angstrom's law	0.305
Sun constant in b_2 Angstrom's law	0.473
Displacement summer time	0
Standard meridian for time zone	24
Beta in Beer's law	0.3
Light extinction coefficient	1
Relative humidity	60 %
Clearness coefficient	65%

Air temperature is considered constant with a value of 30 degrees Celsius over the entire region.

3.2.9 Turbulence

The $k-\epsilon$ turbulence model is used as a turbulence module in the hydrodynamic simulation. Based on the software manual recommendation, the empirical coefficients entering the $k-\epsilon$ turbulence model are based on innumerable experiments and therefore, changing these values should be avoided if possible. As such, no change was made to these values. The empirical recommended values are listed in table (3.5). Eddy viscosity limits in the horizontal plane of $5 \times 10^6 \text{cm}^2/\text{s}$ and in the vertical plane of $0.1 \times 10^6 \text{cm}^2/\text{s}$ are considered.

Table 3.5 Empirical constants in the $k-\epsilon$ Turbulence Model

C_m	C_{1e}	C_{2e}	C_{3e}	σ_k	σ_e	σ_T
0.09	1.44	1.92	0	1	1.3	0.9

3.3 Hydrodynamic Simulation Results and Tuning:

3.3.1 Computed and Measured Tides

Computed water levels at Abu Dhabi and Dubai are compared to measured values from Elshorbagy et al. 2004a. Abu Dhabi data represents the early summer season in April, while Dubai compares for the winter season in November (see figure 3.5).

The comparison time period was chosen based on the actual measurements data time periods. Both comparisons show fair agreement between the measured data and the model water height results

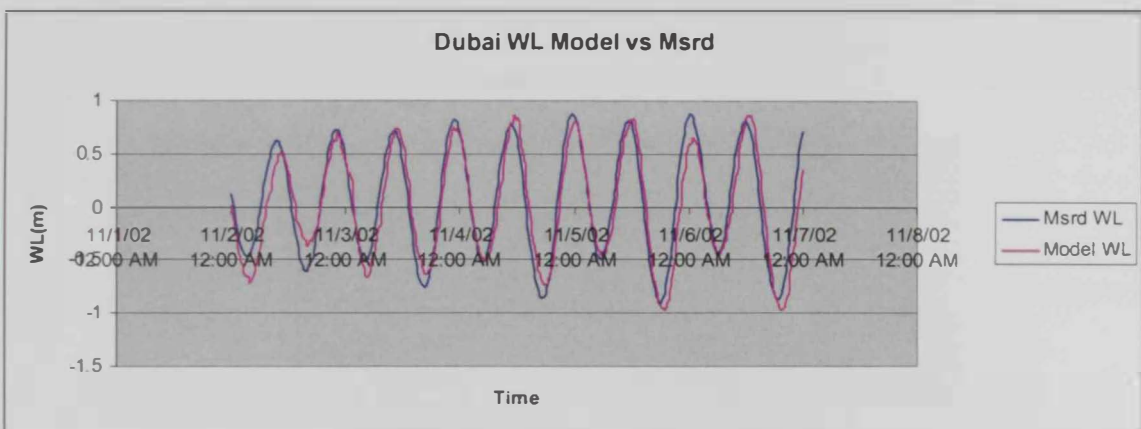
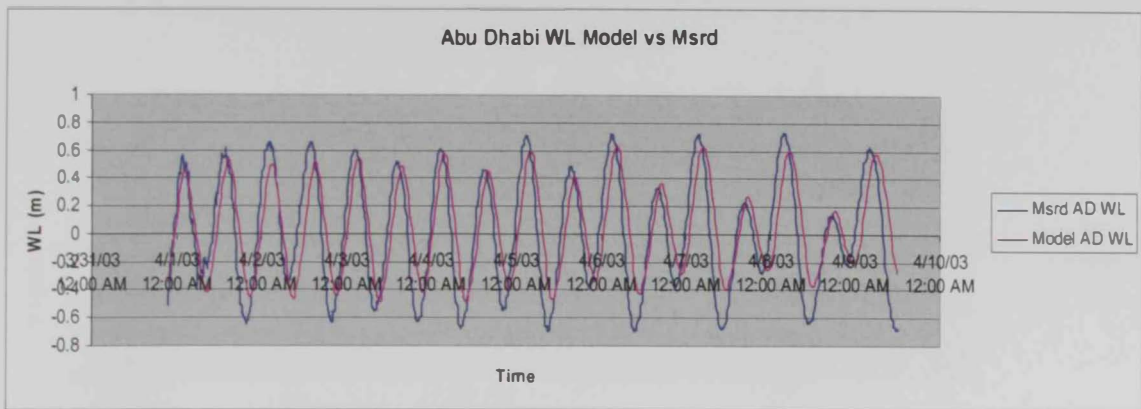


Figure 3.5 comparison of model and measured water level for Abu Dhabi and Dubai

3.3.2 Computed and Measured Residual Currents

For the comparison of currents (fig 3.6), mooring M2 point from the Mt-Mitchell located at Latitude 2622.36 and Longitude 5345.87 is used. The M2 point lies in the deep region of the Gulf along the Iranian coast. This area receives heavy tanker traffic.

Data from the current meter at depth of 10 meters are selected for comparing with the model's 20m deep top layer averaged current. The U and V components were compared for the same period of time. Component U in the model showed fair agreement to the measured data, while the V component showed less agreement. The measured V component data looks quite irregular with abrupt change in local magnitude and this may be attributed to passing ships or winds different from that considered for the study.

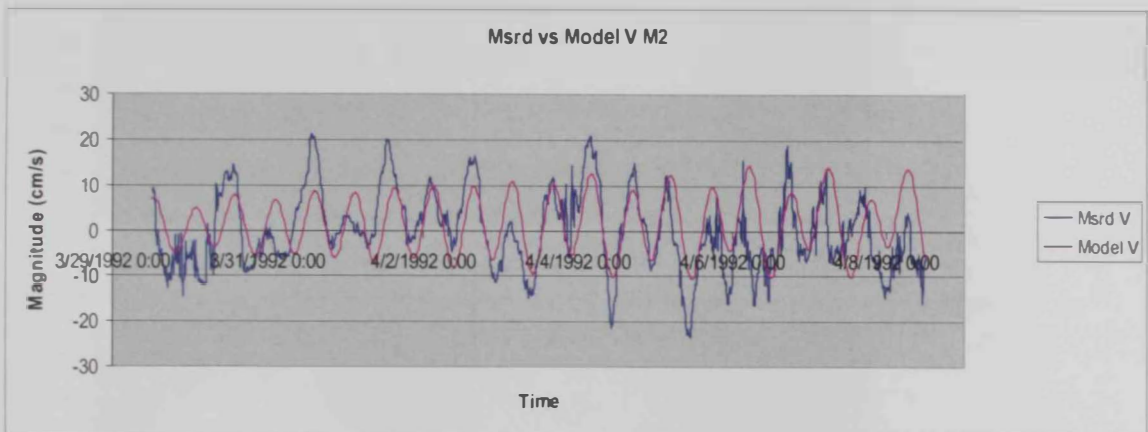
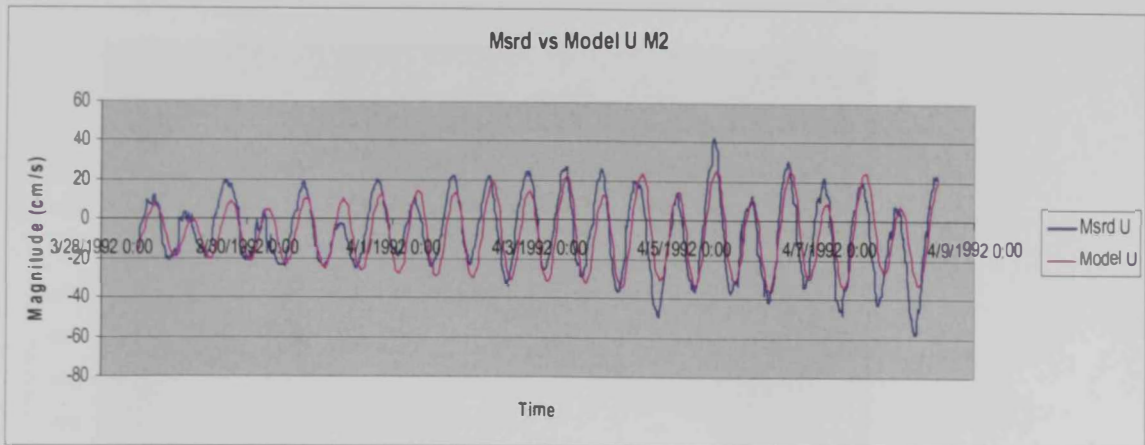


Figure 3.6 Comparison of measured and model current components U and V

3.3.3 Arabian Gulf Residual Flow Pattern

The monthly average wind speed and direction have been used; 5.5 m/s with NW angle 311 degrees for winter and 3.0m/s with NW angle 306 degrees for summer. A 30 day average flow is presented in figure 3-7, “a” for winter and “b” summer.

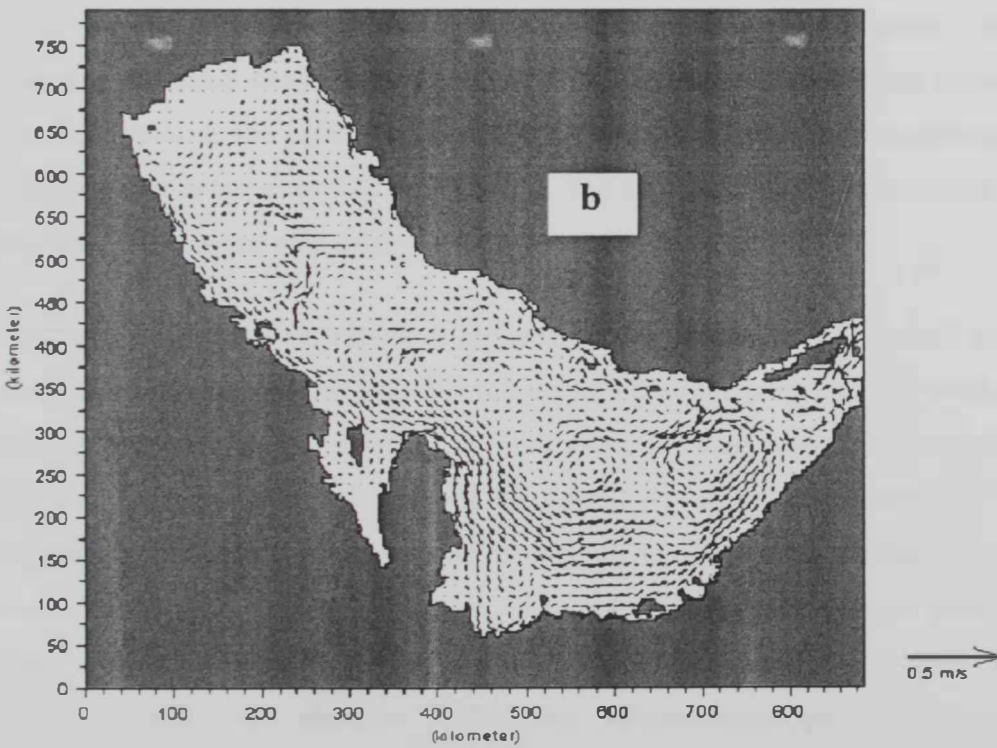
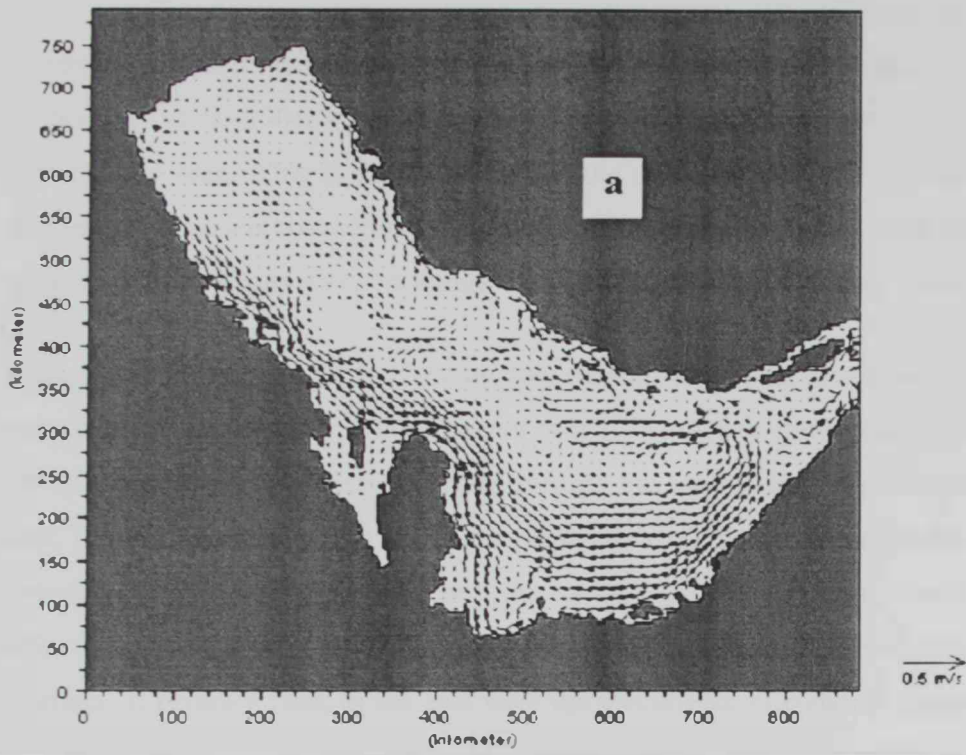


Figure 3.7 Wind and Density driven one month residual surface flow for a) Winter and b) Summer.

The model-predicted average surface flow pattern agrees with the well known general flow pattern features of the Arabian Gulf reported in past studies (Reynolds 1993, Elshorbagy et al. 2004b). In the southern part, the counter clockwise gyre up to Qatar peninsula is seen. Also in the northern half the south westerly jet flow along the Saudi and Iranian coasts is seen while the central and upper portion of the north half of the Gulf is dominated by relatively calm waters with currents hardly exceeding 10cm/s.

Summer: The principal flow feeding the current movement originates along the deep waters of the southern part of the Iranian coast. The surface flow along the Arabian coast always follows the coastline, directed towards the southeast along the Saudi and Qatar coast, turning south following the Qatar peninsula coast then combined with the southern counter-clockwise gyre. The current turns east along the UAE coast, driven by the wind effect on the shallow waters then north-easterly towards the mouth of the Gulf at Strait of Hormuz. It reverses back to the east with the in-currents to combine the gyre again. On the Iranian side of the Gulf, an upward north-western current is active in the southern deep waters to the northern end, turning west at the shallow upper region of the Gulf then reaching the Saudi coast feeding the coastal jet directed southeast in the northern half of the Gulf towards the southeast. The near-shore current is downward south-east current probably due to the river influx to the Gulf. The central portion of the northern half of the Gulf is characterized with calm waters

Winter: The surface currents have higher fluxes than summer. The general pattern is the same except some features probably related to higher magnitude of the wind field in the winter. The main current entering the Gulf along the deep waters of the Iranian coast is directed along the Gulf axes towards the central part of the upper half of the Gulf then splitting very clearly at the upper end of the Gulf to almost equal portions to the east and west. The western current received by the Saudi coast splits again to north and south fluxes. Currents flow along the Kuwaiti coasts are then directed clock-wise to feed the Iranian coastline flow while the south portion follows downward the south-eastern track to Qatar and the UAE coasts with higher fluxes again joining the central gyre at the southern part. The eastern current received by the Iranian coast totally follows the coast

south-eastern downwards till reaching the main flow at the Gulf Axes and is again redirected north-eastern along the Gulf Axes.

In both winter and summer seasons, the flow at the Strait of Hormuz is highly mixed due to high turbulence in the vicinity. In-out waters with steep bathymetric gradients and relatively narrow boundary are factors adding to the complexity and flow turbulence. In conclusion, the residual currents predicted by the model are found to be in fair agreement with the historical and modeling information of the Arabian Gulf.

CHAPTER 4

OIL SPILL MODEL

This chapter is divided into three parts; the first describes the spill analysis model “MIKE3-SA”, its solution technique, and the numerical formulation of the oil spill fate and transport. The second part targets the identification of various model parameters by means of sensitivity analysis simulations in addition to assessing the model performance in association with different crude oil types. The last part of this chapter covers the model validation by testing its performance against the Al Ahmadi oil spill incident. The results of validation along with tables and figures are presented.

4.1 MIKE3 SA Numerical Model

This section describes the physio-chemical processes for the oil spill migration phenomena and their numerical formulation used by MIKE3 SA Module. A major part of the section content is adopted from the software manuals. The module of MIKE3-SA simulates the spreading and weathering of suspended substance in the aquatic environment under the influence of the fluid transport and the associated dispersion processes. The substance may be an oil pollutant, defined according to its distillation properties and chemical structure (alkane or aromatic). The pollutant is transported as discrete particles by a random walk tracking scheme calculating the displacement of each particle as the sum of an advective deterministic component and an independent, random Markovian component which statistically approximates the random and or chaotic nature of time-averaged tidal mixing (MIKE3 Manual Documents, 2002). Such calculations determine the changes of the physical properties (weathering) and describe the movement (trajectory) and performance of oil spilled at the sea. MIKE3 calculates, besides transport due to advection and random walk, the properties of spreading, evaporation, natural dispersion, emulsification, and dissolution. The results of these properties are described in linear scale (millimeters) of the slick thickness. A set of powerful graphical presentation tools are available for pre and post-processing and for data and results manipulation.

4.1.1 Basic Equations

MIKE3 SA module solves the so-called Fokker-Planck equation for suspended oil substances in two dimensions through the introduction of consistent random walk particle method:

$$\frac{\partial f}{\partial t} = \frac{\partial^2}{\partial x_i \partial x_j} \left(\frac{1}{2} B_{ik} B_{jk} f \right) - \frac{\partial}{\partial x_i} (A_i f) \quad (4.1)$$

$A(f,t)$ is a known drift vector representing the deterministic forces which act to change $f(t)$. $B(t)$ is a known diffusion tensor characterizing the random forces and $f = c h$, where c is the concentration and h is the water depth.

The physio-chemical processes affect the movement of each parcel. Once the parcels are released in the water body, their discrete path and mass are followed and recorded as a function of time relative to the reference grid system fixed in space.

The Fokker-Planck equation for suspended oil substances is solved by the Lagrangian Discrete Parcel Method (LDPM). The weathering processes are solved by the Runge-Kutta fourth order method.

4.1.2 Advection/Diffusion

The surface current velocity is based on a nearly logarithmic vertical velocity profile and the wind component is added to the current velocity vectorially in order to determine the total surface drift velocity

Horizontal diffusion due to turbulent fluctuation of the drift velocity is simulated, based on the random walk analysis (Dimou & Adams, 1993). The formulas for the random longitudinal and transversal dispersion are:

$$\frac{1}{2} B B^T = \begin{vmatrix} D_{xx} & D_{xy} \\ D_{yx} & D_{yy} \end{vmatrix} \quad (4.2)$$

where

B = tensor of force

D_{xx} , D_{xy} , D_{yx} , D_{yy} are dispersion coefficients in a Cartesian system

In the special cases where

$D_{xy} = D_{yx} = 0$, ie $D_L = D_{xx}$ and $D_T = D_{yy}$, the displacements in the horizontal and transversal directions are:

$$\begin{aligned} \Delta L &= r \cdot \sqrt{6D_L \Delta t}, \\ \Delta T &= r \cdot \sqrt{6D_T \Delta t} \end{aligned} \quad (4.3)$$

where: r is a random number between -1 and 1.

4.1.3 Evaporation

The evaporation process is modeled by the pseudocomponent approach in which oil is described by a set of fractions. The rate of evaporation adopted in the model was expressed by Spaulding et al., (1982,a) and Payne et al., (1984,b) where a set of hydrocarbons are grouped by their molecular weight as:

$$\frac{dVe_i}{dt} = Ke_i \frac{P_i^{sat}}{RT_{oil}} Xmol_i \frac{M_i}{\rho_i} A_{oil} \quad (4.4)$$

where

dVe_i / dt = the evaporation rate of component i

Ke_i = the mass transfer coefficient of component i

P_i^{sat} = the vapor pressure of component i

R = the gas constant

T_{oil} = oil temperature

$Xmol_i$ = the mole fraction of component i

M_i = the molecular weight of component i

ρ_i = the oil density of component i

A = slick area

And according to Mackay and Matsugu (1973) Ke_i is estimated by

$$Ke_i = 0.029 D_s^{-0.11} Sc_i^{-0.67} u^{0.78} \quad (4.5)$$

where

D_s = slick diameter

Sc_i = Schmidt number for component i

u = wind speed at 10 meters above the sea surface

The slick diameter is calculated by simply assuming a circular shape for the patch.

4.1.4 Natural Dispersion

Crude oils or its refined products after spillage at sea are dispersed by the forming of small droplets of oil to be incorporated in the water column. Besides evaporation the rate of natural dispersion largely determines the life of an oil spill. The model uses a formation of Mackay et al (1980) to compute the entrainment or dispersion on the water column. The fraction of sea surface oil dispersed in the water column is calculated as a lost fraction of sea surface oil per hour given by:

$$D = D_a * D_b \quad (4.6)$$

where D_a is the fraction of sea surface dispersed oil per hour and D_b is the fraction of the dispersed oil not returning to the oil slick, expressed by

$$D_a = Kd_a \cdot \frac{(1+u)^2}{3600} \quad (4.7)$$

where Kd_a is a constant expressing the relationship between dispersed amount and the amount of oil in the surface slick and is taken by the model to be equal to 0.11.

and D_b is the fraction of dispersed oil not returning to the slick calculated by

$$D_b = \frac{1}{1 + 50\mu_{oil}\delta\gamma_{ow}} \quad (4.8)$$

where

μ_{oil} = oil viscosity

δ = slick thickness

γ_{ow} = oil-water interfacial tension

the rate of upwelling of dispersed oil droplets can thus be calculated as

$$\frac{dV_{oil}}{dt} = D_a (1 - D_b) * V_{oil} \quad (4.9)$$

where V_{oil} = spilled volume of oil

4.1.5 Mechanical spreading

Fay's (1971) spreading theory is used to model the slick area growth. The gravity-viscous formulation determines the spreading rate as follows:

$$\frac{dA}{dt} = K_A \cdot A^{1/3} \left[\frac{V_{oil}}{A} \right]^{2/3} \quad (4.10)$$

where

K_A = Constant (s^{-1})

4.1.6 Dissolution

Using the assumption that the actual concentration of hydrocarbons is negligible compared to the solubility, the model uses the rate of dissolution expressed by Payne et al., (1984b) similar to the component approach to calculating evaporation as:

$$\frac{dV ds_i}{dt} = K_{S_i} \cdot C_i^{sat} \cdot X_{mol_i} \cdot \frac{M_i}{\rho_i} \cdot A \quad (4.11)$$

Where

C_i^{sat} = solubility of component i (mg/kg water)

X_{mol_i} = mole fraction of component i

M_i = molar fraction of component i

ρ_i = density of component i

A_{oil} = spilled oil area

The mass transfer coefficient for dissolution is estimated to:

$$K_{S_i} = 2.36 \cdot 10^6 \cdot \epsilon_i$$

Where ϵ_i is the solubility enhancement factor and equals 1.4, 2.2, and 1.8 for alkanes, aromatics, and olefins respectively.

Mixture solubility are calculated by assuming the solubility is proportional to the mole fraction with a correction factor in the solubility of enhancement factor (ϵ) as discussed by Leinonen (1977) who showed that this enhancement factor is necessary in order to predict realistic solubility and the above values of (ϵ) were obtained experimentally (Mackay et al., 1980b).

CHAPTER 5

DESALINATION PLANTS AND SOURCE ZONING

This chapter aims to define points of potential importance to the impact of oil spills with reference to desalination plant intakes along the UAE coast. Further more, zones are laid out to cover the portion of the Arabian Gulf water body adjacent to the UAE. Information on the locations of oil loading terminals and navigation routes of oil tanker are considered in identifying the zoning system distribution.

5.1 Desalination Plants Selection

Intakes of a selected number of strategic desalination plants along the UAE coast mainly in Abu-Dhabi, Dubai, and Sharjah are considered as coastal points of interest in the spill impact analysis. A search has been conducted to determine the selection of points based on their production capacity and their geographical location in an effort to evaluate the risk on the widest range of the UAE coast. The coordinates of the point are considered as observation points and time series is produced in the post processing stage to determine the arrival of oil to these specified locations. Table (5.1) lists the selected desalination plants, coordinates and production capacity in million gallons per day:

Table 5.1 Selected desalination plants along the UAE coast

Emirate	Intake Location	Coordinates in UTM-39		Capacity
		Easting (m)	Northing (m)	(MIG/day)
Abu-Dhabi	Umm Al-Nar	854153	2705831	100
Abu-Dhabi	Taweelah	871950	2744052	95
Abu-Dhabi	Mirfa	748700	2670000	38.7
Abu-Dhabi	Shuwaihat	640254	2663548	200
Dubai	Jebel Ali	937689	2797633	188
Sharjah	Layyah	943657	2809438	40

4.1.7 Emulsification

A result of the emulsification is a large increase in the volume of the oil slick and a significant increase in the density and viscosity of oil.

The incorporation of water is expressed as:

$$\frac{dY}{dt} = R_1 - R_2 \quad (4.12)$$

where R_1 is the rate of uptake. It will increase with increasing temperature and wind speed

$$R_1 = K_1 \frac{(1+u)^2}{\mu_{oil}} (y_{max} - y) \quad (4.13)$$

Where

u = wind speed

y_{max} = maximum water content

y = actual water content

K_1 = emulsification constant ($K_1 = 5.10^{-7}$ [kg/m³])

μ_{oil} = oil viscosity

R_2 is the rate of water release. It decreases with increasing content of asphaltenes, wax and surfactants in the oil and with increasing oil viscosity. This is expressed by:

$$R_2 = K_2 \frac{y}{A_s \cdot Wax \cdot \mu_{oil}} \quad (4.14)$$

Where

A_s = content of asphaltenes in oil [wt %]

Wax = content of wax in the oil [wt%]

K_2 = emulsion coefficient ($K_2 = 1.2 * 10^{-5}$ [kg (wt%)/s²])

4.2 Oil Spill Sensitivity Analysis

Sensitivity analysis is conducted on various selected parameters based on background information of their relevance to oil spill properties such as shape, dimensions, and weathering processes. The study aims to evaluate the effect of these parameters by changing them one at a time and monitoring the results. Eventually, a list of critical

parameters should be short-listed and extensive study will be performed to validate the model for oil spill trajectory based on published literature on oil spill incidents in the Arabian Gulf. The strategy of selecting the values of active parameters is based on the extreme impact in terms of surface total oil slick trajectory and spreading. The weathering parameters used by the model are evaporation, emulsification, dissolution and vertical dispersion. Weathering values will be only of qualitative importance, and no validation will be conducted for them.

The following includes description of the preliminary basic simulation setup utilized in conducting the sensitivity analysis and parameter investigations.

4.2.1 Source and Source Flux

A single oil source releasing 5 particles per time step is assigned at grid location (150, 80) just east of the north end of the Qatar peninsula. The attempt of using 100 particles per time step resulted in increasing the simulation time and produced a smoother slick with no significant difference in predicted trajectory or weathering values. It is decided to adopt continuous release for the sensitivity analysis and to use 5 particles per time step. A continuous source flux of $1\text{ m}^3\cdot\text{s}^{-1}$ is employed which produced 86400 m^3 of oil per day, and is ranked as a major oil spill.

4.2.2 Dispersion Criteria: No Wind, Continuous Source Conditions

This section is meant to serve two purposes. The first, is to identify the dispersion mechanism to use. The second is to estimate the oil spill trajectory due to dispersion, density currents and, tidal currents without including the wind advection. This second purpose will be discussed later with the results of active wind field.

Dispersion criteria is investigated by first adopting it to be proportional to the current (referred to here as case I) and then to be independent of the current (referred to as case II). The case of dispersion being independent from current is most widely used and is suggested in a verified case-study by Proctor et al.(1994) in the Arabian Gulf region where the oil dispersion (diffusion) constants in the horizontal and vertical are $D_h = 10\text{m}^2\cdot\text{s}^{-1}$, $D_v = 0.005\text{m}^2\cdot\text{s}^{-1}$, respectively. The same horizontal value was adopted by Al-Rabeh et al. (1989). These same values are adopted in the simulation, and the dispersion is assumed independent of current. The logarithmic velocity profile was selected to

describe the velocity change with depth. Comparison of simulation results is shown below (Table 4.1)

Table 4.1 Results of total oil dispersion: all dimensions are in grid number (Each grid has an area of 9 km²)

Dispersion	Value	Tot. area	Tot. width	Tot. Length	Oil thickness (mm)
Proportional	10,10,0.005	83	2	31	32
Independent	10,10,0.005	357	12	34	5.52

In case of the dispersion proportional to current, results show that the slick was elongated in shape with maximum width of 2 cells (6 km) and a total area of 83 cells (342 km²) (see fig 4.1) is occupied at the end of a 14 day simulation. On the other hand, in the case where dispersion is independent of current, the results of the slick dispersion were much larger and of an elliptical shape, with a total area of 357 cells (3213 km²) at the end of a 14-day simulation, and the width exceeding 12 cells (36km). The effective length of both slicks was almost equal; where the independent dispersion was 93km while the proportional dispersion was 102km.

Total oil thickness was much larger with velocity-dependent dispersion, exceeding 32 mm, while in the independent dispersion; it was more realistic, barely above 5.5mm. At the end of the simulation, both cases showed that maximum oil thickness location in the slick to be relatively the same on the leading edge. The location of maximum oil thickness at 7 days was generally near the source. In the dispersion proportional to current case, the maximum oil thickness at 7 days is shifted about 30 km downstream more than the independent dispersion. Dispersion independent from the current is adopted for the sensitivity simulations as well as for the final simulations.

At the end of the 14 day simulation, the following is the plot for the dispersion of considered cases. A proportionality ratio of 1 in all three dimensions is considered in case I

Inspecting the results, one can observe that the thickness lost by evaporation was 6 times higher in case II than case I. Also emulsification was 6 times higher in case II and the same ratio was in dissolution and vertical dispersion. In Conclusion:

- ❖ The case of dispersion independent from current produced a total spread area almost 10 times the area covered in the case where the dispersion was proportional to the currents.
- ❖ Case II produced much higher rates of weathering, about 6 times the rates of case I.

From the above findings, it is decided to employ dispersion independent from current in the sensitivity and actual case scenarios based on the conservative approach of employing the extreme conditions for oil spill impact.

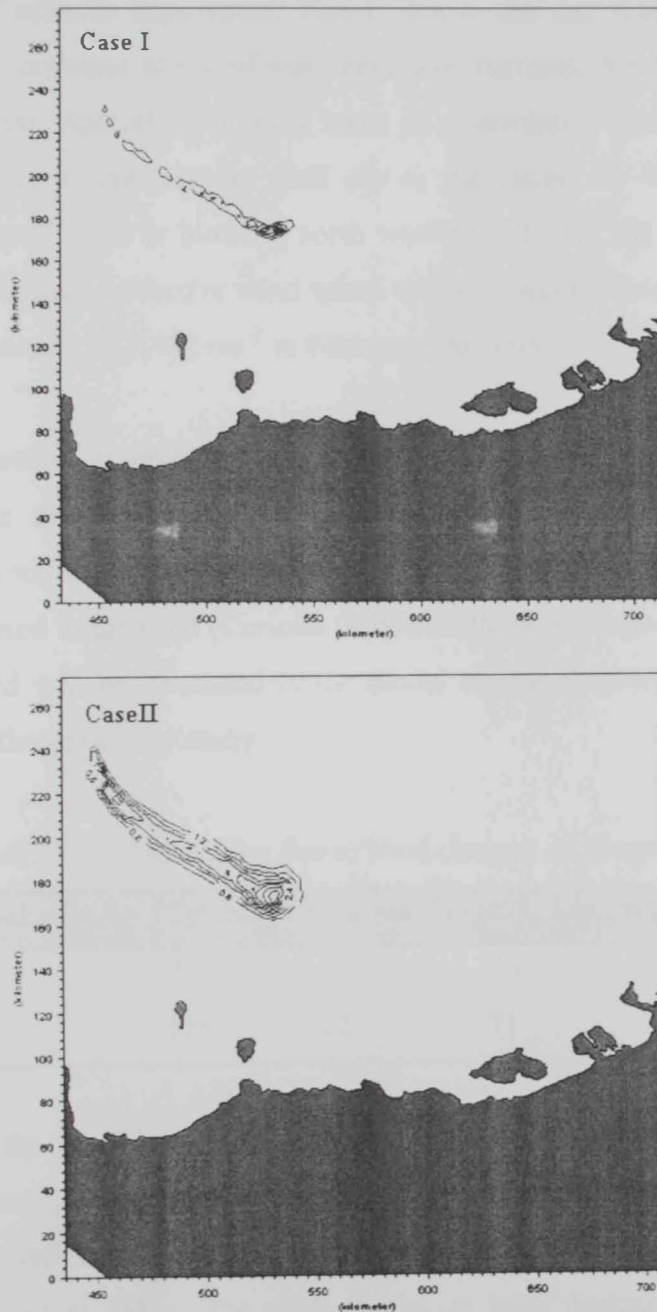


Figure 4.1 Oil Dispersion criteria, 14 Day age (Case I: Dispersion proportional to current, Case II: Dispersion independent of current)

4.2.3 Wind field

Northwesterly wind field, constant in time and space, of 5m.s^{-1} is used for the entire area of the model. Zero wind conditions are tested to evaluate the combined net transport effect of tidal, and density currents in the area adjacent to the UAE coast in absence of the wind advection. Lardner and Das (1991) indicated that, the advection in the Gulf is entirely dominated by wind, except for the North end at Shat Al Arab and the South end at the Strait of Hormoz. It is worth stating that, the wind magnitude and friction coefficient are of extreme importance. This is due to the fact that winds transport oil spills through the combined action of wind-generated currents, wind induced waves, and by direct wind shear. Special attention is taken in determining these values. In general, average wind fields in the Arabian Gulf are in the range of 2 to 5.4 m/s and the dominating "Shamal" wind is blowing north westerly all over the year with -4 to $+10$ degrees range. The mean effective wind speed varies between a minimum of 3.0m.s^{-1} in August and a maximum of 5.487 ms^{-1} in February (Al-Rabeh et al., 1991) (Proctor et al., 1994).

A wind field of magnitude 5m.s^{-1} is used in this sensitivity study. The wind is constant in space and time over the entire model area and directed 315 degree (northwesterly) along the axes of the Arabian Gulf. A constant deflection angle of 15 degrees is considered to the right (Coriolis Effect, northern hemisphere). Wind friction is a tuning value and will be discussed in the model tuning chapter; a constant value of 0.0026 is used in the sensitivity study.

Table 4.2 Results of total oil spreading due to wind change: all dimensions are in cell

Scenario	Value (m/s)	Tot. area	Tot. width	Tot. Length	Max. Oil thick(mm)
No-Wind	0	357	12	34	5.52
Const. wind	5	589	12	71	11.06

Applying the wind field resulted in the increase of the slick covered area due to the added advection force induced by wind field. 40% increase in the area being 5300km^2 and the total effective length to be 312km with an increase of 52%, while the slick width remained unchanged at 36km . The slick maximum total thickness increased 55% to 11.06mm from 5.52mm in the simulation without wind. This increase could be understood due to the effect of breaking waves generated by wind. It is stated by

(Choe1999), that 5m/s is approximately the threshold for generating breaking waves. The maximum thickness in wind conditions simulation was located upstream at grid point (153,76), while in the no-wind conditions simulation the maximum thickness of the slick was located at the leading edge at (177,57).

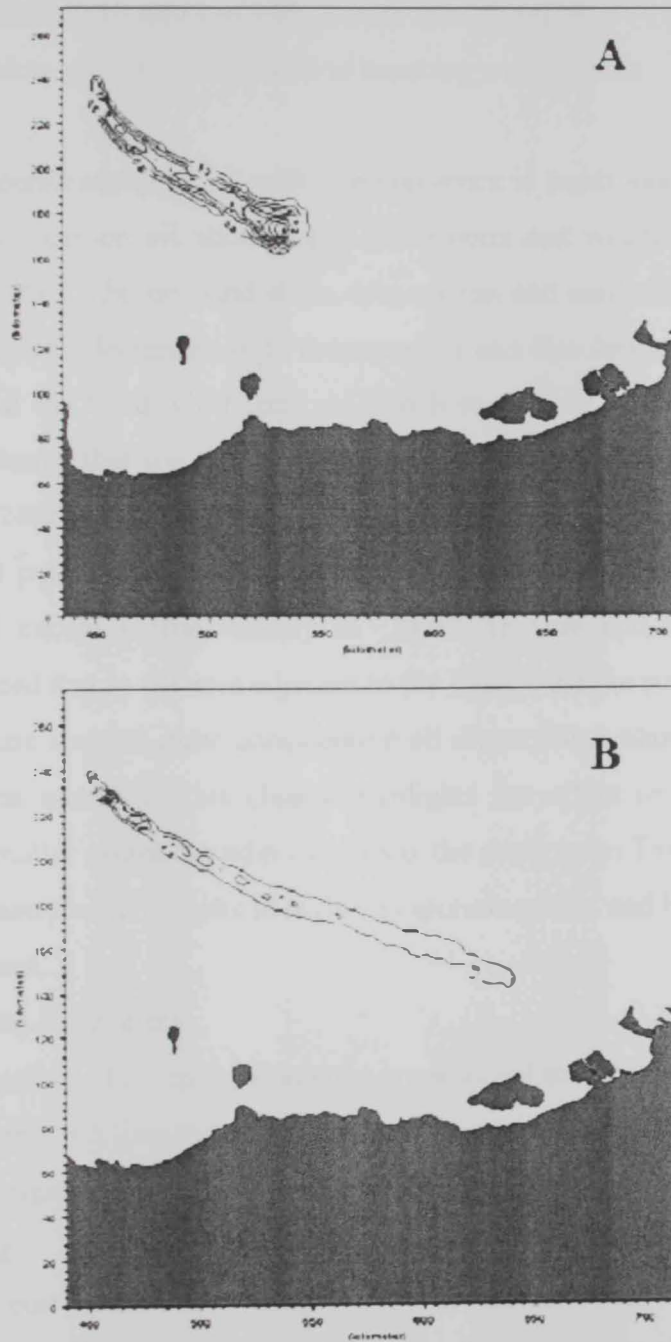


Figure 4.2 Wind conditions effect, Day 14 Oil slick (A: No wind conditions, B: 5m/s constant wind field)

Results of weathering parameters show that:

- ❖ Evaporation loss at the end of 14 day increased 100% from 0.14 to 0.279mm indicating the clear effect of wind presence on increasing evaporation rate.
- ❖ Emulsification formation thickness increased 100% from 4.54 to 9.38mm indicating the clear effect of wind presence on increasing emulsification rate.
- ❖ Dissolution reduce by 10 times to $3.8E-7$ from $3.3E-6$ mm
- ❖ Vertical dispersion greater 30 times due to breaking waves effect

In conclusion, the performance of oil with wind presence is much more active. The wind field effect is very clear on oil slick shape, dimensions and weathering rates. Results show twice the length of the no wind slick, evaporation and emulsification are doubled with wind, while vertical dispersion is 30 times greater and dissolution reduced ten times.

In a study at the Saudi Gulf coast Al-Rabeh et.al. (1992), stated that sensitivity analysis showed clearly that the tidal currents contribute very little to net transport for periods more than 24hr and that the wind driven currents alone are mainly responsible for the net transport of pollutants. Lardner and Das(1991) also stated that the density driven currents are small except in the vicinity of Shatt Al-Arab and Straits of Hormuz. However, it is noticed that in the area adjacent to the UAE were the simulation took place that the no-wind case showed quite considerable oil dispersion, although it was doubled when the wind was included. This clearly highlights the effect of the density driven currents and to a smaller extent the tidal currents in the study area. This is possibly due to the shallow bathymetry which results in higher evaporation rates and hence heavier water that drives the current.

4.2.4 Other Selected Parameters

In this section, a number of oil spill parameters are selected to test their effect on the spill analysis model. Table 4.3 lists the selected parameters of the basic and test setup values that would be investigated for their effect on spill analysis (SA) model performance

Shore Current Zone

The value of shore current zone is investigated for their effect on spill trajectory. Change of shore current zone depth value showed no effect at all when changing from 5m to 2m. results are typical to the basic wind setup.

Table 4.3 Sensitivity analysis parameters

No.	Parameter	Units	Basic setup	Test setup
1	Shore current zone	m	5	2
2	Depth of wind	m	5	10
3	Wind friction (Drag)	Const.	0.02	0.03
4	Cloudiness	%	10	30
5	Albedo (reflectivity)	%	0.14	0.3
6	Oil emmissivity	%	0.82	0.972
7	Emulsion water uptake	kg/ m ³	5.00E-7	5.00E-6
8	Emulsion water release	Kg/ s ²	1.20E-5	1.20E-6
9	Entrainment oil-in-water interfacial tension	Dyne/cm	20	10

Cloudiness

Among air properties, cloudiness value is investigated to estimate its effect. A value of 10% was used with the basic model setup.

Cloudiness was increased from 10% to 30% to evaluate its effect on heat flux. The change did not show any effect on results for total oil spill thickness, shape, or dimensions, nor, on the weathering values. Results show maximum oil thickness with the same value of 11.06 mm at the end of 14 days as in the basic setup.

Albedo

As for heat transport, the Albedo (reflectivity) value, which is an indication of the oil color (the lower the value the darker is the oil) the default value of 0.14 stated by the model is used. Albedo value was increased about 50% to 0.3 from 0.14 (the value of the basic setup) to investigate the effect on heat flux. Looking into the results and comparing revealed no change.

Oil Emmissivity

The effect of the oil emmissivity is investigated. The default value, 0.82 suggested by the model is used. Oil emmissivity was investigated as a parameter in the heat flux dialogue. Changing its value from 0.82 of the basic setup to 0.972 (Sabins, 1997) and reviewing the

results, the change in value proved no effect on oil slick. In conclusion, changing the emissivity value shows no effect on slick shape, dimensions or weathering values.

Emulsion water uptake and water release

The formation of water-in-oil is one of the most important processes affecting a surface slick. It represents a positive flux in which a new component, water, enters the slick. The model of Mackay et al. (1980) is adopted in the software which is fairly simple and derived from extensive experimentation. The Water uptake emulsification constant of $5.00E-7 \text{ kg/m}^3$ and water release emulsion coefficient of $1.20E-5 \text{ kg/s}^2$ constant values are used (DHI SA Manual, 2002). Investigations are made by altering these values as they are suspected to affect the water-in-oil emulsion stability.

Water uptake constant was investigated by increasing its value from $5.00E-7$ to $5.00E-6$ of the basic setup to allow for formation of thicker emulsion.

The results shows that the oil slick maintained its dimensions, shape and, weathering rates with no changes. The emulsion thickness was stable at 9.38 mm with no change from the basic setup results at the 7th day of simulation and at the end of the 14 day simulation.

In conclusion, no effect is shown due to increasing water uptake constant on the oil slick shape, dimensions, or weathering (emulsion thickness).

The other parameter of emulsion formation, water release coefficient value was reduced from $1.20E-5$ to $1.20E-6$ of the basic setup. The reduction was suspected to show larger thickness of emulsion, as this parameter should produce conditions for more stable emulsion as the tendency to release water from emulsion is decreased.

No effect of reducing water release constant value was witnessed. The oil slick maintained the typical shape, dimension, maximum thickness and weathering rates.

In conclusion, reducing water release constant value in the emulsification dialogue has no effect on oil slick spread thickness or, weathering rates.

Vertical dispersion

Vertical dispersion is still a very poorly understood process, and the mathematical description of it is still in an early phase of development (Mackay et al., 1980). The importance of dispersion for a particular spill of crude oil under certain weather conditions, and differences in dispersion behavior of different crude oils, can only be evaluated in a qualitative way. There are fairly reasonable "best estimates" derived from

observations of historical spills (Blaikley et al.1977), which determine the rate of dispersion at sea to be 0-5% oil lost per day depending on the sea state.

Oil-in-water interfacial tension value is important in calculating the vertical dispersion of oil droplets in the water column. AlRabeh et al. (1992) stated that, due to high salinity and low energy of the Arabian Gulf, less oil is expected to enter the water column as compared to less saline and more energetic seas such as the North Sea.

Oil-in-water interfacial tension typical value suggested by (Mackay et al., 1980) is 20-30 dyne/cm. A value of 20dyne/cm is used in the basic simulation and the property is addressed by altering the value to 30Dyne/cm and monitoring the effect. This higher value is suspected to reduce the vertical dispersion due to the stronger interfacial tension that should have allowed for less oil leave the parent oil slick to be dispersed vertically in the water column.

Results showed the value of vertical dispersion reduced with almost 48% from 4.40E-7 mm to 2.96E-7 at the end of the simulation 14 days in the wind condition simulations, still showed no effect on the oil slick spreading, shape, or dimensions. In conclusion, no effect of oil-in-water interfacial tension on slick shape and dimensions

Depth of wind

Change of depth of wind in the wind dialogue from 5 m to 10 m, results showed no change in all comparisons and came to be typical to wind enforced basic setup.

In conclusion, no effect has been witnessed from depth of wind altering.

Wind drift coefficient

This is being an exploratory study that reports the effect of increasing the wind drift coefficient on oil slick development. An increase of wind drift coefficient (wind friction constant) from 0.02 to 0.03 (33 % increase) resulted in a 14% increase in slick area and 16.5% increase in slick length, and also resulted in a reduction of slick width by 16.5%. Total oil thickness was found to be 7.53 mm located upstream with a reduction of 32% from the basic wind setup condition where the coefficient was 0.02. Results of weathering parameters show that:

- ❖ Evaporation: 24 % reduction was encountered.
- ❖ Emulsification thickness was less by 32% with 6.39mm at the end of 14 days.
- ❖ Dissolution 15% reduction is witnessed with the drift increased value.
- ❖ Vertical dispersion 40% reduction is witnessed with the drift increased value.

In conclusion, the increase of the surface wind drift coefficient from 0.02 to 0.03 resulted in increasing the slick area, length, and reduction of slick width and reduced all weathering rates.

4.2.5 Sensitivity to Crude Oil Types

Due to lag of characterization data of crudes produced in the Arabian Gulf. Two representative types medium and, light crude oil (see Table 4.4) are evaluated by comparing the simulation results with the default setup included in the software provider manual (DHI water and environment). The types of crudes used are adopted from literature (Yang and Wang, 1977).

Table 4.4 Selected crude oil samples and their characteristics

Oil sample	General characteristics
Venezuelan Crude	Medium, aromatic, high volume of transport
Nigerian Crude	Light, paraffinic, low in metals

Table (4.5) shows the characterization of crude cuts based on boiling point range and the corresponding %wt of each cut. The hydrocarbon groups for the two selected types are reported in the same table based on their boiling point. Each type has a set of eight cuts representing the crude composition.

Another set of input parameters known to affect the spilled oil weathering rates is used with the relevant crude type in the simulation in order to further evaluate their effect on oil slick trajectory. The values of these parameters are presented below in Table (4.6).

It is important to note that due to lack of data on the addressed crude types, representative values of these parameters are adopted from Canada Environment Website (www.etc-cte.ec.gc.ca) as they are selected based on category classification and are not specifically true for the types of crude addressed. The representative values are for the Arabian medium and light crudes. The main task of the study as stated earlier is focused on the oil slick trajectory and the parameters affecting the weathering rates are only addressed based on the possibility if their variation could affect the oil spill trajectory. The results of the three simulation cases are presented in the following paragraph. Table (4.7) summarizes the 14 day age trajectory and weathering values of the oil slick.

Table 4.5 Hydrocarbon cuts data for selected crudes

Fraction	Description	Boiling Point (°C)	Average Dens	Venezuelan	Nigerian
				Crude (%wt)	Crude (%wt)
1	Paraffin (C6-C12)	69-230	710	10	15
2	Paraffin (C13-C25)	230-405	770	8	15
3	Cycloparaffin (C6-C13)	70-230	810	15	20
4	Cycloparaffin (C13-C23)	230-405	900	20	50
5	Aromatic (mono- & di- cyclic)(C6-C11)	80-240	940	5	5
6	Aromatic Poly- cyclic (C12-C18)	240-400	1000	2	3
7	Naphtheno- Aromatic (C9-C25)	180-400	980	15	7
8	Residual	400	1010	25	15

Table 4.6 Characteristics of medium and light crudes used in oil spill simulation

Parameter	Crude type		
	Default	Medium	Light
Maximum water content (% wt)	0.85	0.85	0.911
Wax content (% wt)	5.7	3.6	6
Asphaltenes content (% wt)	0.05	0.048	0.07
Oil-salt water interfacial tension (dyne/cm)	20	20.4	20
Kinematic viscosity at 38 °C (c St)	3.64	9	7

Weathering

Evaporation value of the light crude is the highest among the three types due to the presence of light components in larger amounts in the light crude characterization groups so that the oil tends to escape by evaporation at ambient temperatures. The reverse

composition is the case with the medium crude, and hence it has less loss in the evaporation process. This is despite the use of the same value for evaporation constant. Weathering and trajectory values are shown in Table (4.7).

Table 4.7 Summary results at 14 day, oil slick trajectory and weathering

		Unit.	Crude type		
			Default	Medium	Light
Trajectory	Area	(km ²)	5301	5301	5301
	Max. Length	(km)	213	213	213
	Max. Width	(km)	36	36	36
	Min. Thickness	(mm)	0.03	0.03	0.03
	Max. Thickness	(mm)	11.06	10.73	16.78
Weathering	Evaporation	(mm)	0.279	0.33	0.41
	Dissolution	(mm)	4x10 ⁻⁷	5x10 ⁻⁷	5x10 ⁻⁷
	Emulsification	(mm)	9.38	9.1	15.24
	Dispersion.	(mm)	4x10 ⁻⁷	3x10 ⁻⁷	1.4x10 ⁻⁷

Dissolution values are typical due to the very limited contribution of this process to total mass balance specially after passing the early hours of oil spilling.

Emulsification of the light crude displays a higher value of 15.24 mm than the medium crude which has a value of 9.1. This is most probably due to the higher content of Asphaltenes 0.07 in the light crude which tends to form stable emulsion than the medium crude which has a value of 0.048 of Asphaltenes forming a less stable emulsion.

The dispersion of the crude in the water column in the form of small droplets is more active in the medium crude having a value two times the light crude. This is due to the condition of the liberal heavier less emulsified crude, while the presence of light crude is more incorporated in stable emulsion and losses in the evaporation process.

Trajectory

A continuous slick is formed of elongated along its axis and expanding its width as it moves downstream. The trajectory and spreading of the three combinations is typical. The total area after 14 days, the maximum length and width and the minimum thickness

at the leading edge are all the same. The value of maximum thickness of the oil varies considerably as it is located upstream only near the source. This difference in oil thickness is not reflected on the trajectory or spreading of the oil slick.

It is concluded from the above analysis that the oil slick movement is solely dependent on the environmental conditions, namely the wind conditions which have clearly showed a substantial effect in driving and directing the oil slick trajectory. To a lesser extent are the density and tidal advective currents. Hence, accurate wind data is essential for accurate trajectory predictions. On the other hand, the change of the physical and chemical properties of the oil had a direct effect on the weathering rates only. Despite the logical expectation of the interrelationship between the weathering processes activities and the retardation and decay of the oil slick with time. The manipulation of the values governing these processes revealed to be of insignificant effect on the oil slick trajectory and spread. And hence the spreading results should be taken with caution as it is understood that the change of the relative oil density -due to the change of the oil type and density- should directly affect the oil spill spreading.

4.2.6 Sensitivity Analysis Conclusion

Despite the effect of a number of the tested sensitivity parameters on various weathering rates, none of the parameters tested in the sensitivity study has a significant effect on the oil spill trajectory except for the wind. The wind driven currents are the dominating force in the oil spill movement in the gulf. It is well known that the oil moves on the sea surface due to the combined action of wind generated currents, wind induced waves, and by direct wind shear. This fact is well documented in previous published articles in the Arabian Gulf. The sensitivity study shows that the density currents in the region adjacent to the UAE coast are of potential importance for oil slick movement. Information found on wind parameters during literature search conducted earlier is usually incomplete. The sensitivity analysis indicates that accurate wind data is essential for accurate trajectory prediction. The wind parameters include comprehensive wind data in terms of magnitude and direction in space and time during the simulation period, wind drift coefficient either constant or variable, and wind drift angle. Lack of information called for the validation of the spill analysis model by using a range of data that was published on the Arabian Gulf and comparing the produced trajectory to a well documented trajectory of an oil spillage occasion in the region.

MIKE 3-SA model applies Fay's Gravity-Viscous (1971) formula for radial spreading which was modified by Mackay (1980) as

$$\frac{dA}{dt} = K_A \cdot A^{1/3} \left[\frac{V_{oil}}{A_{oil}} \right]^{4/3}$$

where:

$$V_{oil} = R_{oil}^2 \pi h_s$$

and K_A is a constant specified internally in the model. It is the term used in Mackey's thin-thick modification to represent the effect of the density difference between water and oil in the original Fay equation.

Reed et. al. (1999), stated that "The resulting spreading rate in the Mackey's thin-thick modification on Fay's spreading formula is therefore independent of the initial oil density and insensitive to subsequent changes in density caused by evaporation and emulsification". This statement clarifies the typical trajectory of oil despite the obvious changes in weathering rates.

4.3 Spill Analysis Model Validation

The combined hydrodynamics and spill analysis models are evaluated against the available information and sightings on AL-AHMADI oil spill that occurred over the period of January-May 1991 in the state of Kuwait in the upper part of the Arabian Gulf (fig. 4.3) adopted from Al-Rabeh et al. (1992).

As a result of hostilities erupted in the area, oil was released into the waters of the Arabian Gulf. Al-Rabeh et al.(1992) stated that the volume of oil released may have been as large as 6×10^6 barrels. Most of the oil was released at or near Mina Al-Ahmadi 25 km south of Kuwait city. This act caused an environmental damage of catastrophic dimensions, inundating well over 550 km of the Saudi coastline. Substantial damage was caused to environmentally sensitive habitat and cleanup requirements were massive. Among several authors who have described and modeled the occasion, the trajectory model (GULFSLIK II) used by King Fahd University of Petroleum and Minerals (KFUPM, Al-Rabeh et al., 1992) provided reasonably accurate predictions and have extensively documented the actual trajectory of the spill. The details of their work are used for the validation of the spill analysis model to be used in this study.

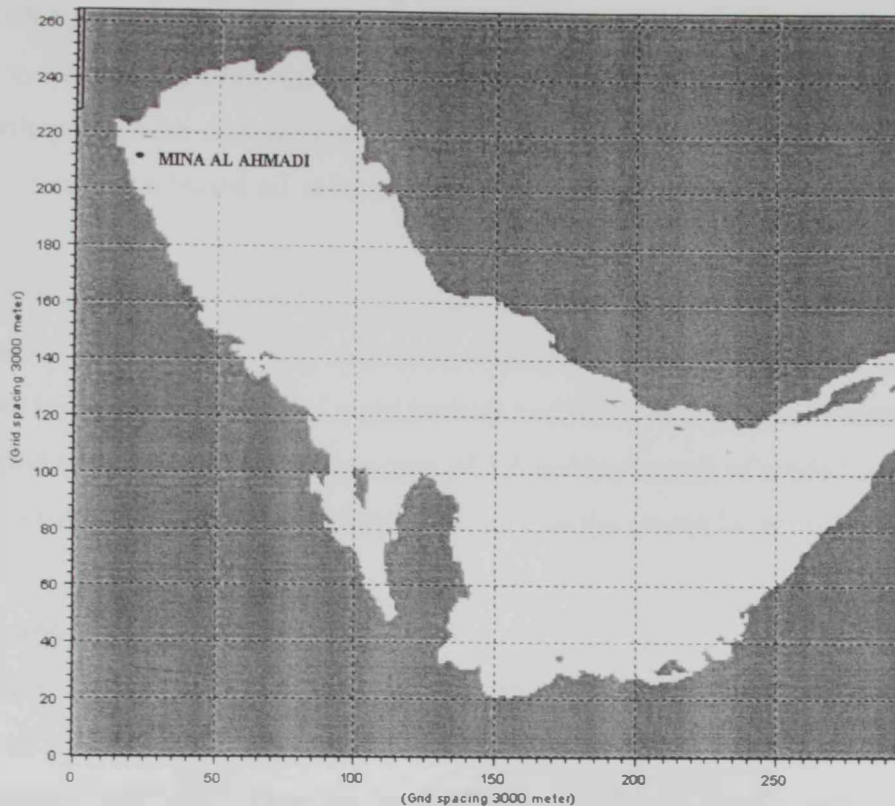


Figure 4.3 Location of Mina Al-Ahmadi

The following is a description of the oil spill parameters used in the model for simulating the oil slick trajectory. The actual trajectory is presented for comparison. Typical values of the input parameters are adopted unless stated otherwise. In that case the aid of other articles or publications of relevance will be sought to verify the required information and reference will be cited where ever necessary.

4.3.1 Al-Ahmadi Oil Spill

Being the largest oil spill incident in history (approximately 3.5 - 10 million barrels), Al-Ahmadi oil spill has put the highly diverse Saudi coastline natural and artificial resources in jeopardy. The following is a review of the King Fahd University of Petroleum and Minerals (KFUPM) effort to simulate the oil spill trajectory along with actual sightings for model validation.

Source location

Based on the description and the information available in Al-Rabeh et al., (1992), Oil was deliberately released from several locations off the coastal area of Kuwait state in addition to Mina Al-Ahmadi itself. The oil pumped from the export terminals at Mina Al-

Ahmadi Single Mooring Point (SMP) at the sea island terminal located 29 07N 48 09E started on January 19, 1991, the major leak was stopped on January 28, 1991. Other north and south piers were damaged and started leaking oil late in January 1991. Mina Al-Ahmadi terminals released oil at an estimated rate of 6000 barrels hr^{-1} .

Mina Al-Bakr released oil from the southern terminal located 29 41N 48 09E started on January 26, 1991 and continued after March 6, 1991. The amount released was estimated to be minor. A total of eight tankers leaked oil into the Gulf waters at the same time period with a total estimated amount of 3.5 million barrels of crude oil. The location of Mina Al-Ahmadi at 29 07N 48 09E is selected as the source location for the simulation

Oil Flux and Duration

To analyze the transport and fate of Al-Ahmadi oil spill, a continuous spill was introduced on January 19, 1991 with an hourly release of 27390 barrels of heavy crude for a period of 144 hours. Thus the total spill size is about 4 million barrels was used in the article study.

Wind Data

The wind parameters include comprehensive wind data in terms of magnitude and direction in space and time during the simulation period, wind drift coefficient either constant or variable, and wind drift angle (Coriolis). Data provided by Saudi Aramco and Meteorology and Environmental Protection Agency of Saudi Arabia were used to determine, on a monthly basis, the average speed of the wind from each of the eight cardinal directions and the percentage of time for which these eight winds blew. The calculated average monthly wind velocity and direction presented in the KFUPM, Al-Rabeh et al., 1992 article are presented in table (4.8) to simulate the wind advection in the long-term. For the real-time model the input of the average daily wind velocity is used instead, this data was not available.

Table 4.8 Average effective monthly wind velocities

Month	Wind velocity	Effective wind direction
Jan	5.324	141.7
Feb	5.487	131.7
Mar	5.006	132.5

Description of Currents

The simulation results of MIKE3 HD model for currents in the western Gulf area-as discussed earlier in the hydrodynamics calibration part confirms to the general circulation towards the southeast. This is typical to earlier findings recovered by the model (HYDRO 1, Lardner et al., 1993) used by the KFUPM to produce the Gulf hydrodynamic current circulation for Al-Ahmadi oil spill. There is a general agreement that wind forcing dominates the surface flow in this region of the Gulf adjacent to the Saudi coastline. Thus, Al-Ahmadi oil spill moved southeasterly almost parallel to the Saudi coast, due to the prevailing northwesterly wind regime in the area.

Actual Oil Spill Trajectory

Al-Rabeh et al., 1992 stated that "Comparisons between predicted trajectories and actual sightings show that GULFSLIK II is reasonably accurate". Figures 4.4 & 4.5 represent the actual and predicted trajectories of the oil spill over the period from January 19, 1991 to March 18, 1991.

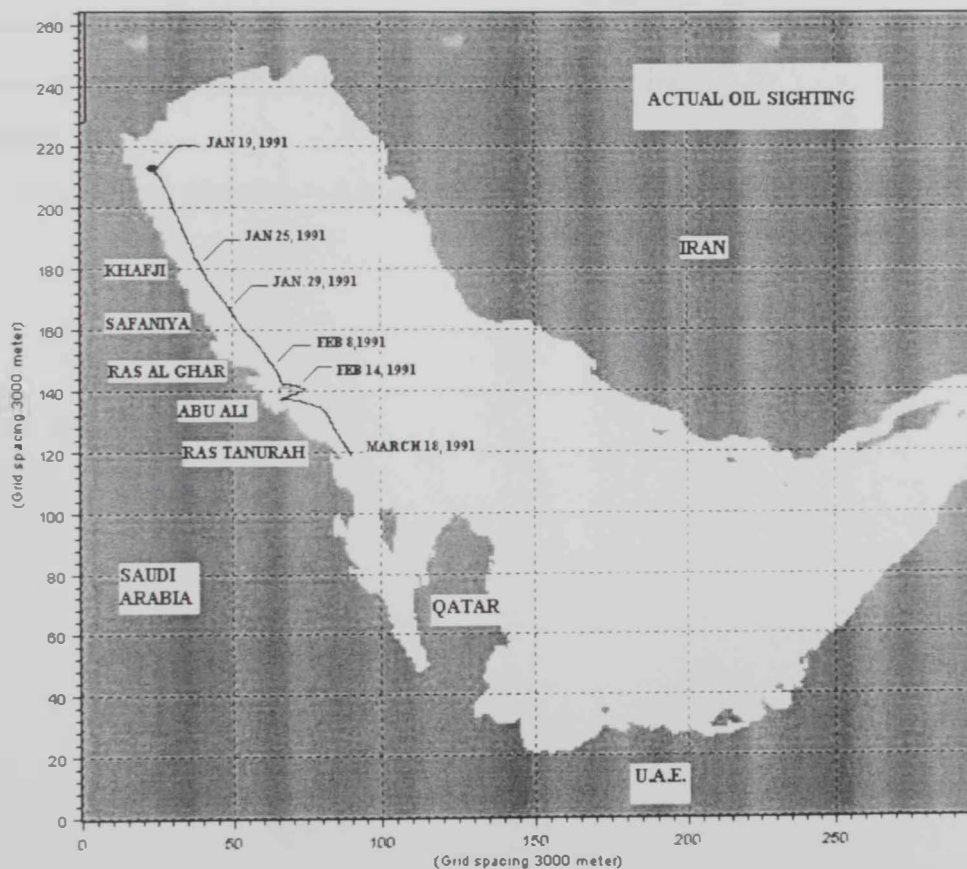


Figure 4.4 Al-Ahmadi actual trajectory of leading edge as reported by Al Rabeh et al, 1992 from the beginning of release

4.3.2 Al Ahmadi oil spill simulation using MIKE3 SA

The spill analysis simulation covers the case study period from January 19, 1991 to March 18, 1991. using a simulation time step of 300 seconds and saving the results at a time interval of 1 hour. The SA model is using the current field produced from a previous hydrodynamic simulation typical to the validated setup in the hydrodynamic part reviewed earlier.

Wind Data

An angle of 180 degrees is added to the wind direction in table (4.9) to account for the wind system adopted by MIKE3 (North wind directed downward =zero degrees), in order to simulate for the Northwestern wind direction..

Optimal values for wind deflection angle (γ) and wind drag coefficient (β) for the Gulf suggested by Al-Rabeh, (1994) to be 26.05 degrees to the right of the wind direction and 0.031 respectively are used in the model. To prepare the wind file used in the simulation, the value of the deflection angle was deducted from the effective wind direction in table (4.9) and again added in the model as a wind parameter input.

And hence,

$$\text{Model wind direction} = \text{Actual wind direction} + 180 - 26.05 \quad (4.15)$$

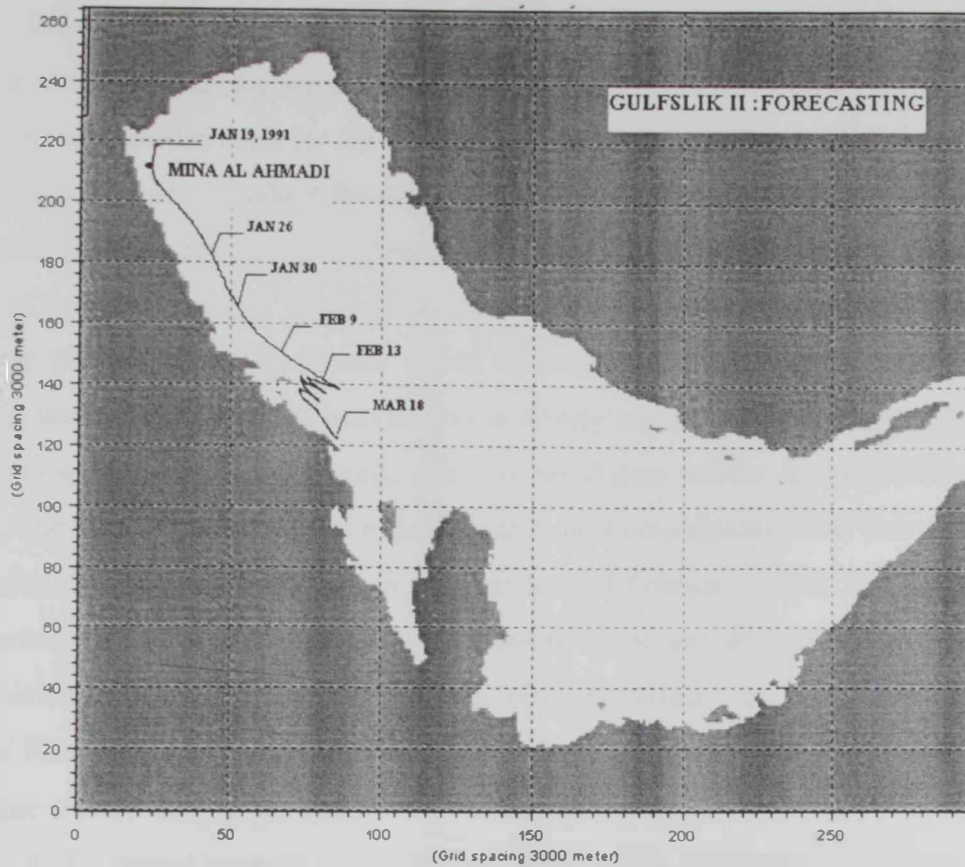


Figure 4.5 Predicted oil trajectory KFUPM model

The average wind velocities in table (4.9) are used to prepare the wind data file which is taken to be constant in space. The data prepared covered the simulation period between January 19, 1991 and March 18, 1991.

Table 4.9 Al Ahmadi spill Simulation wind data

Month	Wind velocity	Wind direction
Jan	5.324	295.67
Feb	5.487	285.67
Mar	5.006	286.47

It is worth noting that the use of such coarse data is expected to cause some disagreement between the simulated in this study and the one based on average daily wind velocity and direction for the same period, depending on the normalization constant value that was used to produce the average monthly effective wind velocity vector.

Later in the MEPA report on Al-Ahmadi oil spill, Nizari and Olsen (1993), stated that "A series of European weather fronts passed through the Gulf Area during much of February, reversed the prevailing Northwest winds to Southeast and held the spill front from moving south". This piece of information is clearly neither stated nor considered in the preparation of the monthly average effective wind data profile in the KFUPM article, despite the fact that the predicted trajectory showed a considerable slow down of the spill movement towards the Southeast in the first half of February. Also, the spill trajectory has occasionally been reversed to the Northwest in the second half of the month. Such information would cause the predicted trajectory by MIKE3 to deviate during the first half of February and more considerable deviation is expected during the second half of the same month. Hence, the prediction validity of the used wind data is expected to be limited to the period prior to early February only. This highlights the vitality of using precise wind data in successfully predicting the trajectory of an oil spill.

Oil data

Due to lack of data on heavy Kuwaiti and Iraqi crudes characterization and breakdown, the medium Venezuelan crude oil was arbitrarily selected. This simplification was justified based on the fact that the sensitivity analysis on MIKE3 showed that the type of crude did not affect the trajectory. Similar to the case study condition of release, a rate of $1.65 \text{ m}^3/\text{s}$ release of oil was used for the same duration of 144 hours or 5 days producing an oil spill of size $7 \times 10^5 \text{ m}^3$ equivalent to 4×10^6 barrels. The release point was 25 km south of Kuwait city at the location of Mina Al-Ahmadi at 29 07N 48 09E. Table (4.10) lists the oil parameters used for the spill analysis model setup considered in the validation process.

Table 4.10 SA Parameters for validation simulation

parameter	Value
maximum water content	85%
asphaltenes content	0.07 %
wax content	6 %
dissolution mass transfer coefficient	2.3×10^{-6}
oil-water interfacial tension	20 dyne/cm
oil diffusion coefficients	10,10, 0.005 (x,y,z) m ² /s
kinematic viscosity/ref. temp	9 cs / 38degree
oil emmissivity	0.82
water emmissivity	0.95
air emmissivity	0.82
evaporation constant	0.029

4.3.3 Results of Al Ahmadi oil spill simulation using MIKE3 SA

Using MIKE3 SA model with the simulation revealed the following results of the leading edge location with time. The location recovered from the actual oil spill sighting, KFUPM GULFSLIKII model, and MIKE3 SA model are compared in table (4.11) at five stations along the Saudi coast.

Table 4.11 Al-Ahmadi oil spill, Actual and predicted trajectory comparison

Location	Date of actual oil sighting	Predicted date of impact using GULFSLICKII	Predicted date of impact using MIKE3
Al-Ahmadi(Start)	January 19, 1991	January 19, 1991	January 19, 1991
Khafji	January 25, 1991	January 26, 1991	January 26, 1991
Safaniya	January 29, 1991	January 30, 1991	January 30, 1991
Ras Al Ghar	February 08, 1991	February 09, 1991	February 07, 1991
Abu Ali	February 14, 1991	February 13, 1991	February 09, 1991
Ras Tanura	March 18, 1991	March 18, 1991	February 15, 1991

4.3.4 Discussion and Conclusion

Trajectory

MIKE3 SA is showing fair agreement to sighting dates and track of both, the actual and predicted findings in the first three stations of Khafji, Safaniya, and Ras Al-Gar until the end of the first week of February (Figures 4.6a, 4.6b, and 4.6c). Deviation from the KFUPM predicted sighting dates starts to increase with time after that date. This was expected, as stated earlier, based on the limitation of using the average effective monthly wind data by MIKE3 instead of the daily average used for prediction in the KFUPM model. Yet, the predominant average effective monthly wind data produced a fair prediction during the first 19 days of the spill period. The deviation was amplified due to the effect of the less frequent reversed southeastern wind front documented in the MEPA report by Nizari and Olsen, (1993) which occurred after February 7, 1991 and acted to retard the propagation of the spill further southeast. The absence of this occasional reversed wind data caused MIKE3 SA to carry over the simulation with the average effective monthly wind data and drive the spill further southeast (see figure 4.6.d) while the actual spill was held back with the reversed wind forcing.

In general, the predicted MIKE3 SA trajectory resembles the prediction of the KFUPM model track which does not come into interference with Abu-Ali island but else is drifted to the east and the retardation of the trajectory is only due to the reversed wind direction, while the actual trajectory retardation was partially due to the fact that the spill was held northeast of Abu-Ali (Spaulding, 1993) for a long time before it started circling around the island and again moving southwest.

Although it is speculated that a constant value of the spreading rate (K_A) in calm water is considered in the model, the good agreement between the simulated (Al Ahmadi) oil spill trajectory with observations suggests that the constant value used in the model is appropriate to simulate the spreading in the case of real sea-state conditions at least for Arabia Gulf. The fair agreement during the first stage of the simulation does also ensure the ability of MIKE3 SA model current setup to accurately predict the oil spill trajectory provided that accurate wind data is applied.

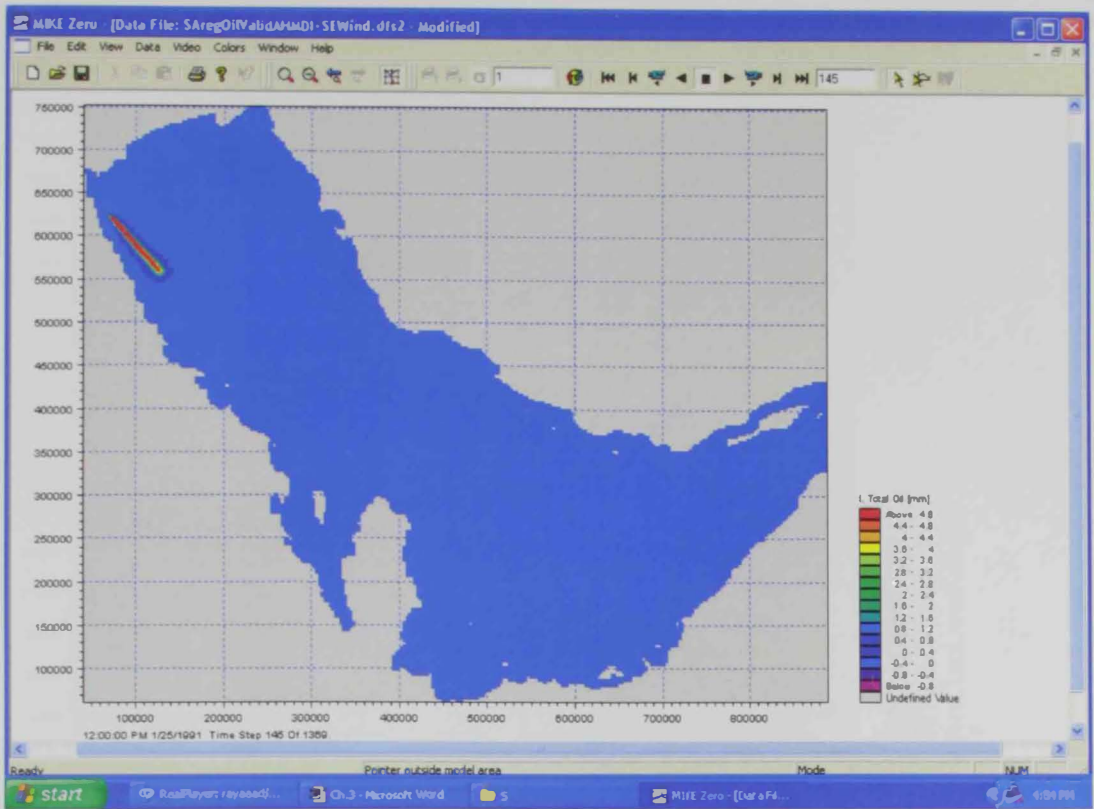


Figure 4.6a Al Ahmadi oil spill trajectory at January 25, 1991- monthly average wind

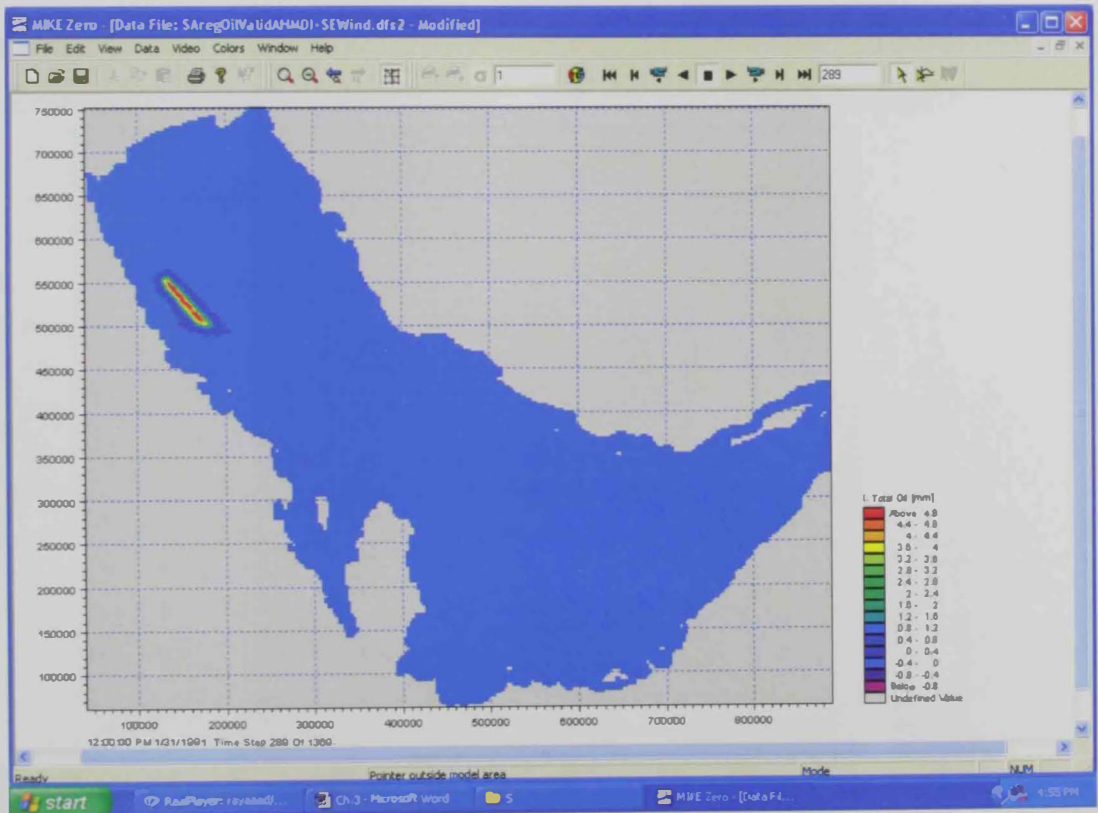


Figure 4.6b Al Ahmadi oil spill trajectory at January 31, 1991- monthly average wind

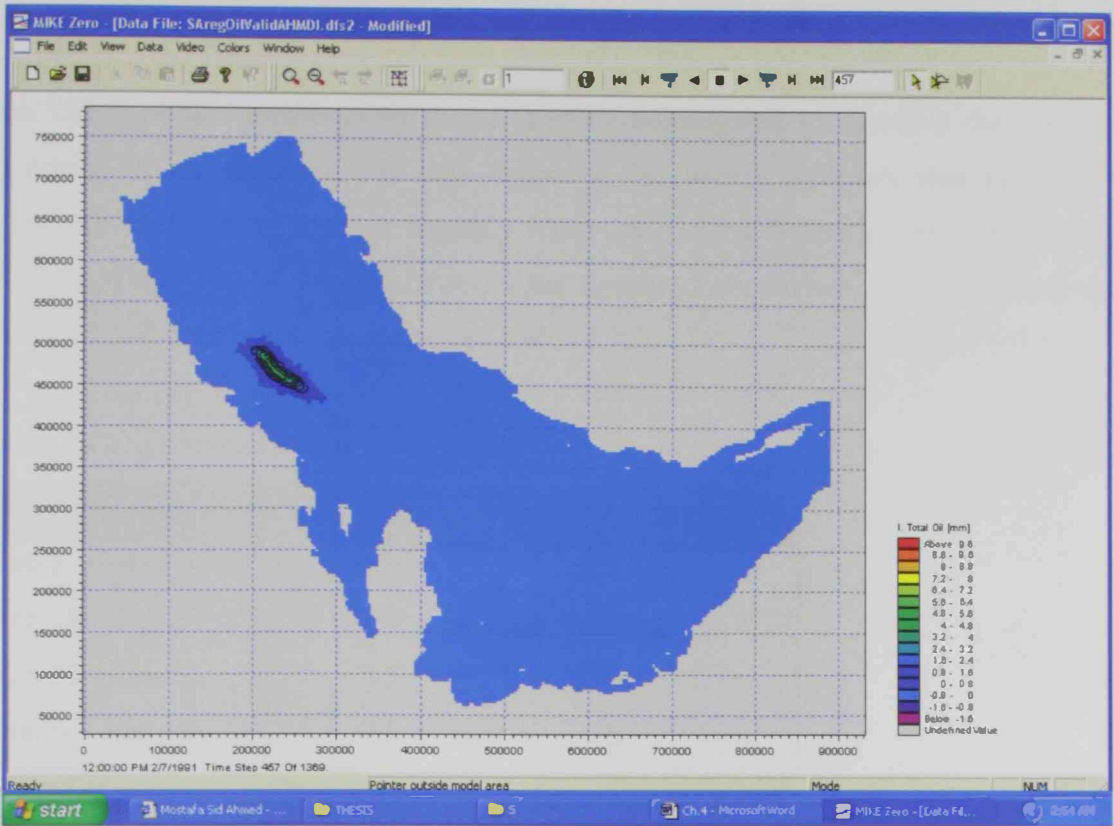


Figure 4.6c Al Ahmadi oil spill trajectory at February 7, 1991- monthly average wind

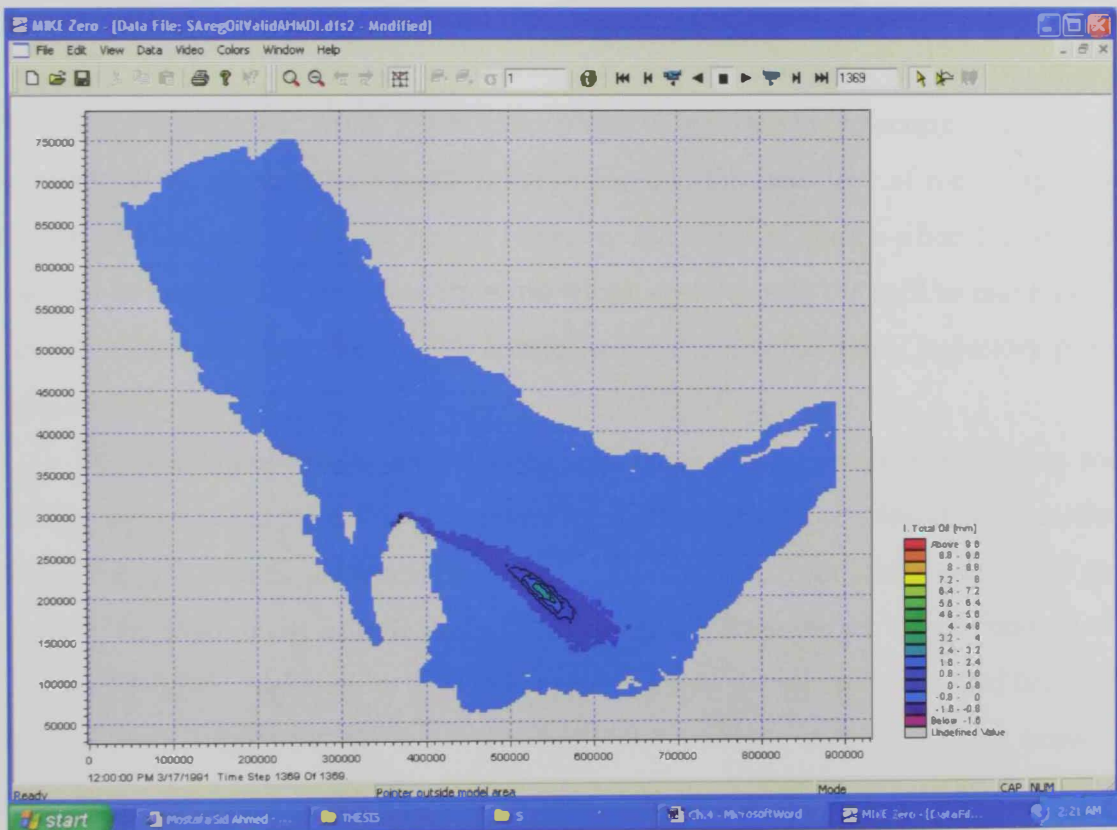


Figure 4.6d Al Ahmadi oil spill trajectory at March 17, 1991- monthly average wind

Southeast Wind Front

The effect of the southeast wind was further investigated to discover the mode of trajectory. A set of speculated data based on the actual trajectory was prepared to substitute the effective average monthly wind data during the period from February 5, 1991 to March 18, 1991 which showed the deviation occurrence from the actual spill track due to the revised wind effect, see table (4.12).

Table 4.12 Speculated February wind data

Date	Wind velocity	Wind direction
Feb 5 – Feb 17	1.0	315
Feb 18 – Feb 23	1.0	120
Feb 24 – Mar 5	0.5	290
Mar 6 – Mar 18	0.5	315

The simulation was conducted from January 19, 1991 to March 18, 1991. A combination of the effective average monthly wind and the speculated February wind data was used.

The results of the simulation showed that after the first week of February, a non-prevailing southeastern wind front took place. This caused lowering the velocity magnitude of the northwestern wind in the region and the trajectory of the oil spill was reversed and delayed during the rest of February and some of March when the net wind blow was in favor of the northwestern wind which again caused the spill to move slowly in the southeast direction. Relatively, a trajectory similar to the actual trajectory plot is produced.

The simulation results also showed that much more horizontal spreading took place during the holding conditions in February as this was typically found by Spaulding, (1993). The spill moved northwest due to the southeast wind front which caused the spill to impact the Saudi coast from latitude 28 40' to 27 20' from the period of February 11, to March 18, 1991. Al-Rabeh et al., (1992) reported that the oil spill impacted the Saudi shoreline from latitude 28 44' to 27. The MIKE3-SA results showed that the impacted region along the Saudi coast was almost similar to the actual. The extent of shoreline impact is less in the simulation than actual; this is probably due to the difference in the wind data combination of magnitude, direction, and duration from the real data.

The comparison results proved that the southeastern wind front has affected the trajectory in a typical manner to the actual trajectory and that the spill holding and backward movement was the cause for the spill to reach the Saudi mainland coast. The findings revealed that in case of two opposite wind fronts facing each other, the oil tends to spread horizontally much faster and covers larger areas in that region. The results are considered fair to reflect the effect of the southeastern wind front on Al-Ahmadi oil spill trajectory. The set of figures 4.7a, 4.7b, 4.7c and 4.7d, show the oil spill trajectory due to the speculated wind field after February 7 at various time intervals as indicated in the figure caption.

The model correctly predicted the movement trajectory of Al-Ahmadi oil spill during the first 19 days of release due to the consistency of the wind data being used with the prevailing wind conditions. While the trajectory deviation beyond that date was due to reversed actual wind data not reflected in the used wind data file.

On the other hand, the results of the simulation for the combined data proved the competency of MIKE3-SA to handle the trajectory efficiently provided the correct data is plugged in. Starting at Mina Al-Ahmadi on January 19, 1991, moving downward parallel to the Saudi coast the oil spill reached Ras Tanura on March 17. By this exact timing the predicted oil spill is typical to the actual trajectory. Also, the predicted shore line deposition using MIKE3-SA took place along the Saudi coast at latitude 28 40' to 27 20' while Al-Rabeh et al., (1992) reported that the oil spill impacted the Saudi shoreline from latitude 28 44' to 27 this limited difference is possibly due to the difference in the estimated wind data combination from actual.

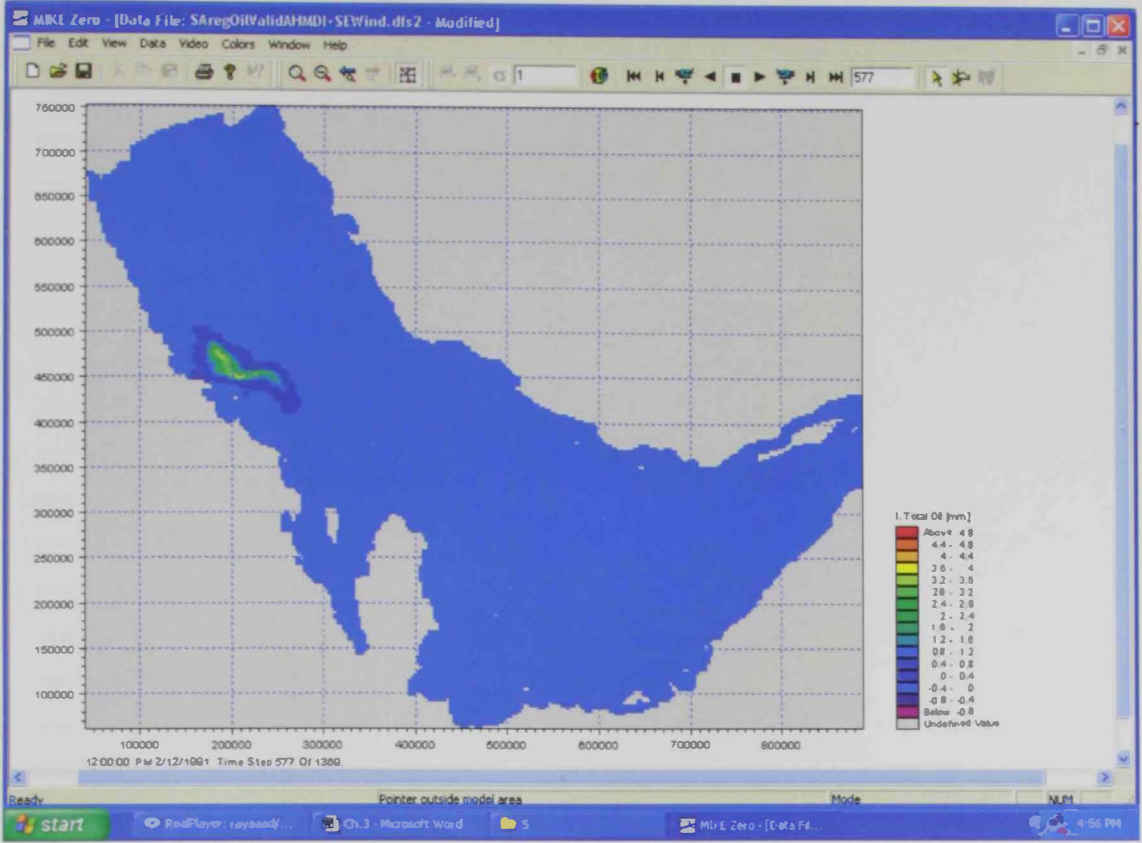


Figure 4.7a Al Ahmadi oil spill trajectory at February 12, 1991-specified wind field

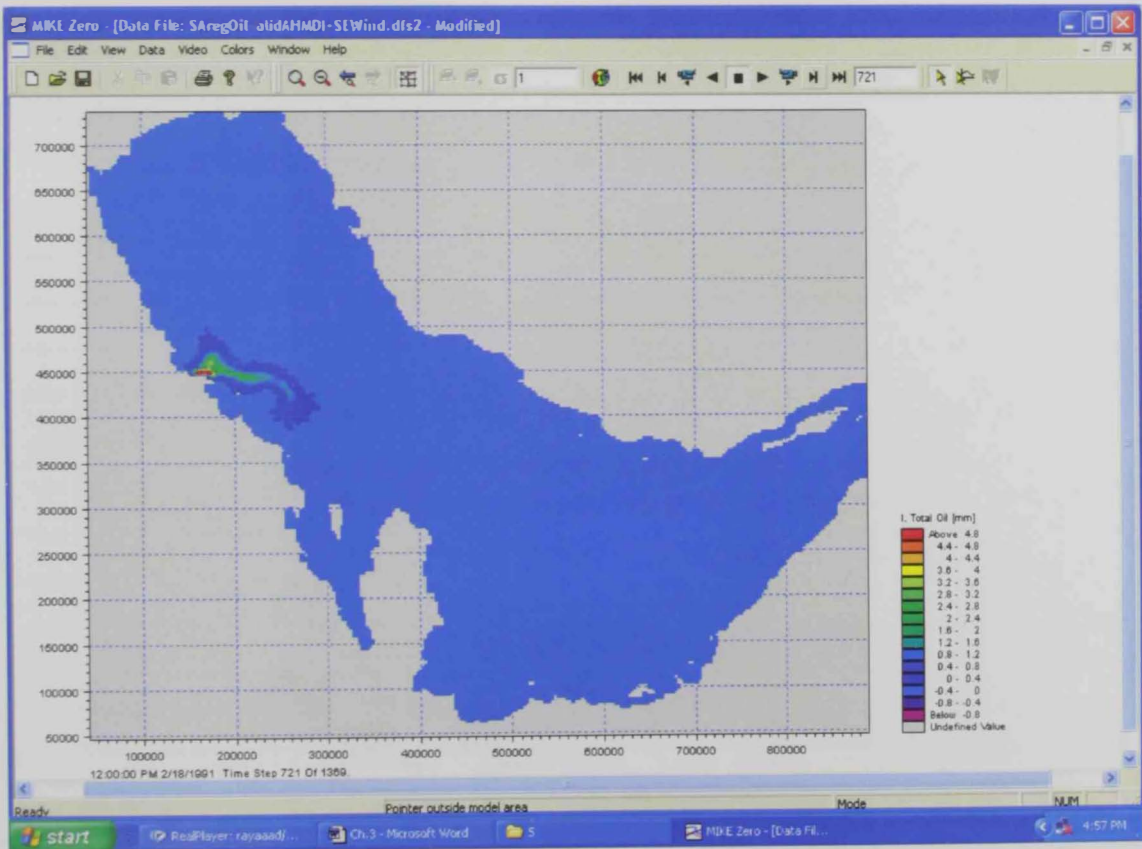


Figure 4.7b Al Ahmadi oil spill trajectory at February 18, 1991-specified wind field

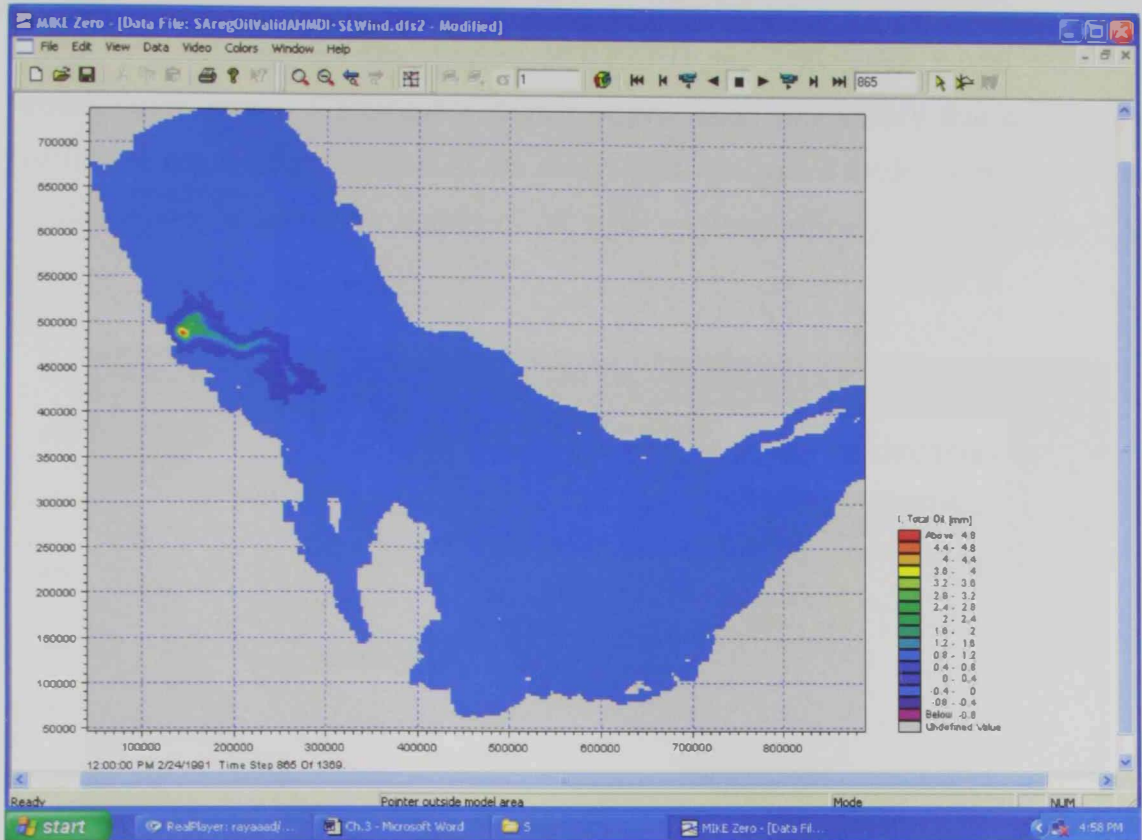


Figure 4.7c Al Ahmadi oil spill trajectory at February 24, 1991-specified wind field

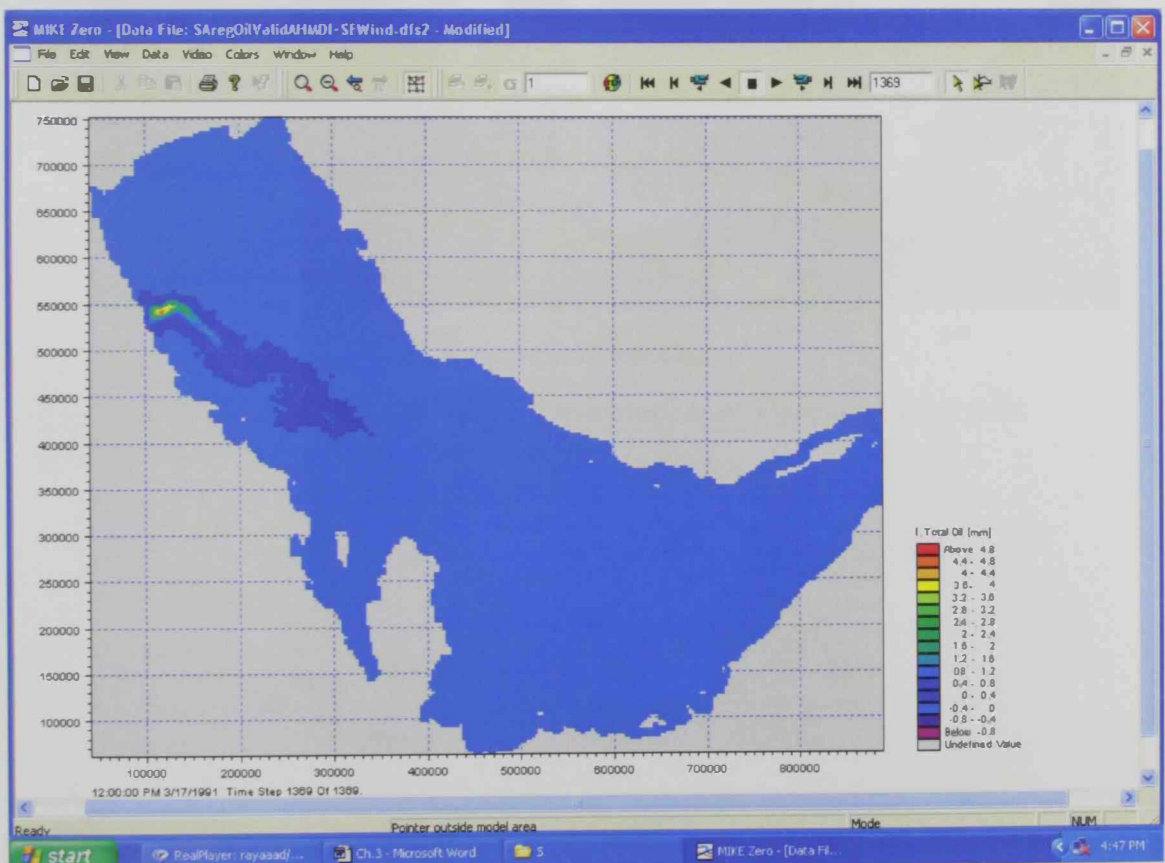


Figure 4.7d Al Ahmadi oil spill trajectory at March 17, 1991-specified wind field

It can be concluded that the coupled MIKE3-HD and MIKE3-SA model with their current setups enjoys a reasonable degree of prediction competency that enables and justifies its use for the next part of the study. That configured model is employed as a simulating tool to assess the impact of oil spills on desalination plants along the UAE coast.

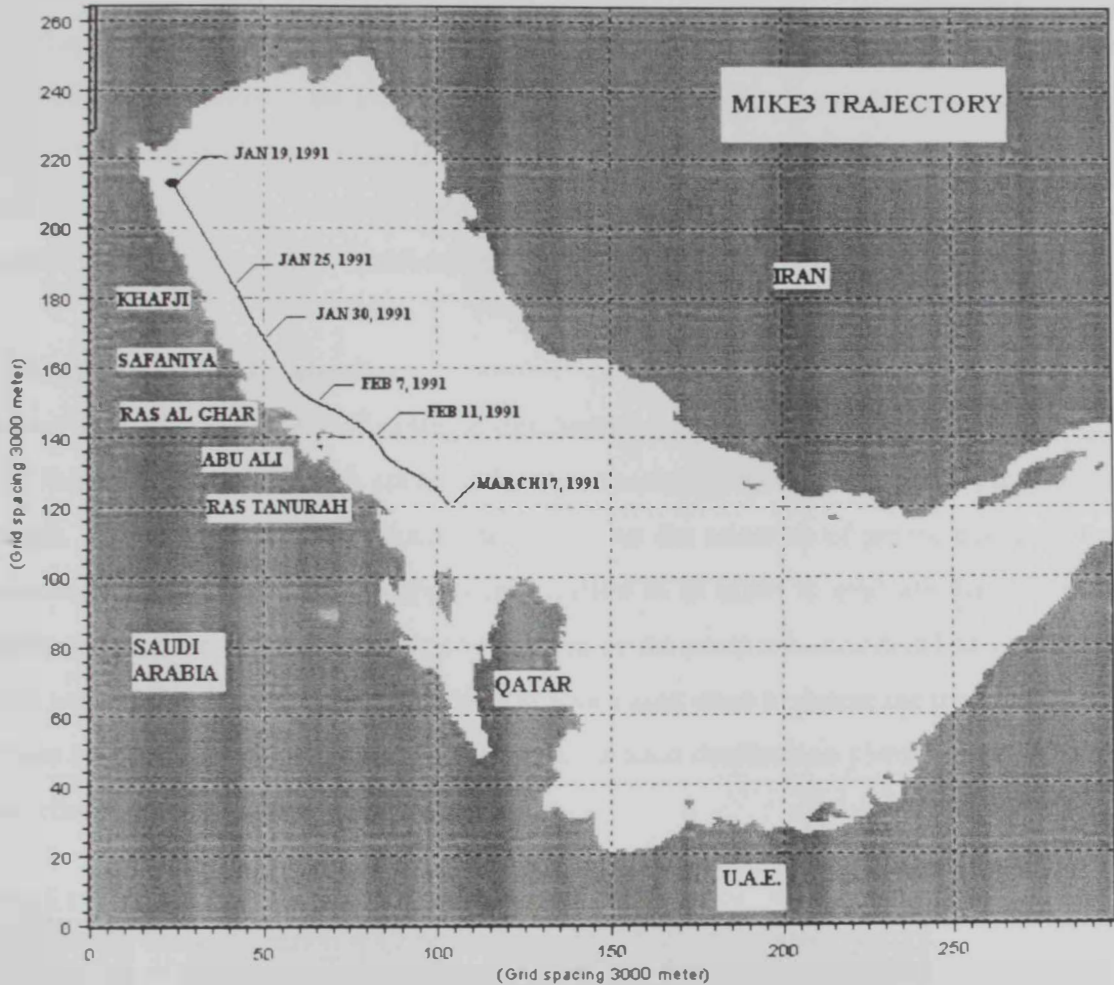


Figure 4.8 Al Ahmadi oil spill trajectory with speculated wind field

CHAPTER 5

DESALINATION PLANTS AND SOURCE ZONING

This chapter aims to define points of potential importance to the impact of oil spills with reference to desalination plant intakes along the UAE coast. Further more, zones are laid out to cover the portion of the Arabian Gulf water body adjacent to the UAE. Information on the locations of oil loading terminals and navigation routes of oil tanker are considered in identifying the zoning system distribution.

5.1 Desalination Plants Selection

Intakes of a selected number of strategic desalination plants along the UAE coast mainly in Abu-Dhabi, Dubai, and Sharjah are considered as coastal points of interest in the spill impact analysis. A search has been conducted to determine the selection of points based on their production capacity and their geographical location in an effort to evaluate the risk on the widest range of the UAE coast. The coordinates of the point are considered as observation points and time series is produced in the post processing stage to determine the arrival of oil to these specified locations. Table (5.1) lists the selected desalination plants, coordinates and production capacity in million gallons per day:

Table 5.1 Selected desalination plants along the UAE coast

Emirate	Intake Location	Coordinates in UTM-39		Capacity (MIG/day)
		Easting (m)	Northing (m)	
Abu-Dhabi	Umm Al-Nar	854153	2705831	100
Abu-Dhabi	Taweelah	871950	2744052	95
Abu-Dhabi	Mirfa	748700	2670000	38.7
Abu-Dhabi	Shuwaihat	640254	2663548	200
Dubai	Jebel Ali	937689	2797633	188
Sharjah	Layyah	943657	2809438	40

Given the relatively close distance between Umm Al-Nar and Taweela plants in Abu-Dhabi Emirate, it was decided to consider both plants as one single observation point and labeled "Abu Dhabi". Figure 5.1 shows the approximate location of the selected plants and observation points.

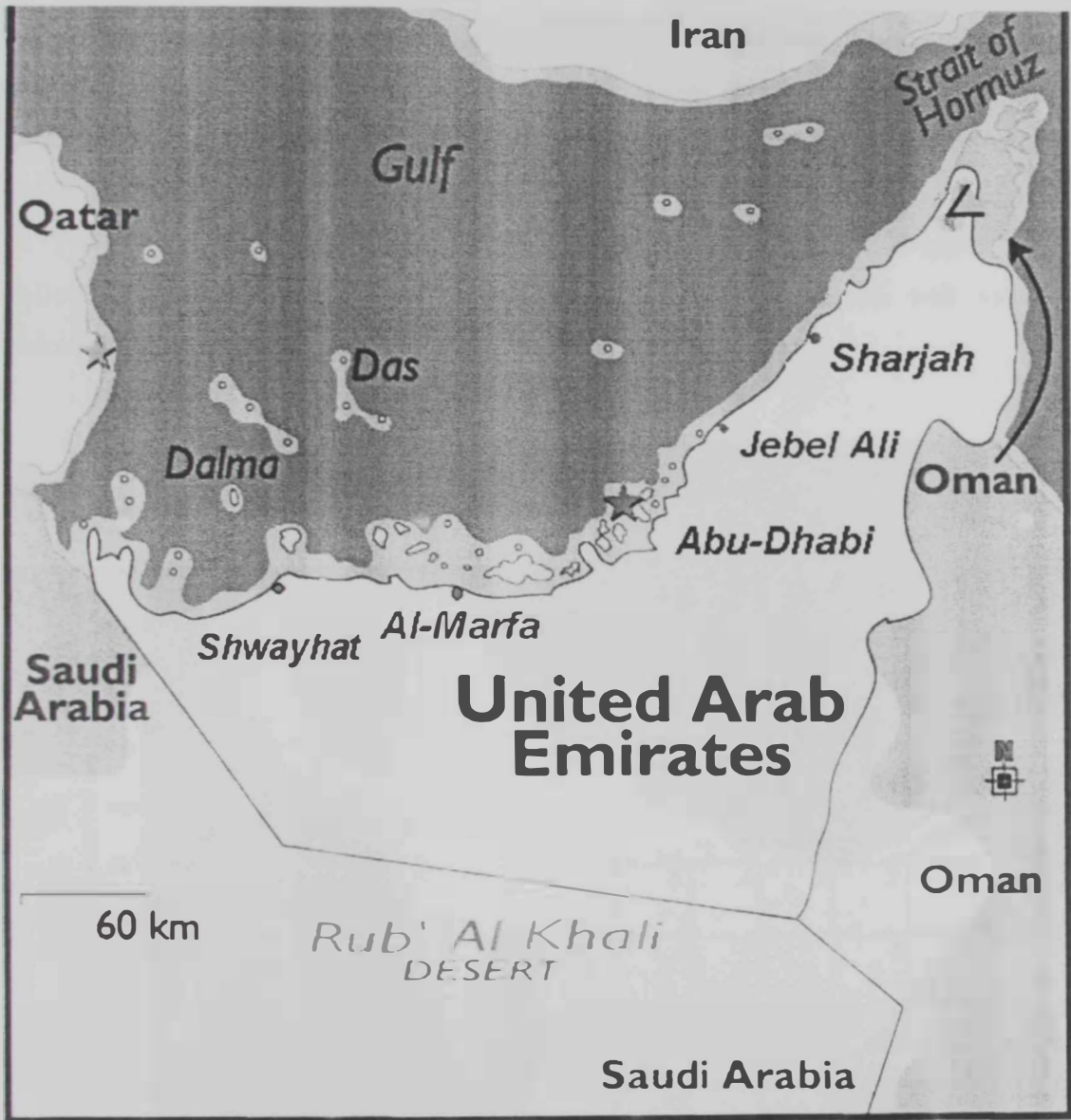


Figure 5.1 Locations of the selected desalination plants

5.2 Zoning

A zoning pattern has been produced for the area of the Arabian Gulf adjacent to the UAE (see fig 5.2). A system of 12 consecutive boxes of 75 km² each constitutes the potential oil source release zones. The adopted distribution was determined based on two constraints, first, is the actual location distribution of the oil loading terminals in the area, and second, the navigation routes followed by the oil tankers.

The use of these two determinants covers the whole journey of oil tankers in and out of the Gulf and also during loading and unloading of oil so that most potential locations of oil spill occurrence are enclosed by such zones. The information used is recovered from the Admiralty Navigation Chart no. 2889 for the Arabian Gulf. Gupta et al. (1993) includes a generalized plot describing the main navigation routes to be following the deep waters along the Iranian Coast. That plot agrees well with the Admiralty Charts.

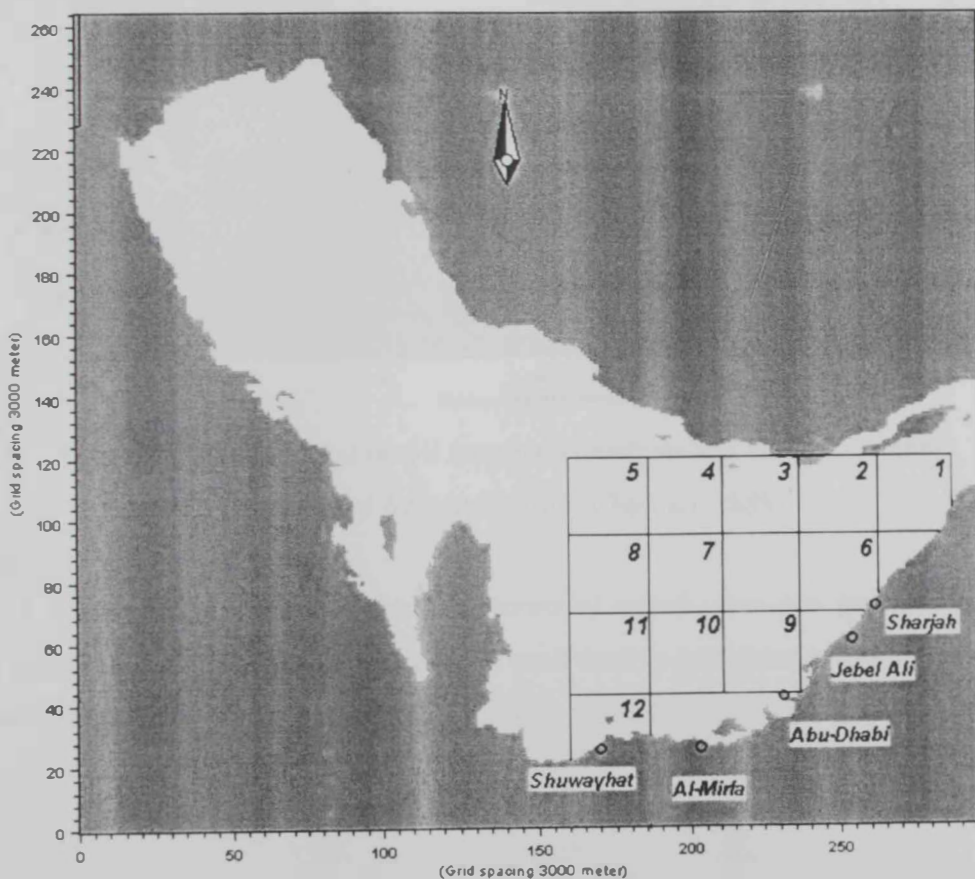


Figure 5.2 Oil spill source zones

The navigation in the shallow waters is restricted to a well defined navigation network through which oil tankers are guided by pilot tug boats in and out from the oil loading terminals. Figure (5.3) illustrates the zoning boxes in association with navigation lines and loading terminals.

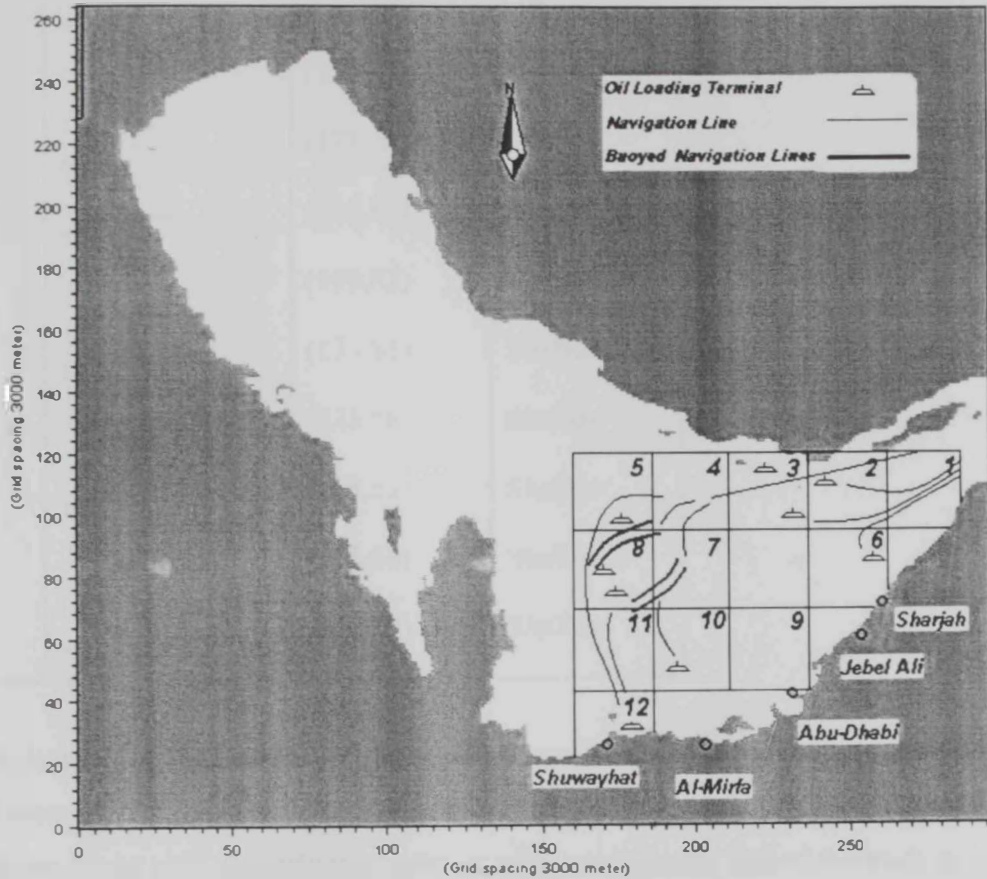


Figure 5.3 Zoning based on oil terminals locations and navigation lines
(Reproduced from Admiralty Chart no. 2889)

Table 5.2 describes the selected zones in terms of significance and point source. The point source is taken to be the center point of each zone in grid point coordinates (x,y).the symbol (\triangle) represents an oil loading terminal, while (---) indicates a navigation route.

Table 5.2 zone significance and relative oil spill source

Zone	Significance	Point source	Bathymetry
1	—	(273,108)	Deep
2	▰	(248, 108)	Deep
3	▰	(223, 108)	Deep
4	—	(198, 108)	Deep
5	▰	(173, 108)	Deep
6	▰	(248,83)	Deep
7	—	(198,83)	Shallow
8	▰	(173,83)	Shallow
9	—	(223,58)	Shallow
10	▰	(198,58)	Shallow
11	—	(173,58)	Shallow
12	▰	(173,32)	Shallow

Oil spills generated at each point source will be evaluated based on the time it reaches the desalination plant intake. Details on the oil spill scenarios and the applied wind conditions along with the various simulation results will be the aim of the study presented in the next chapter.

CHAPTER 6

OIL SPILL RESULTS AND IMPACT ASSESSMENT ON DESALINATION PLANTS

This chapter is divided into two sections; the first presents a detailed description of a sample oil spill event and the second presents the main assessment outputs of oil spill impact on major desalination plants in the UAE represented by contour maps of shortest travel times and associated wind directions. Based on oil spill trajectory, the arrival duration of the oil slick from its source point to the target desalination plant is recorded in association with the wind direction.

6.1 Results of Sample Oil Spill Event

A hypothetical oil spill event with a continuous discharge rate of $0.5\text{m}^3/\text{s}$ was introduced at zone 5 (refer to fig. 5.3) being the furthest among the designed zone distribution that could impact the UAE coast. A constant northwesterly wind with direction 274 degree, and 7m/s magnitude is applied. The trajectory and weathering rates are reported after 1, 2, and 3 weeks of spillage. The plots of trajectory and weathering estimates are demonstrated as a representative typical case to show the ability of the model to actually estimate various parameters in an oil spill occasion. Table (6.1) shows the spill parameters for the spill center, and spill leading edge at the end of the 1st, 2nd, and 3rd weeks. Figures (6.1a), (6.1b), (6.1c) represent the results extracted from the simulation at the end of week 1, 2, and 3.

The slick originating in the center point of zone 5 travels towards the UAE coast elongating in the direction of the wind and spreading laterally perpendicular to its axis. The lateral spreading is maximum at the leading edge of the migrating slick and minimum at the source release location.

The point of maximum thickness of the slick is skewed more to the releasing source location. It has a average thickness of 4.5 mm over the 3-week simulation period. Emulsification has a maximum value at the point of maximum thickness. It comprises 93% of the oil thickness at the first week, while it remains constant at the rest of the simulation at 85%. The rest of the processes are of much less contribution. Evaporation is the highest

among them with a maximum of 2% at the end of the third week, while dissolution and dispersion are of minimal rates and trace values.

An approximate constant total thickness is considered for the slick center line at each time period which is clearly decreasing with time as the slick propagates downstream away from the source supply due to the losses of weathering. The slick center line shows a constant value of maximum emulsification is constant at 85% for the total simulation period.

The leading edge thickness is the least among the slick area, having a maximum of 0.0155mm at the end of the first week and decreasing to 0.0013mm as the slick later reaches the shoreline. Emulsification percentage of the total thickness drops from 85 % during the first and second weeks to 77% as it reaches the shoreline. Losses due to evaporation at the leading edge are insignificant as it takes place at the early stages (hours or few days) of the oil spill incident.

Table 6.1 Total oil thickness and weathering estimates in

Location in the spill	Thickness (mm)	Week1	Week2	Week3
Point of maximum	Total	4.49	3.99	5.09
	Emulsification	4.19	3.37	4.32
	Evaporation	0.037	0.083	0.11
	Dissolution	3.5E-8	9.87E-8	1.18E-7
	Dispersion	1.1E-5	2.48E-5	3.49E-5
Spill center line	Total	2.82	1.35	1.08
	Emulsification	2.4	1.14	0.92
	Evaporation	0.0015	3.4E-5	1.4E-5
	Dissolution	7.2E-10	2.67E-10	1.8E-10
	Dispersion	2.86E-6	2.89E-6	1.9E-6
Leading edge	Total	0.0155	0.0026	0.0013
	Emulsification	0.0132	0.0022	0.001
	Evaporation	6.5E-9	2.66E-10	1.3E-10
	Dissolution	3.9E-14	3.36E-15	1.7E-15
	Dispersion	4.25E-10	2.56E-11	1.7E-11

The slick covers an approximate total area of 13 000 km² as it reaches the shoreline. The leading edge of the slick is moving at an average velocity of 16.8 km/day reaching the UAE shoreline at Jebel Ali in approximately 433 hrs (18 days).. It is also clear that the slick direction is dominated by the 7m/s wind field driving force. Currents are insignificant in the total slick movement. After 11 days of release and about 80 km offshore the slick enters the shallow waters which tend to distort the track of the slick deflecting its leading edge from southeast to the south.

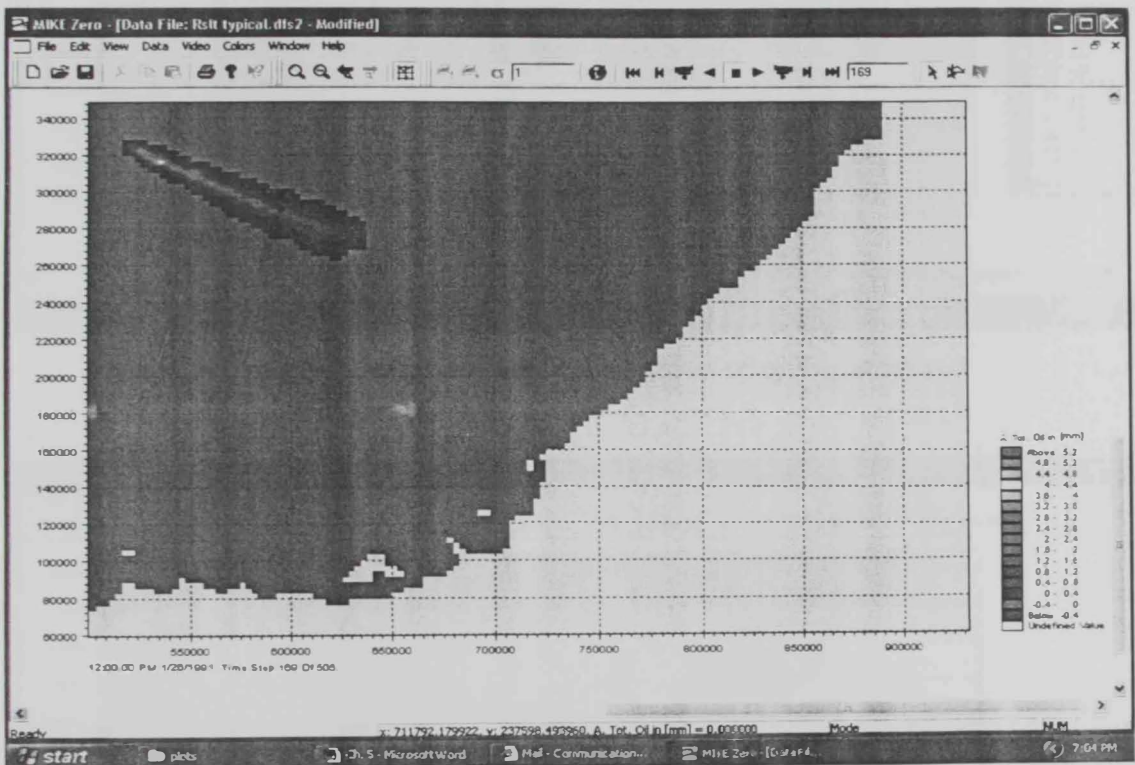


Figure 6.1a Trajectory and total thickness of spill-1 week age

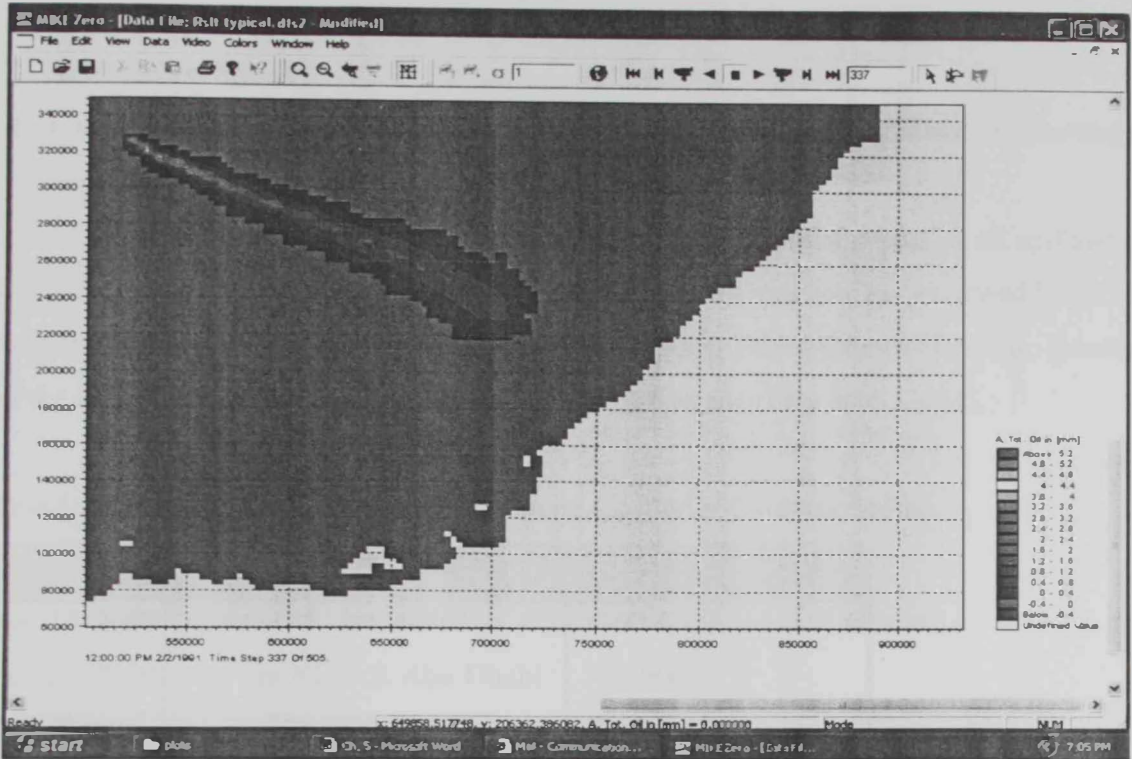


Figure 6.1b Trajectory and total thickness of spill - 2week age

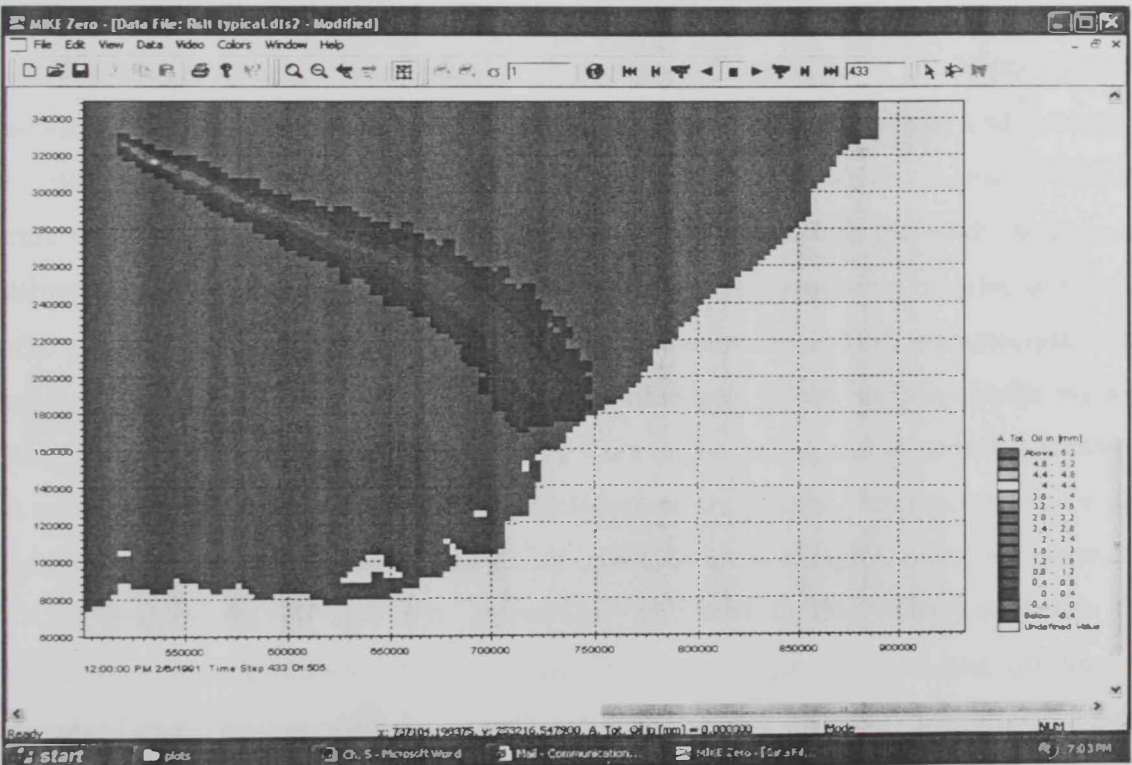


Figure 6.1c Trajectory and total thickness of spill - 3week age

6.2 Oil Spill Impact Assessment on Desalination Plants

6.2.1 Release Conditions

In this section oil spill release conditions and wind parameters are discussed and the target case scenarios are outlined.

Oil spills threat in the UAE is significant. Among numerous events of oil spillage in the UAE waters, some events, reported with very limited information, are reviewed herein to establish basis for oil spill scenarios release characteristics. Table (6.2) lists the date, location and the spilled volume of major events during the last decade (Essa et al., 2004).

Table 6.2 Reported oil spill events, approximate location and volume spilled

Date	Location	Volume spilled (ton.)
Jan. 14, 2001	1.6 km O.S. Jabal Ali	1300-1500
Jan. 24, 2000	11.5 km NE O.S. Abu Dhabi	300-900
Jan. 7, 1998	8 km O.S. Ajman	5000-1000
Mar. 30, 1994	16 km O.S. Fujairah	16000

It is noticed that these reported events are all occurring in the winter season from January to March, which is characterized with strong winds and high sea conditions. Another observation is that all occasions are occurring at locations near the coast and extending northeast from Abu Dhabi city along the coastline towards Sharjah and Ajman. While no events west of Abu Dhabi city are reported, Fujairah is outside the study area as no desalination plants have been designated in these areas. Such events are reported to receive public attention due to their visual impact on coastal communities. They are associated with small general-purpose tankers that could possibly navigate in the shallow depths without getting wrecked. Much larger events occurring from larger tankers and oil terminal accidents that would have an impact at less developed locations are possibly not reported due to the remoteness of the occasions and the less direct impact on areas of high population centers.

Therefore, the oil spill risk assessment addressed in this study and hence the considered zones are selected to cover the crowded navigation routes and oil loading terminals. The navigation of Shallow depth non-restricted GP tankers is partially addressed by oil spills from zones 1, 6, 9, and 12 at 10 to 50 km offshore.

The oil spill modes of release are very erratic and governed with a case by case special features associated with the cause of release, tanker size, sea state, oil type, site conditions and other factors. Therefore, further numerical tests were made to investigate the effect of release mode on slick migration.

Two modes of release; continuous and intermittent, were tested using the SA model against arrival time and location. Both cases showed very close results with about 1 hour deviation in the simulated travel times out of a three-week simulation. Both spills impacted the same location. Furthermore, the release discharge rate was investigated using 10.5 and 0.5 m³/s respectively. Both results have also showed identical arrival times and final destinations. Table (6.3) summarizes the output of the above tests on the stated parameters.

Such results rule out the need to use different discharge rates in the current study. Hence, any estimate of oil release would fulfill the requirement of reporting the arrival time and still serve the current objectives.

Table 6.3 Shore arrival time using different release modes

Type	Rate (m ³ /s)	Amount (m ³)	Arrival (hrs)	Max. thickness (mm)
Continuous	0.5	907 200	431	5.6
Intermittent 1 day	10.5	907 200	432	15.5
Intermittent 1 day	0.5	43 200	433	0.67

The dates of the reported oil spill accidents indicate that winter season conditions are more critical for oil spill occurrence. The stronger residual currents observed in the winter hydrodynamic simulation results compared to the summer currents (Ch.3) would result in shorter travel times of the migrating slicks. Another fact is that winter conditions produce less losses from the oil slick due to retarded evaporation which counts for more than 25% of the losses and hence would have more damaging potential. Hence, winter conditions are adopted on basis of extreme case scenarios.

Simulations are applied on a set of hypothetical oil spills located at the center point of each zone. The source of oil spills at all zones consider medium crude (Venezuelan) with an intermittent 1 day release and an average discharge rate of 0.5m³/s.

6.2.2 Approaches of Identifying Critical Trajectories

Considering the worst extreme cases and observing the historical records of wind conditions in the gulf, constant wind with magnitude of 7m/s is applied.

Thirteen consecutive wind directions are applied starting from the west (270 degree) and ending with the east (90 degree) with 15 degrees increment one at a time. Three additional incremental wind fields are considered to account for the deflection caused by the Coriolis effect in the southern western quadrant.

A set of oil spill events are simultaneously released from all 12 zones (figure 6.2) and subjected to incremental wind fields. The travel times of different slicks hitting the neighborhood of various desalination plants are reported for each wind field. The results of the thirteen incremental wind fields are analyzed and sorted in terms of the shortest arrival times associated with slicks generated from various zones to a given desalination plant. In such manner, the arrival time would be conservative over any other indirect wind combination. Using the shortest arrival times in association with each source zone, a shortest-arrival-time contour map is produced for each destination (desalination plant).

The above approach however, produces some cases of uncertainty as the oil slicks in some incidents did not hit the desalination plant directly and needed additional time for along-shore movement. While in other cases, some islands located in the course of migrating slicks extend the arrival time significantly. Another case related to this approach, is the overlap of new slicks reaching the shore following earlier ones that have spread along the shoreline. In such case, some approximation is made to estimate the arrival time of the new spill to the destination in the presence of the older one. To overcome such implications, the visual judgment is directed to report somehow underestimated travel time for conservative determination.

In order to verify the first approach and to minimize the effect of observed cases of uncertainty, a second approach is investigated to produce the shortest arrival time and critical wind direction. In this approach, the exact angle between the source and the destination was measured and the Coriolis effect is considered to specify the wind direction in order to direct the slick hitting the destination exactly. However, the calculated angle is modified using trial and error approach to account for the trajectory deflection taking place once the slick enters the shallow areas close to the shore (see fig 6.1c).

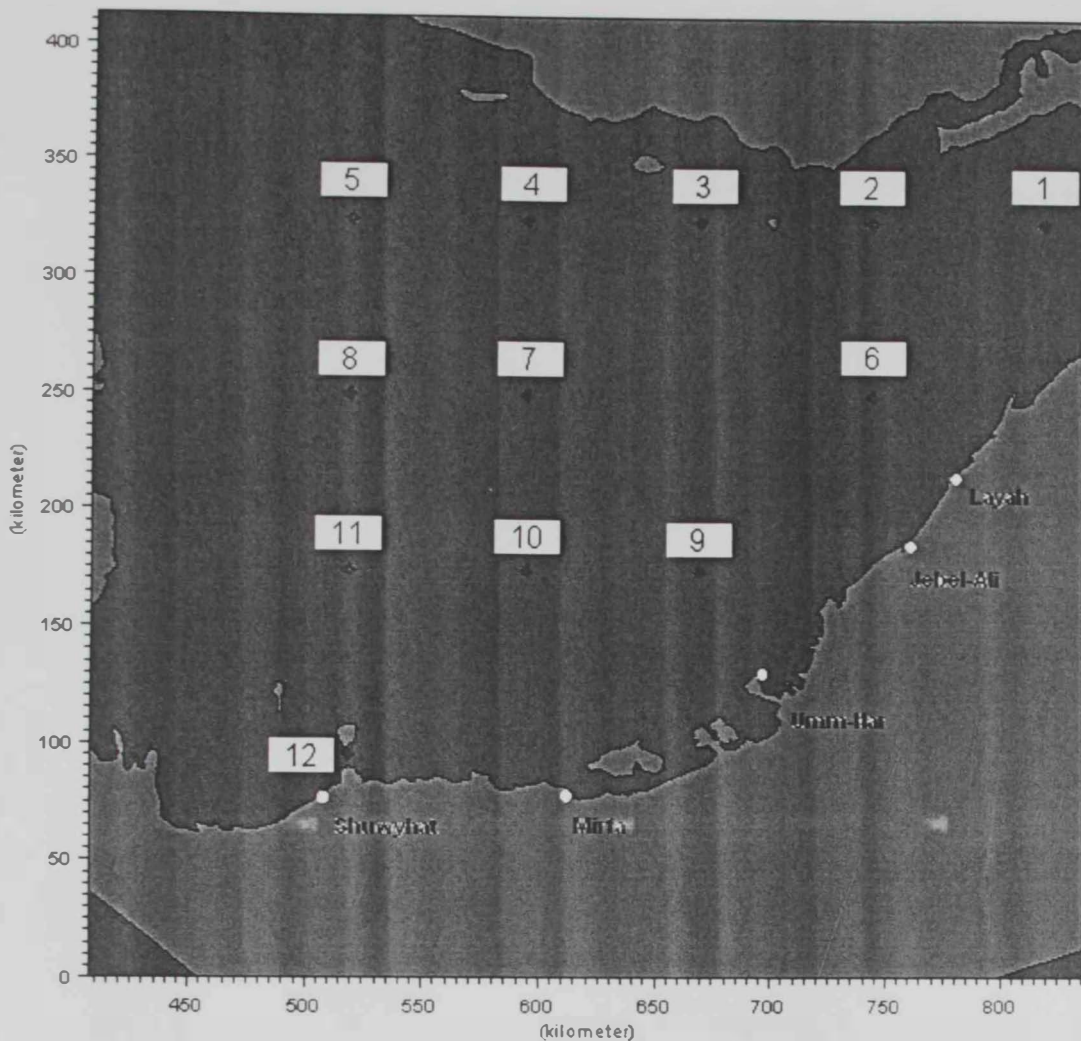


Figure 6.2 Locations of oil spill sources and destinations

The second approach produces either similar or shorter travel time in cases of unrestricted slick courses, while it has proved that visual approximation adopted in cases of oil overlapping in the first approach has been underestimated. The second approach has also over ruled all the uncertainties of the first approach. Therefore the results of the second approach are considered in producing the final contour maps of the travel time and wind direction for the five desalination plants.

Upon inspection of the early versions of contour maps, it was decided to introduce 3 supplementary zones (13, 14, 15) in several maps in order to refine the coarse resolution of travel time and wind direction observed in some areas (see figure 6.3).

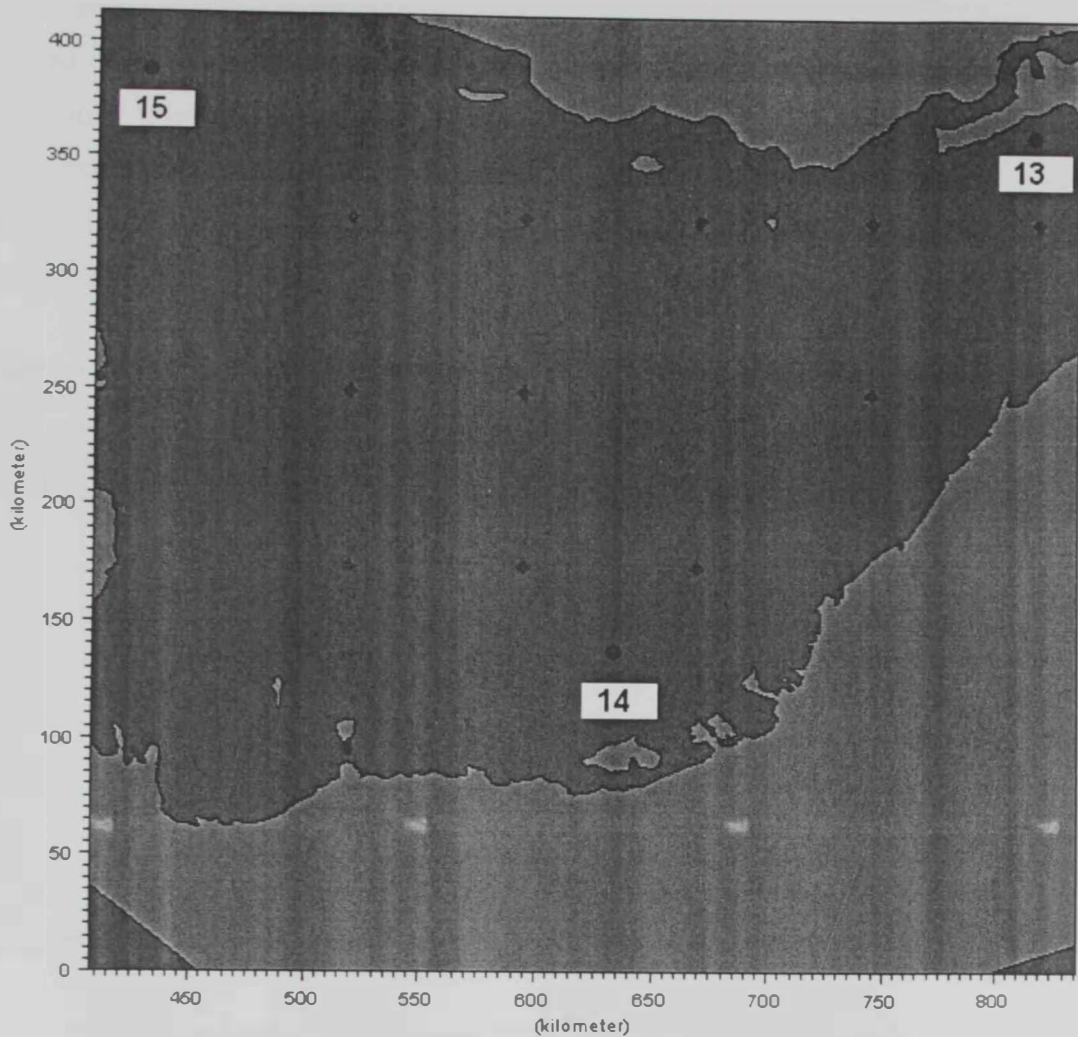


Figure 6.3 Supplementary enhancement zones

A 30 day simulation period using winter conditions is conducted in all considered scenarios from January 19 to February 18. The results of a total number of 64 simulations are analyzed and tabulated and contour maps are produced for travel time and associated wind directions for each desalination plant. Such contour maps are presented and described for each desalination plant in the following sections.

It is worth noting here that due to interpolation confusions, values for wind directions from the first quadrant has been added to 360° in order to be able to represent them correctly in the contour map. Hence to obtain the right direction for a wind value that exceeds 360° , 360° should be subtracted.

6.2.3 Shuwayhat Desalination Plant

Located at about 28km Southwest Jebel Dhanna oil loading terminal, Shuwayhat desalination plant has the shortest oil travel time as it is the closest destination point to the source representing zone 12. Oil spills propagation from other sources is always delayed by the presence of Sir Bany-Yas Island forming a natural barrier. Delay time has a maximum value of 49 hrs.

Table 6.4 Critical arrival times and corresponding wind direction for Shuwayhat desalination plant

zone	Travel time (hrs.)	Travel time (days)	Wind direction (clockwise from North)
1	472	19.66	26
2	421	17.54	17
3	359	14.95	1
4	333	13.87	347
5	320	13.33	330
6	322	13.41	26
7	236	09.83	353
8	233	09.70	328
9	210	08.75	28
10	146	06.08	8
11	119	04.95	330
12	21	00.87	352

Travel time contours range from 50 to 450 hrs. (approximately 2-19 days) over the modeled area. Large travel times (greater than 300 hrs) are occurring from the northern eastern corner in association with northeastern wind (40°). Most critical travel times associated with spills originated from the northern areas straight above the plant are brought about by the northwestern winds (330°). Wind direction contours are forming a hand fan shape with its origin at the shuwayhat plant.

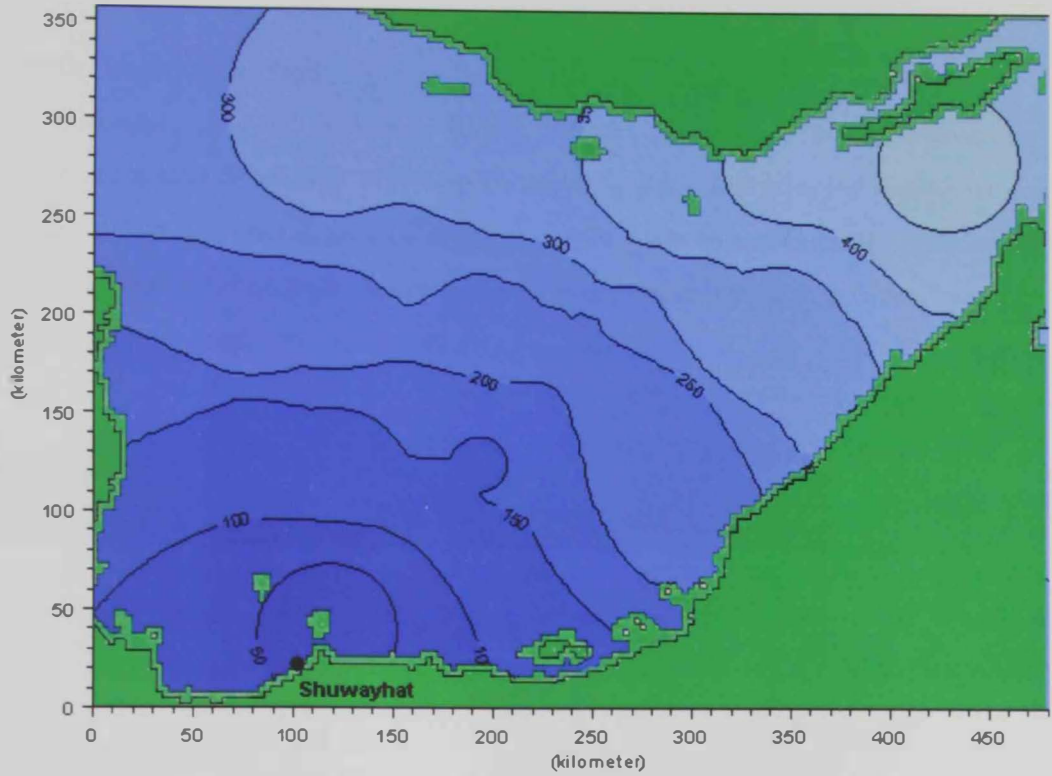


Figure 6.4a Shortest arrival times to Shuwayhat desalination plant

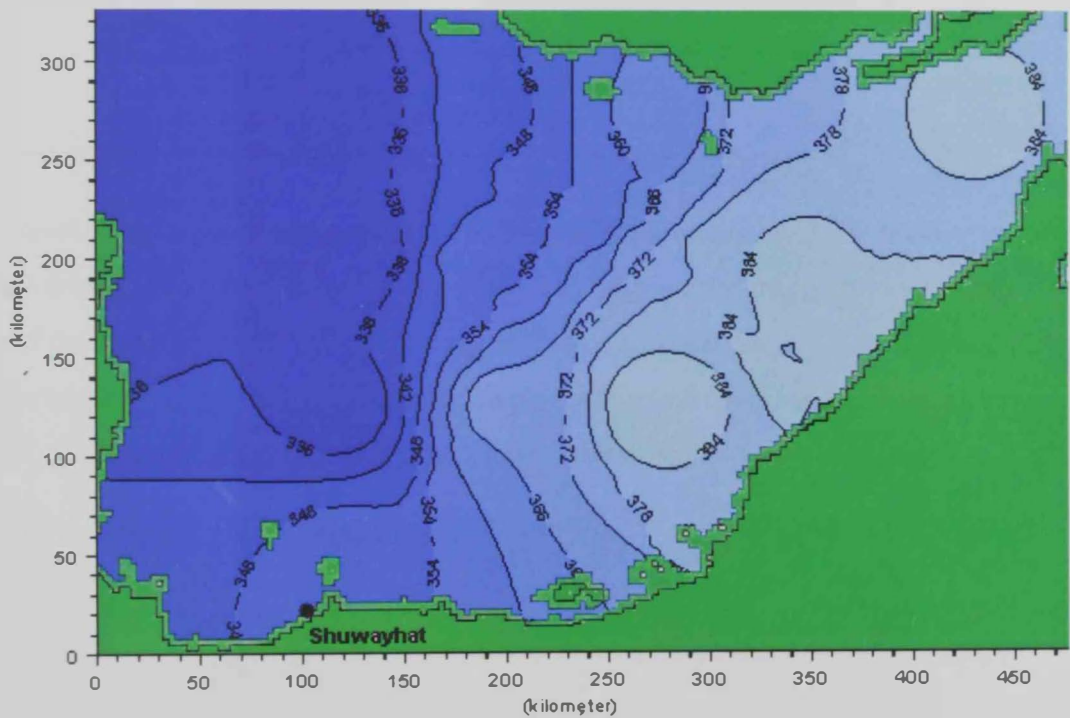


Figure 6.4b Critical wind direction in association to oil zones targeting Shuwayhat (note: values exceeding 360° should be reduced by 360°)

6.2.4 Mirfa Desalination Plant

Located Southwest of Abu AlAbiad Island, Mirfa desalination plant receives a considerable protection from most of the spills targeting the plant from the source zones which in turn delays the arrival time of oil spills to the plant to a maximum value of 65 hrs. The supplementary zone # 14 was introduced to the contour map in order to improve the Mirfa arrival time contour map.

Table 6.5 critical arrival time and wind direction to Mirfa in association with each zone

zone	Travel time (hrs.)	Travel time (days)	Wind direction (clockwise from North)
1	333	13.87	13
2	318	13.25	356
3	332	13.83	337
4	318	13.25	321.5
5	378	15.75	306
6	210	08.75	7
7	220	09.16	315
8	336	14.00	297.5
9	118	04.91	355
10	140	05.83	305
11	195	08.12	280
12	145	06.04	245
14	70	02.91	335

Travel time contours range from 80 to 360 hrs (approximately 3-16 days) over the modeled area. Large travel times (greater than 280 hrs) are occurring from the northern region of the study area with critical forcing of wind directions ranging from 255 to 360°. Winds originating at the fourth quadrant and at part of the first quadrant are most critical to drive oil slicks to the plant as it dominates over the entire study area from northwest to north.

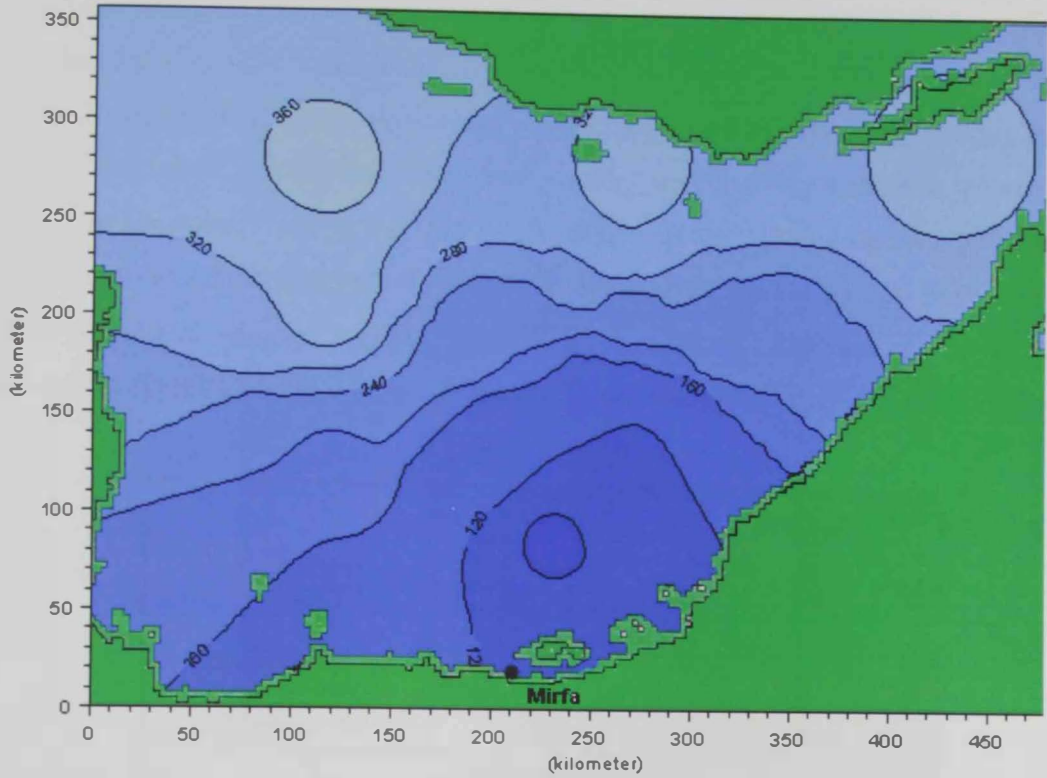


Figure 6.5a Shortest arrival times to Mirfa desalination plant

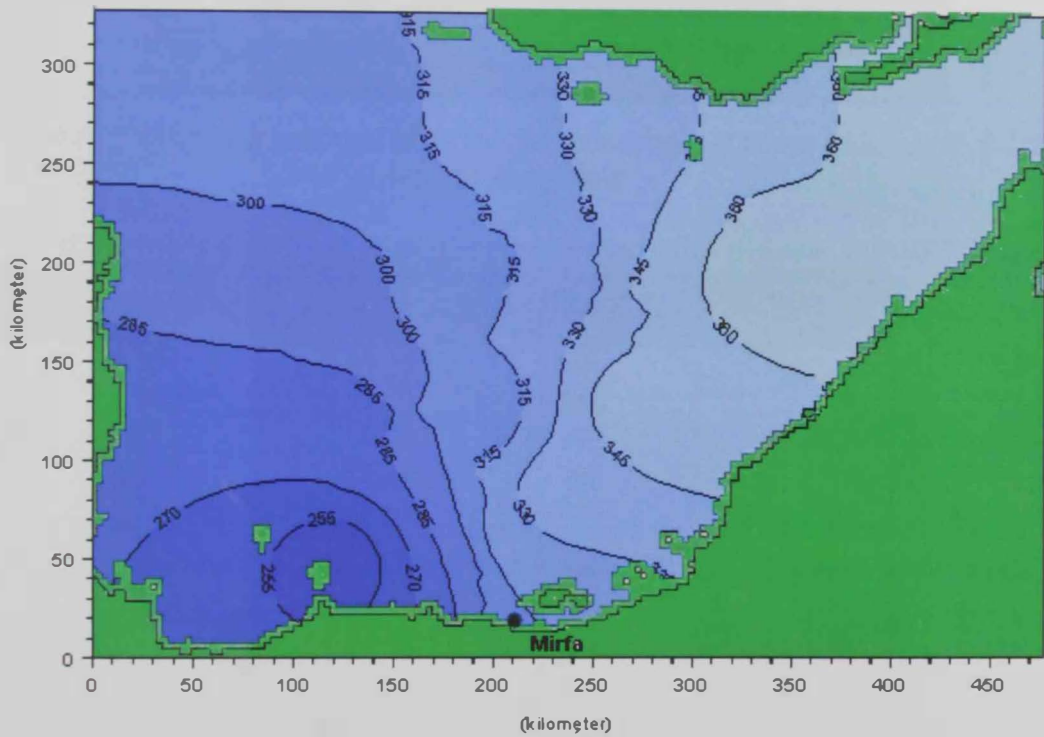


Figure 6.5b Critical wind direction in association with shortest arrival times to Mirfa Plant (note: values exceeding 360° should be reduced by 360°)

6.2.5 Abu Dhabi Desalination Plants:

Two mega desalination plants of Abu Dhabi (Umm AlNar and Taweelah) are serving the emirates of Abu Dhabi, the capital of the UAE. As they are relatively located in the same area, they are considered here as one destination. The location of Mina Zayed is selected as a destination to give conservative estimate of the shortest arrival time to both plants that are located inside the lagoon system of Abu Dhabi. Simulations from the supplementary zone #15 was introduced to improve the resolution of arrival time contour map.

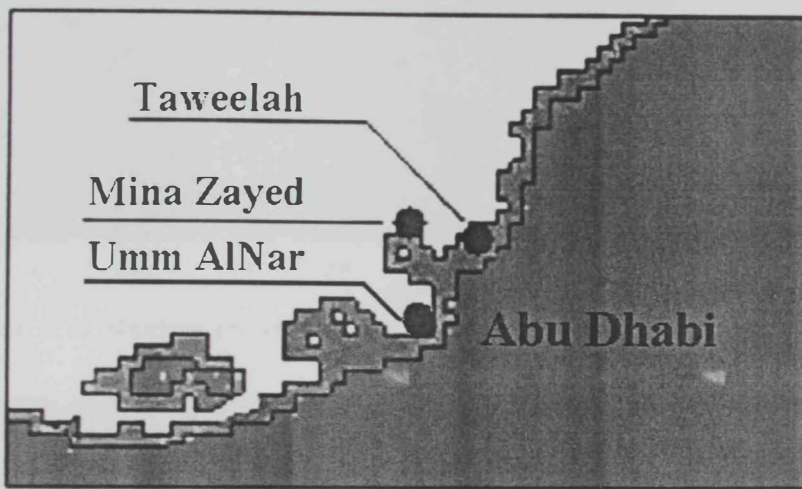


Figure 6.6 Approximate location of Mina Zayed, Taweelah and Umm AlNar desalination plants in Abu Dhabi

Table 6.6 critical arrival time and wind direction to Abu Dhabi in association with zones

zone	Travel time (hrs.)	Travel time (days)	Wind direction (clockwise from North)
1	234	09.75	6
2	203	08.45	348
3	222	09.25	322
4	267	11.12	303
5	327	13.62	290
6	118	04.91	351
7	205	08.54	285
8	306	12.75	272
9	57	02.37	296
10	176	07.33	258
11	292	12.16	252
12	268	11.16	233
15	466	19.41	283

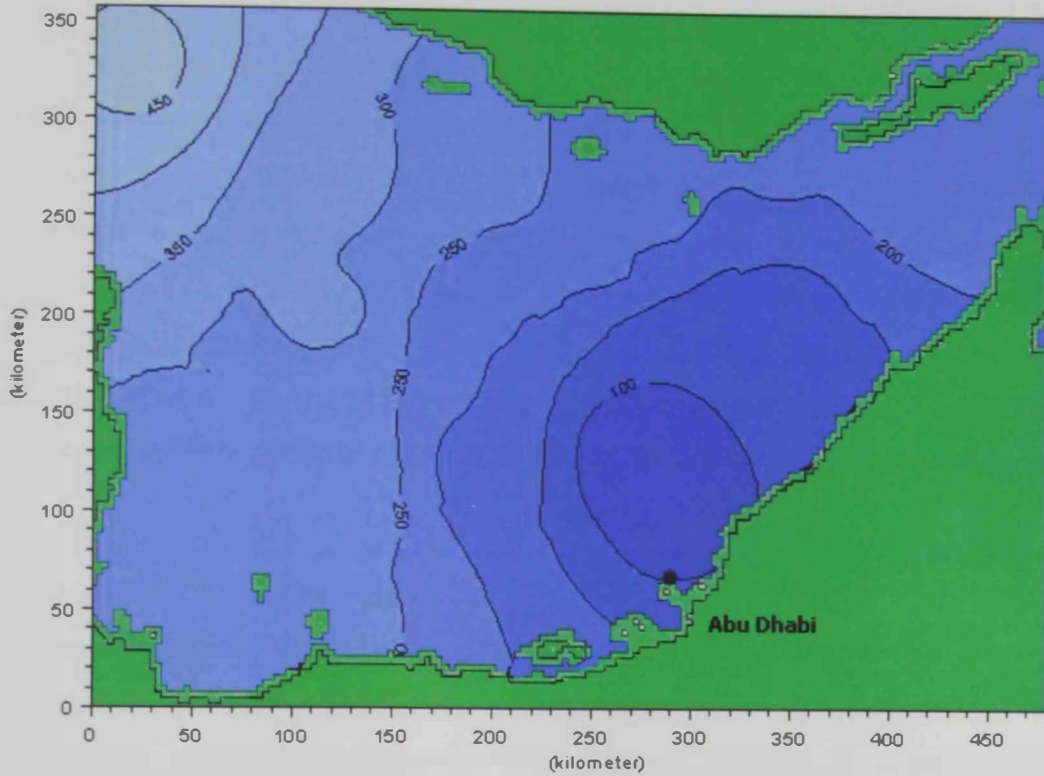


Figure 6.7a Shortest arrival times to Abu Dhabi desalination plant

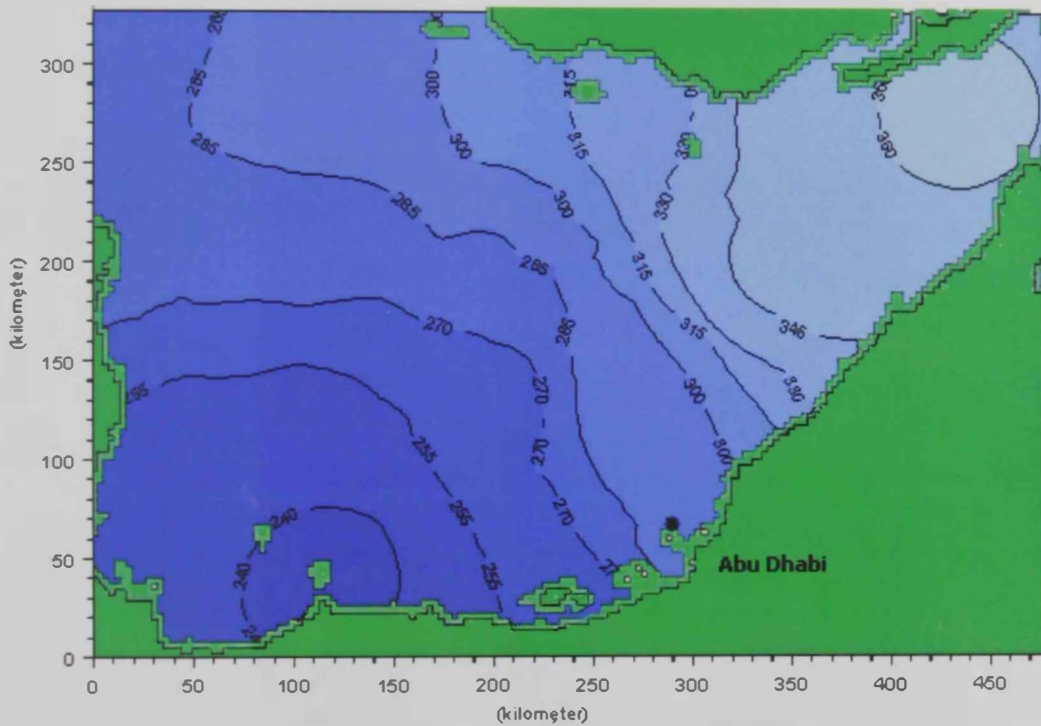


Figure 6.7b Critical wind direction in association with shortest arrival times to Abu Dhabi des. Plants (note: values exceeding 360° should be reduced by 360°)

Travel time contours range from 100 to 450 hrs (approximately 4-19 days) over the modeled area. Large travel times (greater than 400 hrs) are occurring from the northwestern corner in association with northwestern wind (280°). The wind direction contour lines are evenly distributed towards the northeast and southwest from 240 to 360° except for the two far corners comprising the minimum and the maximum effective directions. The even distribution suggests that all wind directions originating at the fourth quadrant and part of the first and third quadrants are thought to have equal importance and hence Abu Dhabi plants have the widest critical wind direction range among other plants.

6.2.6 Jebel-Ali Desalination Plant:

Approximately 100 km Northeast of Abu Dhabi, Jabal-Ali desalination plant is located with its 180 million gallons per day capacity, being the only desalination plant serving Dubai Emirate. A supplementary zone #13 is introduced to improve the contour of travel time northeast of Jebel-Ali Desalination plant. It is thought at this stage that the introduction of other supplementary zones at the west and northwest would further improve the travel time contours in that area.

Table 6.7 Critical arrival time and wind direction to Jebel-Ali in association with zones

zone	Travel time (hrs.)	Travel time (days)	Wind direction (clockwise from North)
1	159	06.62	357
2	140	05.83	325
3	182	07.58	297
4	265	11.04	281
5	329	17.70	274
6	67	02.79	314
7	249	10.37	255
8	337	14.04	256
9	164	06.83	238
10	267	11.12	235
11	272	11.33	239
12	396	16.50	224
13	231	09.62	356

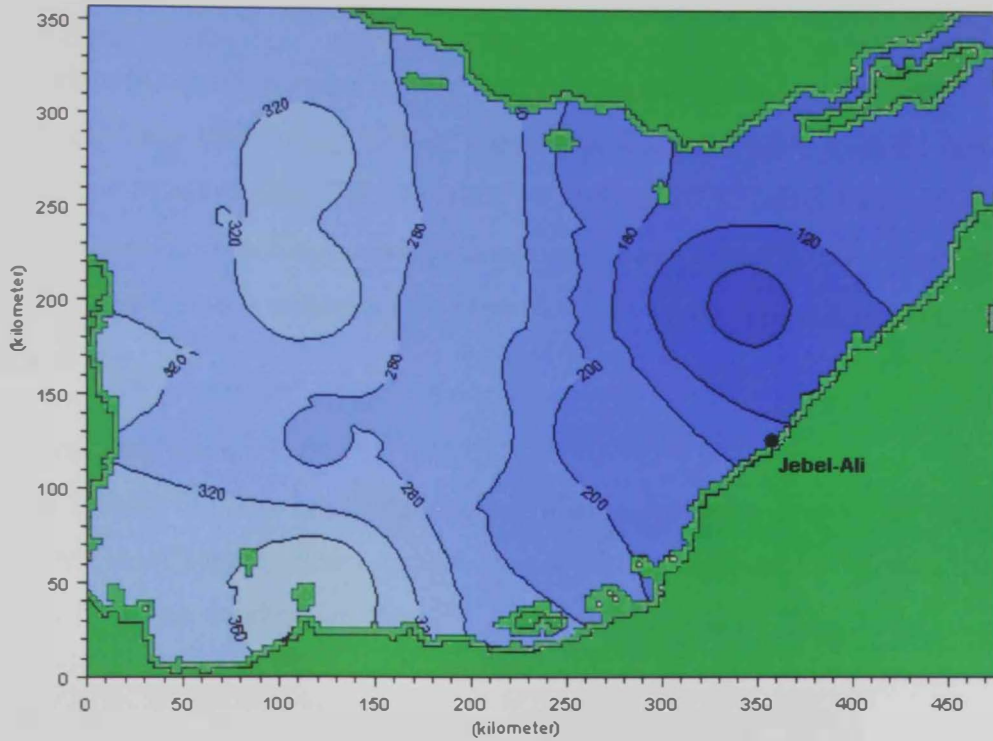


Figure 6.8a Shortest arrival times to Jebel-Ali desalination plant

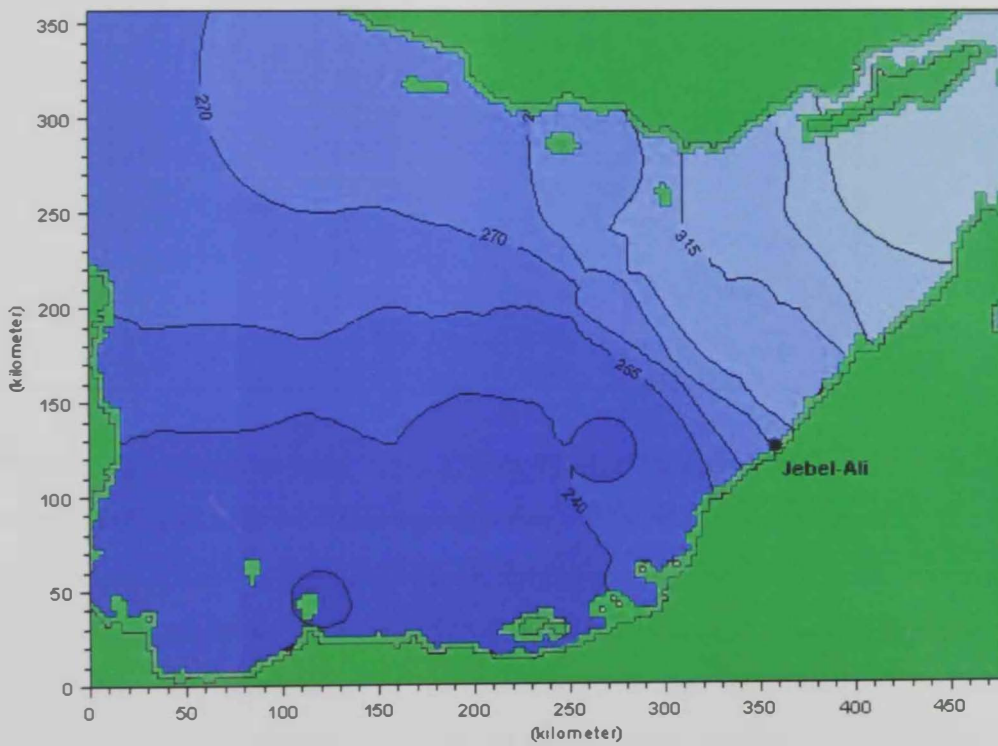


Figure 6.8b Critical wind direction in association with shortest arrival times to Jebel-Ali des. plant (note: values exceeding 360° should be reduced by 360°)

Travel time contours range from 80 to 360 hrs (approximately 3-15 days) over the modeled area. Large travel times (greater than 300 hrs) are occurring from the northern western corner in association with northwestern wind (270°). Travel times associated with spills originated from the northwestern to northern areas straight above the plant are brought about by the northwestern winds (240-315°). Contours are again fanning around the origin at Jebel Ali.

6.2.7 Layah Desalination Plant:

Located in Sharjah Emirate, Layah desalination plant supplies fresh water to well over 500 000 persons. A supplementary zone # 13 was used to improve the Contour map of arrival time for Layah desalination plant.

Table 6.8 critical arrival time and wind direction to Layah in association with zones

zone	Travel time (hrs.)	Travel time (days)	Wind direction (clockwise from North)
1	119	04.95	351
2	115	04.79	310
3	171	07.12	282
4	259	10.79	271
5	331	13.79	264
6	62	02.58	268
7	261	10.87	248
8	352	14.66	248
9	225	09.37	215
10	302	12.58	227
11	407	16.95	233
12	455	18.95	220
13	167	06.95	346

Travel time contours range from 120 to 440 hrs (approximately 5-18 days) over the modeled area. Large travel times (greater than 400 hrs) are occurring from the west and northwestern corner in association with northwestern wind (270°). The travel time contours are denser in the west, and the 120-80 hrs smallest contour covers the area near the plant. Again the application of supplementary zones has refined the contour distribution. The wind direction of 270° is the most critical direction acting at the area above the plant.

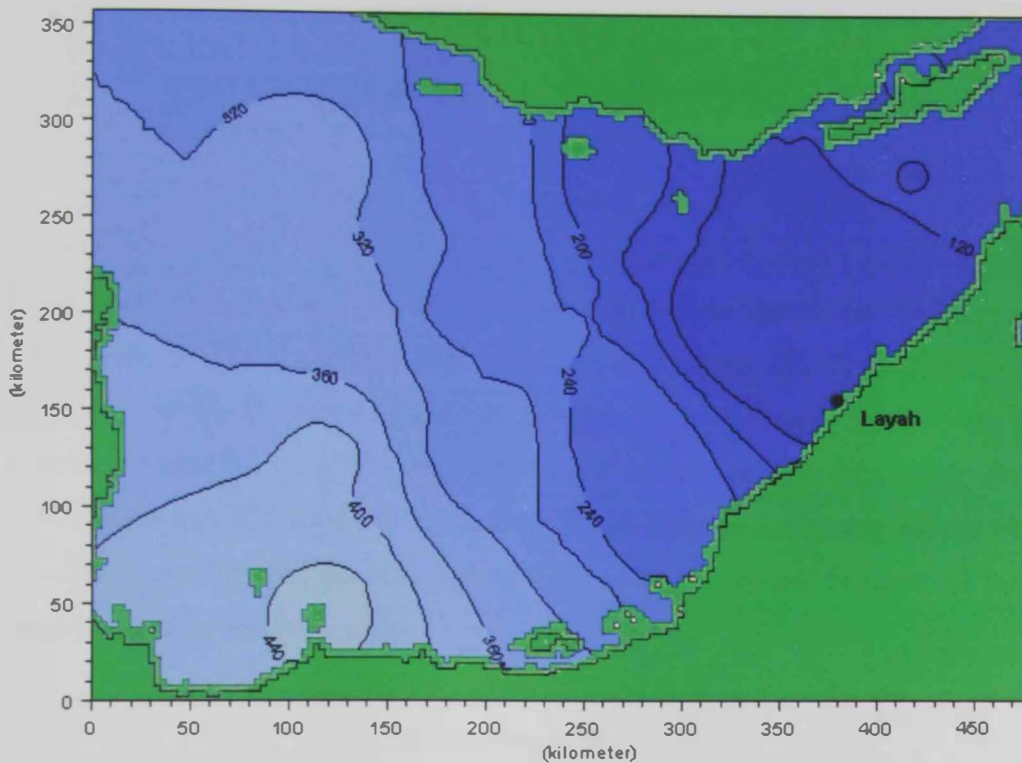


Figure 6.9a Shortest arrival times to Layah desalination plant

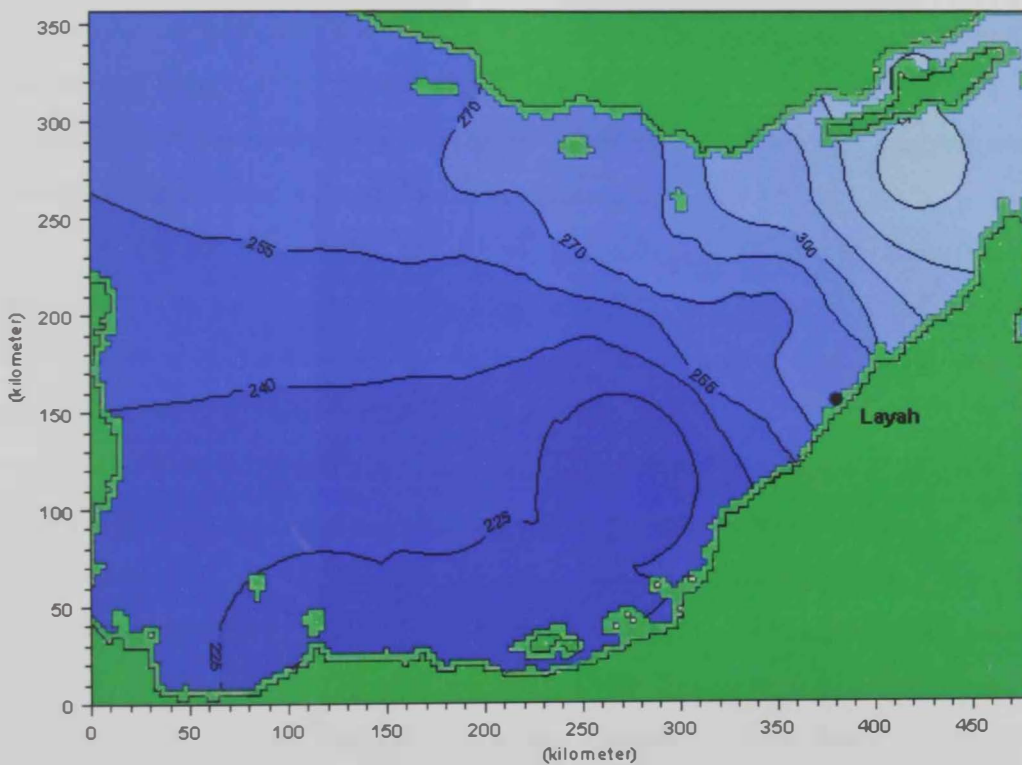


Figure 6.9b Critical wind direction in association with shortest arrival times to Layah des. Plant (note: values exceeding 360° should be reduced by 360°)

CHAPTER 7

SUMMARY AND RECOMMENDATIONS

The current study has aimed to produce a set of 10 hazard contour maps for the prediction of oil spill travel time and critical wind direction in association with five selected mega desalination plants along the UAE coast. Al-Shuwayhat, Al-Mirfa, Umm AlNar and Taweelah, Jebel Ali and Al-Layah were selected as the most vital plants and their locations were set as observation points. To achieve such a task, three stages were carefully designed to form the operational frame work of the study; the hydrodynamic simulation, the oil spill simulation, and the impact assessment in terms of the contour maps processing and production.

Advanced modeling techniques were employed to simulate the 3D dynamics of water motion and oil weathering and transport in the Arabian Gulf.

The hydrodynamic model is set based on light of previous work conducted in the Gulf and a comprehensive review of literature on the topic. The hydrodynamic model was further tuned and validated against actual field data of tides and currents. Also the comparison of the model results with published articles describing summer and winter residual surface currents showed to be in agreement.

In the oil spill model, sensitivity analysis is conducted to identify the model parameters. The assigned model setup was tested against the available information on Al Ahmadi oil spill travel time, spreading and shore impact. The model proved to be performing fairly in agreement with the published data.

The stage of impact assessment comprised of assigning a set of 12 zones covering the oil tankers routes and loading terminals in the area adjacent to the UAE coastline. Three additional zones supplemented the original zones during the first stage of reviewing the output of contour maps in order to improve its resolution. The testing of oil releasing conditions yielded the decision to use intermittent oil spill. Extreme case scenario approach was adopted and winter conditions were found statistically more critical for oil spills to occur. Two approaches were tested to ensure a refined production

of travel time. The direct approach from source to destination is adopted as it has ruled out the indirect approach implications and uncertainties.

By assigning a constant wind field over the study area, a total number of 64 simulations were conducted to produce the contour maps for the five desalination plants. Two maps were produced for each plant, the first reports the shortest arrival times from different source points and the second shows the critical wind direction that causes the oil spill to hit the plant in association with its counterpart arrival time.

The produced maps are of practical and direct benefit for the operators of the desalination plants and the water authorities and further, the environmental agencies in the United Arab Emirates. The source/destination travel time of an oil slick at any time is directly spotted and the associated critical wind direction is pointed out by locating the spill on the contour maps. Such identification will enable the desalination plant operators to prepare in advance for combating oil spill incidents.

It's worth noting that wind effect is found to dominate the trajectory of oil spill in the entire area of simulation with an exception at the Straits of Hormuz. The residual currents are found to dominate the spills originated in Hormuz vicinity. The application of an oil spill at that area shows that the surface currents flowing out of the Arabian Gulf are quite considerable. This area is not considered in the study due to the complications of prevailing dynamics taking place over there and the produced contours may not necessarily yield accurate representation of the events originated there.

The current study could be further expanded using the same model and setup to produce more sophisticated contour maps in terms of larger study area, various wind magnitudes, and assigned to other potential coastal resources. Also the application of summer prevailing water and environmental conditions and other simulation periods would be important to address. Finally other models reflecting the effect of weathering processes on the migrating slick can be further investigated. The produced maps hence can be linked to different oil types as well as critical weathering parameters.

REFERENCES

- [1] Al-Hajri, K., 1990. The circulation of the Arabian (Persian) Gulf: A model study of its dynamics. The Catholic University of America, Washington, DC. Ph.D. Dissertation
- [2] Al-Rabeh, A. H., 1994. Estimating surface oil spill transport due to wind in the Arabian Gulf. *Ocean Engineering*. 21, 461-465.
- [3] Al-Rabeh, A. H., Gunay, N., 1991. On the application of particle dispersion model. *Coastal engineering*. 17, 195-210.
- [4] Al-Rabeh A. H., Gunay, N., and Cekirge, H. M., 1990. A model of tidal and wind driven circulation in the Arabian Gulf. *Applied Math. Model*. 14, 410-419.
- [5] Al-Rabeh A. H., Cekirge, H. M., and Gunay, N., 1992. Modeling the fate and transport of Al-Ahmadi oil spill. *Water and Air Pollution* 65, 257-279.
- [6] Al-Rabeh A. H., Lardner, R., Gunay, N., and Khan, R. 1993. On Mathematical and empirical models for surface oil spill transport in the Gulf. *Marine Pollution Bulletin*, 27, 71-77.
- [7] Al-Rabeh A. H., Lardner, R., Gunay, N., 2000. Gulf spill version 2.0: a software package for oil spill in the Arabian Gulf. *Environmental Modeling and Software*, 15, 425-442.
- [8] Atlas, R. M., 1981. Microbial degradation of petroleum hydrocarbons: an environmental prescriptive. *Microbial Reviews* 45(1), 180-209.
- [9] Admiralty Tide Table (ATT), 2001. Hydrographer of the Navy, United Kingdom,
- [10] Audunson, T., (1979). Fate of oil spill on the Norwegian continental shelf. Oil spill conference, Los Angeles. California.

- [11] Blaikley, D. R., Dietzel, G. F. L., Glass, A.W., and Cankleef, P.J. Siltrak.. 1977. a computer simulation of offshore oil spills, cleanup, effects and associated costs. Proc. Oil Spill Conf., API, Washington, D.C., 45-52.
- [12] Brewer, P. G. and Dyrssen, D (1985). Chemical oceanography of the Persian Gulf. Prog. Oceanog. 14, 41-55
- [13] Cekirge, H. M., Al-Rabeh, A. H. & Gunay, N. (1989). Determining surface currents in
- [14] the Arabian Gulf. Computers and Mathematics with Applications 17(11), 1449-1453.
- [15] Chebbi, R., 2001. Viscous-Gravity spreading of oil in water. American Institute of Chemical Engineers Journal, vol. 47, No. 2
- [16] Chao, S-Y., Kao, T.W. and K.R. Al-Hajiri, 1992. A numerical investigation of circulation in the Arabian Gulf. Journal of Geophysical Research (C. Oceans), 97 (C7). 11219-11236.
- [17] Chu, W. S., Bark, B.L. & Akbar, A.M. (1988). Modeling tidal transport in the Arabian Gulf. J. Waterway, Port, Coastal , Ocean Engineering, 114(4), 455-71
- [18] Daling, P.S., Brandvik, P.J., 1988. A study of the formation and stability of water-in-oil emulsions. In: Proceedings of the 11th Arctic and Marine Oil Spill Program (AMOP) Technical Seminar. Environment Canada, pp. 153-170.
- [19] Delft Hydraulics Lab. Report "Modeling tides, currents and waves in the Gulf"
- [20] Delvigne, G. A. L., Sweeny, C. E., 1988. Natural dispersion of oil. Oil and Chemical Pollution 4, 281-310.

- [21] DHI MIKE3-SA Manual, 2002
- [22] Dimou, K. N., Adams, E. E., 1993. A Random-walk, Particle tracking model for well mixed estuaries and coastal waters. *Estuarine, Coastal and Shelf Science* 33, 99-110.
- [23] Elshorbagy, W., Mir, H. A., and Taguchi, K., 2004a. Hydrodynamic characterization and modeling of the Arabian Gulf. Submitted to ASCE, *Journal of Waterway, Port, Coastal, and Oceanic Engineering*.
- [24] Elshorbagy, W., Mir, H. A., Ichikawa, T., and Terasawa, T. 2004b. A three dimensional model application to study the residual flow in the Arabian Gulf. Submitted to ASCE, *Journal of Waterway, Port, Coastal, and Oceanic Engineering*.
- [25] Emery, K. O., 1956. Sediments and water of the Persian Gulf. *Bull. Amer. Assoc. Petroleum Geologists*, 40,10
- [26] Evans-Roberts, D.J., 1981. *Tides in the Persian Gulf, hydrology*, Hydraulics Research Station. Wallingford, England
- [27] Fannelop, T. K., Sjoen, K., 1980. Hydrodynamics of underwater blowouts. *Norwegian Maritime Research* 4, 17-33.
- [28] Fay, J. A., 1971. Physical processes in the spread of oil on a water surface. In: *Proc. Conf. Prevention and Control of Oil Spills*, 15-17 June. American Petroleum Institute, Washington, DC, 463-467.
- [29] Fay, J. A., 1969. The spread of oil on a calm sea. In: D. Hault (Ed.), *Oil on the sea*. Plenum Press.

- [30] Fingas, M., 1997. The evaporation of oil spills: prediction of equations using distillation data. In: proceedings of the 20th Arctic and Marine Oil Spill Program (AMOP) Technical Seminar. Environment Canada, 1-20
- [31] Fingas, M., 1999. The evaporation of oil spills: development and implementation of new prediction methodology. Spill Science and Technology Bulletin.
- [32] Galt, J. A., Payton, D. L., Torgrinson, G. M., and Watchayaski, G. 1983. Trajectory analysis for the Nowruz oil spill with specific applications to Kuwait, Modeling and Simulation Studies. Hazardous Materials Response Branch, NOAA, Seattle, WA, USA.
- [33] Grasshoff, K. 1976. Review of hydrographical and productivity conditions in the Gulf region. Marine Sciences in the Gulf Area, UNESCO Technical Papers in Marine Sciences, 26. 39-62
- [34] Gundlach, E. R. and Boehm, P. D., 1981. Determine fates of several oil spills in coastal and offshore waters and calculate a mass balance denoting major pathways for dispersion of spilled oil, Final Report. NOAA Grant
- [35] Gupta, R. S., 1993. State of oil pollution in the northern Arabian Sea after the 1991 Gulf oil spill. Marine pollution Bulletin. 27, 85-91
- [36] Harrison. W., Winnik, M. A., Kwong, P.T. Y. and Mackay, D. 1975. Disappearance of aromatic and aliphatic components from small sea-surface slicks. Environmental Science and Technology 9(3). 231-4
- [37] Henaidi, A. K., 1984. Preliminary report on drifting buoy movements. MEPA, Gulf Area Oil Companies Mutual Aid Organization, Doc. No. GO-86/87-70

- [38] Horowitz, A. and Atlas, R. M., 1977. Continuous open flow-through system as a model for oil degradation in the Arctic ocean. *Applied and Environmental Microbiology* 33(3), 647-53
- [39] Horton, C., Clifford, M., Cole, D., Schmitz, J., and Kantha, L., 1992. Operational modeling at the naval oceanographic office. *Oceanography* 5(1), 69-72.
- [40] Huang, J. C., 1983. A review of the state-of-the-art of oil spill fate/behavior models. In: *Proceedings of the 1983 oil spill conference*. American petroleum Institute, 312-22
- [41] Hughes, P. and Hunter, J. R. 1979. Physical oceanography and numerical modeling of the Kuwait Action Plan Region, UNESCO, Kuwait.
- [42] Hunter, J. R., 1982a. The physical oceanography of the Arabian Gulf: A review and theoretical interpretation of previous observations. Paper presented at the First Gulf Conference on Environment and pollution, Kuwait, 7-9 February 1982
- [43] Hunter, J. R., 1982b. Aspects of the dynamics of the residual circulation of the Arabian Gulf. In *coastal oceanography*. Plenum Publishing Corp., New York, USA.
- [44] Hydrographer of Navy, 1976. Admiralty co-tidal chart-Persian Gulf. Principal harmonics constituents, Chart 5081. Hydrographer of Navy, Taunton, Somerset, UK.
- [45] IMCOS Marine Ltd., 1981. Handbook of the weather in the Gulf, Surface Wind Data. London, UK.
- [46] Jones, R. K., 1997. A simplified pseudo-component oil evaporation model. *Proceedings of the 20th Arctic and Marine Oil Spill Program (AMOP) Technical Seminar*. Environment Canada, pp. 43-61.
- [47] Kolpak, R. L., Plutchak, N. B., and Stearns, R. W., 1977. Fate of oil in a water environment – Phase II, a Dynamic model of the mass balance for released oil. University

of Southern California, prepared for American Petroleum Institute, API publication 4313, Washington D.C.

- [48] Lardner, R. W., and Das, S., 1991. On the computation of Flow driven by density gradient: residual currents in the Arabian Gulf. *Applied Mathematical Modeling*, 15. 282-294.
- [49] Lardner, R., Al Rabeh, A. H., Gunay, N., Khan, R., Hossani, H., Reynolds, R. M., and Lehr, W. J., 1993. Computation of the residual flow in the Gulf using the Mt Mitchell data and KFUPM/RI Hydro dynamical models. *Marine Pollution Bulletin*, 27. 61-70.
- [50] Lardner, R. W., Lehr, W. J., Faraga, R. J., and Sarhan, M. A., 1987. Residual circulation in the Arabian Gulf. 1: Density-driven flow. *The Arabian Journal for Science and Engineering* 12(3). 341-354.
- [51] Lardner, R., Lehr, W. J., Fraga, R. J., Sharhan, M. A., 1988a. Residual currents and pollutant transport in the Arabian Gulf. *Applied Mathematical Modeling*, 12. 379-390
- [52] Lardner, R., Cekirge, H. M., Al Rabeh, A. H., Gunay, N., 1988b. Passive pollutant transport in the Arabian Gulf. *Advanced Water Resources*. 11. 158-161
- [53] Lehr, W. J., Fraga, R. J., Belen, M.S., Cekirge, H. M., 1984. A new technique to estimate initial spill size using a modified Fay-type spreading formula. *Marine Pollution Bulletin*, 15, 326-329
- [54] Linden, O., 1990. State of marine environment in the ROPME Sea area. UNEP Regional Seas Reports and Studies No. 112, Rev. 1:1-34.
- [55] Mackay, D. and Matsugu, R. S., 1973. Evaporation rates of liquid hydrocarbon spills on land and water. *Canadian J. Chem. Engng*, 51, 434-439.

- [56] Mackay, D., Leinonen, P.J., 1977. Mathematical model of the behavior of oil spills on water with natural and chemical dispersion. Tech. Review Report no. EPS-3-EC-77-19. Fisheries and Environment Canada.
- [57] Mackay, D., Paterson, S., 1980. Calculation of the evaporation rate of volatile liquids. Proc. 1980 National Conf. on Control of Hazardous Material spills, Louisville, KY.
- [58] Mackay, D., Paterson, S., Trudel, K., 1980a. A mathematical model of oil spill behavior. Environment Canada Report EE-7.
- [59] Mackay D., Buist, I., Mascarenhas, R., Paterson, S., 1980b. Oil spill processes and models. Environmental Canada Report EE-8
- [60] Meshal, A. H., and Hassan, H. M., 1986. Evaporation from the coastal waters of the central part of the Gulf. Arab J. Sci. Res. 4(2), 649-655.
- [61] MIKE3 Manual Documents, 2002
- [62] Milgram, J. H., 1983. Mean flow in round bubble plumes. J. Fluid Mech. 133, 345-376
- [63] Milgram, J. H., Burgess, J. J., 1984. Measurements of the surface flow above round bubble plumes. Applied Ocean Research 6(1), 41-44
- [64] Nizari, T., and Olsen, D. A. 1993. Saudi Arabia's response to the 1991 Gulf oil spill. Marine Pollution Bulletin, 27, 333-345.
- [65] NOAA final report on the Mt Mitchell research vessel in the Arabian Gulf, February – June 1992.
- [66] The Mt Mitchell cruise, 1992. US department of commerce, National Oceanic and Atmospheric Administration, Final Report.

- [67] Payne, J. R., and Philips, C. R., 1985a. Petroleum spills, Lewis Publishers, Inc., Chelsea, Michigan.
- [68] Payne, J. R., and McNabb, G. D., Jr., 1985. Weathering of petroleum in the marine environment. *Marine Technology Society Journal* 18(3).
- [69] Payne, J. R., McNabb Jr, G. D., Lambach, JI., Redding, R. Y., Jordan. R. E., Hom, W., de Olivera, C., Smith, G. S., Baxter, D M. and Gaegel, R., 1984b. Multivariate analysis of petroleum weathering in the marine environment-sub arctic, In: Environmental assessment of the Alaskan continental shelf – Final reports of the principal investigations. Vols. 21 and 22, US department of commerce, National Oceanic and Atmospheric Administration, Juneau, AK, USA.
- [70] Payne, J. R. et al., 1987. Development of the predictive model for the weathering of oil in the presence of sea ice. US department of commerce, National Oceanic and Atmospheric Administration, OCSEAP Final Report.
- [71] Pearson, W. H., Al-Ghais, S. M., Neff, J. M., Brandt, C. J., Wellman, K., Green, T., 1994. Assessment of damages to commercial fisheries and marine environment of Fujairah, United Arab Emirates, resulting from the Seki oil spill of March 1994:A case study. *YALE F&ES BULLETIN*, Middle eastern Natural Environments, p 407-428.
- [72] Persian Gulf Pilot (1967). Comprising the Persian Gulf and its approaches (11th edn.). Hydrographer of the Navy, London UK.
- [73] Price, A. R. G., and Sheppard, C. R. C., 1991. The Gulf: Past, Present and possible future states, *Marine Pollution Bulletin*, 22, 222-227.

- [74] Price, A. R. G., Brooks, W. H. and Younes, T., 1982. Saudi Arabia and the Gulf region: An Environmental overview. Report prepared for IUCN/MEPA for the Expert Meeting of the Gulf coordinating council to review environmental issues.
- [75] Price, A. R. G., Sheppard, C. R. C. and Roberts, C. M., 1993. The Gulf : its biological setting. *Marine Pollution Bulletin*, 27, 00-00.
- [76] Privett, D. W., 1959. Monthly charts of evaporation from the North Indian Ocean, including the Red Sea and the Persian Gulf. *Q. J. R. Meteor. Soc.* 85, 424-428.
- [77] Proctor, R., Elliot, A., Flather, R., 1994. Forecast and hind cast simulations of the Braer oil-spill. *Marine Pollution Bulletin* 28(4), 219-229.
- [78] Reed, M., Gundlach, E. and Kana, T., 1989c. A coastal zone oil spill model: development and sensitivity studies, *Oil Chem. Pollution.*, 5, 419-449.
- [79] Reed, M., Ekrol, N., Rye, H, Turner, L., 1999. Oil spill contingency and response (OSCAR) analysis in support of environmental impact offshore Namibia. *Spill Science and Technology Bulletin* 5(1). 29-38.
- [80] Reed, M., Spaulding, M. L., 1981. A fishery-oil spill interaction model: simulated consequences of a blowout. NATO Conference on Operations Research in Fisheries, Trondheim, Norway. August, 1979. In: K.B. Haley (Ed.), *Applied Operations Research in Fisheries*. Plenum Press, New York, pp. 99-114.
- [81] Reed, M., Johansen, O., Brandvik, P. J., Daling, P., Lewis, A., Fiocco, R., Mackay, D., and Prentki, R., 1999. Oil spill modeling towards the close of the 20th century: Overview of the state of art. *Spill Science and Technology Bulletin*, 5. 3-16.
- [82] Rye, H., and Brandvik, P. J., 1997. Verification of subsurface oil spill models. In: *Proceedings 1997 Oil Spill Conference*. API Publication No.4651, Washington DC, pp.551-557.

- [83] Reynolds, R. M., 1993. Physical oceanography of the Gulf, Strait of Hormuz, and Gulf of Oman – results from the Mt Mitchell expedition. *Marine Pollution Bulletin*, 27, 35-59.
- [84] Rodi W., 1980. Turbulence models and their applications in hydraulics, state of the art paper article sur l'état de connaissance. Paper presented by the IAHR- Section of Fundamentals of Division II: Experimental and Mathematical Fluid Dynamics, The Netherlands.
- [85] Sabins, F. F., 1997. *Remote Sensing: principles and interpretation-3rd edition*, p 138
- [86] Samuels, W. B., Huang N. E., and Amstutz D. E., 1982. An oil spill trajectory analysis model with a variable wind deflection angle. *Ocean Engineering*, 9 (4), 347-360
- [87] Severin, T., 1982. *The Sindbad Voyage*. Hutchinson, London
- [88] Shen, H.T., Yapa, P, Petroski, M., 1987. A simulation model for oil spill transport in lakes. *Water Resources Research*. 23 (10), 1949- 1957.
- [89] Sheppard. C. R. C. 1993. Physical environment of the Gulf relevant to marine pollution: an overview. *Marine Pollution Bulletin*, 27, 3-8
- [90] Spaulding, M. L., Saila, S.B., Reed, m., Lorda, E., Walker, H., Isaji. T., Swanson, J. and Anderson, E.. 1982a. Assessing the Impact of oil spills on a commercial fishery. Final report to Minerals Management Services. Contract No.AA851-CTO-75.NTIS No. PB83-149104.
- [91] Spaulding, M. L., Odulo, A., Kolluru, V. S.,1992 . A hybrid model to predict the entrainment and subsurface transport of oil. In *Proceedings of the 15th Arctic and Marine Oil Spill Program (AMOP) Technical Seminar*. Environment Canada. pp. 67-92.

- [92] Spaulding, M. L., Anderson, E. L., Isaji, T. and Howlett, E., 1993. Simulation of the oil trajectory and fate in the Arabian Gulf from the Mina Al Ahmadi spill. *Marine Environmental Research*, 36, 79-115.
- [93] Spaulding, M. L., 1988. A state-of-art review of oil spill trajectory and fate modeling. *Oil and Chemical Pollution*, 4, 39-55.
- [94] Stolzenbach, K., Madsen, O., Adams, E., Pollack, A., and Cooper, C., 1977. A review and evaluation of basic techniques for predicting the behavior of surface slicks. Report No. 222, Ralph M. Parsons Laboratory, Massachusetts Institute of Technology, Cambridge, MA.
- [95] Sugden, W. 1963. The hydrology of the Arabian Gulf and its significance in respect to evaporate deposition. *Ame. J. Sci.*, 261.
- [96] Swan, C., and Moros, A., 1993. The hydrodynamics of a sub-sea blowout. *App. Ocean Res*, 15, 269-280.
- [97] Tibbetts, G. R., 1971. Arab navigation in the Indian Ocean Before the coming of Portuguese. Royal Asiatic Society, London
- [98] Wheeler, R. B., 1978. The fate of petroleum in marine environment. Special report. Exxon production research Co.
- [99] Williams, G. N., Hann, R. and James, W. P., 1975. Predicting the fate of oil in the marine environment. Proceedings of conference on prevention
- [100] World Resources Institute. 1996. World Resources, 1996-97. Oxford University Press, New York
- [101] www.dewa.gov.ae

- [102] www.etc-cte.ec.gc.ca
- [103] www.itopf.com
- [104] www.response.restoration.noaa.gov
- [105] www.trade.uktradeinvest.gov.uk/water/abu_dhabi/
- [106] www.water-technology.net/projects/umm/
- [107] Yang, W.C., and Wang, H., 1977. Modeling of oil evaporation in aqueous environment. *Water Research*, 11, 879-887.
- [108] Zheng, L. and Yapa, P. D., 1997. A numerical model for buoyant oil jets and smoke plumes. In: *Proceedings of the 20th Arctic and Marine Oil Spill Program (AMOP) Technical Seminar*. Environment Canada, pp. 963-979.
- [109] ZoBell, C. E., 1973. Microbial degradation of oil: Present status, problems and perspectives. In: D. G. Ahearn and S.P. Meyres (Eds), *The Microbial Degradation of Oil Pollutants*. Center for Wetland Resources, Louisiana State University. Pub. No. LSU-SG-73-01

ملخص الدراسة

تهدف هذه الدراسة الى انتاج خرائط تقييم أخطار كـنـتـورية تستخدم لتوقع أقل زمن لانتقال البقع النفطية و اتجاه الرياح الحرج المصاحب لها وذلك لعدد من محطات تحلية المياه الاستراتيجية على طول ساحل الامارات العربية المتحدة. لقد تم اختيار خمسة محطات للتحلية على ساحل الدولة المطل على الخليج العربي باعتبارها نقاط مستهدفة ذات أهمية من حيث أخطار البقع النفطية وهي الشويهات، المرفأ، أم النار و الطويلة، جبل علي و النية.

من أجل تحقيق هدف البحث فقد تم توظيف و استخدام برنامج للنمذجة الرياضية لمحاكاة الهيدروديناميكا الساحلية الطبيعية للخليج العربي. و قد تمت مقارنة النتائج الواردة من البرنامج مع القياسات الخاصة بارتفاع المد و سرعة واتجاه التيارات البحرية بعد عمل التوفيقات اللازمة على أداء نموذج المحاكاة، كما تم مقارنة توزيع التيارات البحرية السطحية المتوسطة مع تلك الواردة في أوراق بحثية سابقة لمنطقة الخليج العربي، وقد وجدت النتائج في توافق جيد وعلى ذلك تم التأكد من قدرة النموذج الهيدروديناميكي على تمثيل واقع الحالة البحرية الى درجة جيدة.

تم تفعيل النمذجة الرياضية الخاصة بمحاكاة البقع النفطية بالاعتماد على قاعدة النتائج الصادرة من المرحلة الاولى والخاصة بحقل توزيع التيارات البحرية و النتائج الهيدروديناميكية الاخرى، وقد تم اجراء تحليل لمدى حساسية مختلف العناصر المستخدمة في حساب مسار تحرك البقع النفطية و عمليات التجوية الخاصة بها للتعرف و عليه فقد تم استخدامها لضبط عمل نموذج المحاكاة.

لقد تم اختبار اداء النموذج بشقية الاول، الهيدروديناميكي و الثاني الخاص بالبقع النفطية في تلك المرحلة و ذلك باجراء نمذجة لحادثة تسرب نفطي حقيقية في الخليج العربي و مقارنة النتائج الصادرة مع واقع أرصاد تحرك البقعة الحقيقية وقد وجدت النتائج في توافق جيد. وبذلك تم التأكد من معيارية عمل النموذج بشقية.

تم استخدام النموذج في تلك المرحلة لعمل سلسلة من عمليات النمذجة لعدد من البقع النفطية الافتراضية اعتمادا على مبدأ أسوأ الأوضاع التي يمكن حدوثها.

لقد تم تقسيم مساحة الدراسة الى مناطق تغطي الممرات الملاحية البحرية لناقلات النفط بالإضافة الى منصات تحميل النفط. وقد تم تحديد أقل زمن لانتقال البقع النفطية من كل من تلك المناطق إلى كل محطات التحلية مع تحديد اتجاه الرياح الحرج الذي يدفع البقعة باتجاه محطة التحلية مباشرة.

وفي النهاية تم استخدام قيم أقل زمن انتقال واتجاه الرياح الحرج لإنتاج خرائط كـنـتـورية للخضر بحيث تم إنتاج زوج من الخرائط الكنتورية تمثل القيمتين لكل محطة من محطات التحلية محل الدراسة.



جامعة الإمارات العربية المتحدة
عمادة الدراسات العليا
برنامج ماجستير علوم البيئة

محاكاة التسرب النفطي في البيئة البحرية للخليج العربي
وتقييم الخطر المرتبط به على محطات تحلية المياه الساحلية
بدولة الامارات العربية المتحدة

مقدم من الطالب
أبو بكر عوض الحكيم

الي

جامعة الإمارات العربية المتحدة

استكمالاً لمتطلبات الحصول على درجة الماجستير في علوم البيئة

يناير 2005